



NTNU – Trondheim
Norwegian University of
Science and Technology

Drug Delivery Using Oral Vehicles

Controlled Release in the GI-tract

Maren Sæther

Biotechnology (5 year)

Supervisor: Kurt Ingar Draget, IBT

Norwegian University of Science and Technology
Department of Biotechnology

Preface

The laboratory work presented in this thesis was performed from august 2011 to april 2012 at the Norwegian Biopolymer Laboratory (NOBIPOL), Department of Biotechnology, Norwegian University of Science and Technology (NTNU), Trondheim.

I would like to express my thankfulness to my supervisors Professor Kurt I. Draget, Dr. Ingvild J. Haug and PhD. Magnus N. Hattrem for excellent practical and theoretical guidance. A special thank to Magnus for valuable input and discussions throughout the study, and for always being patient and cheerful. I would also thank staff engineer Ann-Sissel Ulset, who performed the SEC-MALLS experiments, and all my other fellow co-workers who made this work a great experience.

To Øystein, thank you for all help and support.

NTNU, Trondheim
May 15th 2012

Maren Sæther

Abstract

Oral delivery is considered a convenient route for administration of pharmaceuticals. Great effort has been made to optimize oral delivery vehicles to increase the bioavailability of the pharmaceutical, and enhance patient compliance to ease swallowing. Emulsion-based gelled matrices have shown promising features as delivery systems. They are soft chewable matrices that are easy to swallow, and have the ability to entrap the pharmaceutical, providing prolonged, and controlled release to avoid fast dissolution in the stomach.

The purpose of this study was divided into two main objectives. The first aim was to study emulsion-based gelatin matrices intended for oral drug delivery by investigation of the influence of gelatin type and/or oil content on the matrix properties. The second aim was to investigate the properties of multiple emulsions, regarding their potential as oral drug delivery systems for water-soluble pharmaceuticals, and controlled drug delivery.

Emulsion-based matrices stabilized by 160g Bloom gelatins, either type A or B, and containing various amounts of corn oil (0, 10, 30 and 50 wt %) were subjected to rheological characterization and *in vitro* dissolution studies at simulated gastric conditions. The results showed an increase in viscosity, storage modulus and gelling and melting temperatures in line with increased oil content in the matrix, and to a larger extent for matrices with type A gelatin compared to type B. Longitudinal deformations of the gelled matrices did show a trend of slightly increasing Young's modulus when oil was added to the matrix, but no clear trend was observed for force and strain at break. A correlation between rheological matrix properties and dissolution time was observed: An increase in dissolution time with higher fractions of oil and prolonged dissolution time for matrices with type A gelatin compared to type B. Overall the results showed that different oil contents and gelatin types changed the physical properties of the matrices, providing a possibility to tailor matrices to obtain suitable delivery systems for various pharmaceuticals.

Water-in-oil-in-water double emulsions, stabilized by either 226g Bloom gelatin type B or tween80 was examined by long time stability studies, and by *in vitro* lipolysis studies simulating small intestinal conditions. The water-soluble marker tartrazine, was entrapped in the inner water phase of the emulsions. The release of tartrazine was measured during a period of 78 days and both double emulsions with gelatin and tween80 were found to possess long-term stability at room temperature. *In vitro* lipolysis of gastric stable double emulsions stabilized by gelatin was conducted in a dissolution medium containing bile extracts, with or without lipases. A complete release of tartrazine was obtained; both in the presence and absence of lipases, while a faster release was observed when lipases were present. Although the release mechanism was not completely determined, the results indicate that release of drugs can occur in the small intestines due to lipolysis. The double emulsions thus offer great potential in delivery of gastric unstable pharmaceuticals.

Sammendrag

Oral administrering av legemidler er en praktisk og enkel leveringsmetode. En stor innsats har blitt lagt i å øke biotilgjengeligheten til legemidler som leveres oralt, og det er i tillegg viktig at formuleringen gjør det enkelt å svelge medikamentet. Emulsjonsbaserte matriser har vist seg å ha egenskaper som gjør de egnet som leveringssystemer. De er myke, tyggbare og lette å svelge. Leveringssubstansen kan dispergeres i matrisen, som vil fungere som et reservoar og kan gi kontrollert frigivelse av legemiddelet over tid, samt beskytte det mot degradering i magesekken.

Dette studiet hadde to hovedmålsettinger. Det første målet var å studere hvordan gelatintype og/eller oljeinnhold i emulsjonsbaserte gelatinmatriser påvirket matrisens egenskaper. Det andre målet var å undersøke egenskapene til doble emulsjoner, med tanke på et eventuelt bruksområde som leveringssystemer for vannløselige legemidler og for kontrollert frigivelse av medikamenter.

De reologiske egenskapene til emulsjonsbaserte matriser, stabilisert av 160g Bloom gelatin, type A eller B, og forskjellig innhold av maisolje (0, 10, 30 og 50 wt %), ble karakterisert. Matrisene ble i tillegg utsatt for *in vitro* oppløsningsstudier under simulerte mageforhold. Resultatene viste en økning i viskositet, lagringsmodul, geling- og smeltetemperatur i takt med økende oljekonsentrasjon i matrisen. Økningen ble observert i større grad for matriser stabilisert med type A gelatin. Langsgående deformasjonsstudier av matriser i gelform viste en trend av svakt økende Young's modul med økt oljeinnhold, men ingen klare resultater ble sett ved målinger av bruddstyrke. En sammenheng mellom de reologiske egenskapene og oppløsningstid for matrisen ble observert: Økte oljefraksjoner i matrisen forlenget oppløsningstiden, og oppløsningstiden var også lengre for matriser med type A gelatin. Resultatene viste at det er mulig å skreddersy matriser for levering av ulike legemidler ved å endre gelatin type og/eller oljeinnholdet.

Doble emulsjoner av vann-i-olje-i-vann, stabilisert av 226g Bloom gelatin type B eller tween80, ble undersøkt gjennom langtidsstabilitetsstudier og *in vitro* lipolyseforsøk under simulerte tynntarmsbetingelser. Den vannløselige markøren tartrazine var inkorporert i den indre vannfasen i emulsjonene. Frigivelsen av tartrazine fra den indre vannfasen ble målt over en tidsperiode på 78 dager, og begge dobbeltemulsjonene var stabile i romtemperatur. *In vitro* lipolyseforsøk ble utført med syrestabile dobbeltemulsjoner i et oppløsningsmedium som inneholdt galleekstrakt, med eller uten lipaser tilstedet. Tartrazine ble fullstendig frigjort, både med og uten tilstedeværelse av lipaser, men frigivelse skjedde raskere med lipaser tilstede i oppløsningsmediet. På tross av at frigivelsesmekanismen ikke ble fullstendig kartlagt, indikerte resultatene at frigivelse vil skje i tarmen. De doble emulsjonene har dermed et stort potensial som leveringssystemer for legemidler som er ustabile i det sure miljøet i magesekken.

List of abbreviations and symbols

A	area
API	active pharmaceutical ingredient
Bloom	gel strength measured under standard conditions
CCx	Concordix
DE	double emulsion
E	Young's modulus
F	force
G'	storage modulus
IEP	isoelectric point
L ₀	original length
ΔL	change in length
M _n	number average molecular weight
MQ	MILLI-Q water
M _w	weight average molecular weight
N	number of replicates
PE	primary emulsion
PGPR	Polyglycerol Polyricinoleate
PI	polydispersity index
rpm	revolutions per minute
SEC-MALLS	size exclusion chromatography coupled to multi-angle laser light scattering
Type A	gelatin obtained from acidic collagen processing
Type B	gelatin obtained from alkali collagen processing
T _g	gelling temperature
T _m	melting temperature
WP	water phase
wt %	weight percentage
δ	phase degree
η	viscosity
σ	stress
γ	strain
ω	angular frequency

Table of contents

INTRODUCTION	1
1.1 BACKGROUND AND AIM OF THESIS.....	1
1.2 GELATIN	2
1.3 EMULSIONS.....	3
1.4 THE GASTROINTESTINAL SYSTEM.....	6
1.5 PHARMACEUTICALS.....	7
1.6 RHEOLOGICAL CHARACTERIZATION	8
1.7 MOLECULAR WEIGHT DISTRIBUTION OF BIOPOLYMERS	11
2. MATERIALS AND METHODS	12
2.1 MATERIALS	12
2.1.1 Gelatin.....	12
2.1.2 Milli-Q water.....	12
2.1.3 Ingredients used to prepare Concordix matrices.....	12
2.1.4 Artificial gastric acid	13
2.1.5 Acetaminophen	13
2.1.6 Trizma® base.....	13
2.1.7 Tartrazine.....	13
2.1.8 Polyglycerol Polyricinoleate (PGPR).....	13
2.1.9 Parabenes.....	13
2.1.10 Intestinal Digestion Fluid	14
2.1.11 Concentrated Pancreatic Lipase solution.....	14
2.2 METHODS	15
2.2.1 SEC-MALLS.....	15
2.2.2 Preparation of Concordix matrices	15
2.2.3 Mastersizer 3000	17
2.2.4 Viscosity measurements	17
2.2.5 Small strain oscillatory measurements	18
2.2.6 Longitudinal deformations	18
2.2.7 Dissolution studies.....	20
2.2.8 Double emulsions.....	22
3. RESULTS AND DISCUSSION	26
3.1 SEC-MALLS	26
3.2 DROPLET SIZE DETERMINATION OF CONCORDIX MATRICES.....	28
3.3 VISCOSITY MEASUREMENTS OF CONCORDIX MATRICES.....	30
3.4 RHEOLOGICAL CHARACTERIZATION OF CONCORDIX MATRICES.....	38
3.4.1 Small strain oscillatory measurements of Concordix matrices.....	38
3.4.2 Longitudinal deformation of Concordix gels	41
3.5 IN VITRO DISSOLUTION STUDY OF CONCORDIX MATRICES.....	45
3.6 STABILITY STUDY WITH DOUBLE EMULSIONS STABILIZED BY GELATIN VERSUS TWEEN80	50
3.7. IN VITRO LIPOLYSIS OF DOUBLE EMULSIONS.....	59
3.8 PROSPECTIVE RESEARCH.....	64
4. CONCLUDING REMARKS	65
REFERENCES	66
LIST OF APPENDICES	70

INTRODUCTION

1.1 Background and aim of thesis

Oral delivery is considered the most convenient route of administration for active pharmaceutical ingredients (APIs). Usual dosage forms comprise tablets, capsules, suspensions, solutions and emulsions. Although it is a simple route for API delivery, several disadvantages complicate the formulation process. For instance, low solubility in the stomach and intestines reduces the bioavailability of the pharmaceutical. Additionally, fast dissolution in the stomach, possibly followed by destruction of the API by enzymatic secretions of the gastrointestinal (GI) tract may occur (Aulton, 2007). Another problem is that many people, especially children and the elderly, have difficulties swallowing tablets and capsules. A questionnaire study showed that 26 % of 1576 patients had problems swallowing tablets (Andersen *et al.*, 1995).

Based on the demand for improved drug formulation, NOBIPOL (Norwegian Biopolymer Laboratory) together with Ayanda AS developed a new technology, *Concordix* (CCx, patent number US 2011/0268770 A1), for oral delivery (Seternes *et al.*, 2009). CCx was originally an emulsion-based delivery system for drugs and nutraceuticals, stabilized by a gelling agent, resulting in a soft, chewable matrix. An emulsion consists of two immiscible liquids, usually a water and a lipid phase, where one phase is uniformly distributed throughout the other (McClements, 2005). In the CCx vehicle, lipid droplets are distributed in a gelled water phase with gelatin as a stabilizing agent.

Currently the CCx technology is on the market for delivery of omega-3 (ω -3) fatty acids and has shown improved bioavailability of the ω -3 fatty acids docosahexaenoic acid (DHA) and eicosapentaenoic acid (EPA) compared to traditional soft gel capsules (Haug *et al.*, 2011). It is desirable to utilize the same technology for delivery of pharmaceuticals, due to the known benefits of CCx: The matrix is easy to swallow, leading to increased patient compliance and it may also affect the bioavailability of the API, by increasing the API solubility. There is an increasing interest for development of lipid based systems for oral delivery of poorly water-soluble pharmaceuticals to enhance absorption and thus the bioavailability of the API (Sek *et al.*, 2001). Another advantage is the potential of reduced misuse of pharmaceuticals by drug addicts, as extraction of pure API from the matrix is difficult compared to e.g. traditional tablets and capsules.

This thesis focuses on the optimizing and further development of the existing Concordix technology for oral delivery of pharmaceuticals. The relation between matrix properties and dissolution rate was studied to gain knowledge of how the CCx matrices behave in the gastrointestinal tract. Another aim was to study the properties of multiple emulsions, considering the use of multiple emulsion systems for drug delivery of water-soluble pharmaceuticals. According to Garti (1997), multiple emulsions are so-called “emulsions of emulsions” where the droplets of the dispersed phase contain even smaller dispersed droplets. Multiple emulsions have the potential to serve as an entrapped reservoir of APIs and offers prolonged release, as the content can be released from inner to outer phase in a controlled and sustained manner (Garti, 1997). The goal was to make stable *water-in-oil-in-water* (w/o/w) double emulsions,

utilizing the Concordix technology, where the API is not released as a function of time during storage, but rather by lipolysis in the small intestine, making it a highly controllable delivery system.

1.2 Gelatin

Gelatin is a versatile biopolymer with numerous applications in food, pharmaceuticals, cosmetics and technical products. It is a widely used gelling agent in the food industry due to its texture and the “melt-in-mouth” feeling. Its advantages in pharmaceutical and medical applications are owed primarily to its biocompatibility and low immunogenicity, and the possibility to control its physical parameters (Veis, 1964, Haug and Draget, 2009).

Gelatin is produced from collagen, and the raw material can be any collagen-containing tissue. Common sources are mammalian hides, skins and bones, but gelatin may also be produced from fish skin (Haug and Draget, 2009). Collagens are a family of fibrous proteins found in all multicellular animals, and is the most abundant class of proteins in animals (Ward and Courts, 1977, Alberts *et al.*, 2008). A typical collagen molecule has a right handed, triple stranded helical structure, formed by three intertwined collagen peptide chains, called α chains. Glycine-X-Y is the general amino acid sequence of the α chains, where X is commonly proline and Y is commonly hydroxyproline (Veis, 1964, Haug, 2003). The high content of proline and glycine facilitates the triple helical structure. The ring structure in proline stabilizes the helical conformation in each α chains and glycine allows tight packing of the chains (Alberts *et al.*, 2008).

Gelatin is produced by partial degradation of collagen. The collagen is treated with either dilute acid or alkali to partially cleave the cross-links, resulting in gelatin, which is soluble in warm water. The acid or alkali treatment gives rise to type A gelatins and type B gelatins, respectively (Ward and Courts, 1977). Type A gelatins have an amino acid composition very similar to the native collagen molecule, and have an average isoelectric point (IEP) in the pH range 7-9.4. The alkali treatment gives rise to type B gelatins, by converting glutamine and asparagine residues into their carboxyl forms (aspartic and glutamic acid, respectively), resulting in a more acidic gelatin compared to type A. Type B gelatins therefore have a lower IEP, in the pH range 4.8-5.5 (Schrieber and Gareis, 2007, Haug and Draget, 2009).

The gelatin structure consists of three classes of fragments based on molecular weight, denoted α , β and γ chains. The α chain is a single peptide chain with a molecular weight average of approximately 100 kDa (Norland, 1990). β chains and γ chains corresponds roughly to two and three covalently linked α chains, respectively. The different fragments contribute to the broad molecular weight distribution of gelatin obtained by SEC-MALLS.

Physical properties of gelatin

Gelatins are thermo-reversible, having the ability to interconvert between a liquid and solid state upon heating and cooling, by absorbing between five and ten time their own weight of water (Rowe *et al.*, 2009). Gelatin from mammalian sources has a coil-

helix transition temperature at approximately 40°C. Above this temperature the gelatin exists as a flexible, random coil. Below the transition temperature, the gelatin retains the helix formation and gels as long as the gelatin concentration is above a critical gelation concentration, C_0 , typically in the range of 0.4-1.0 wt % (Gilsenan and Ross-Murphy, 2000). Gelatin is soluble over the whole pH range, but if the pH in the dilution medium is close to the isoelectric point of the gelatin, the solution will become turbid (Ward and Courts, 1977). The coil-helix transition process is illustrated in figure 1.1.

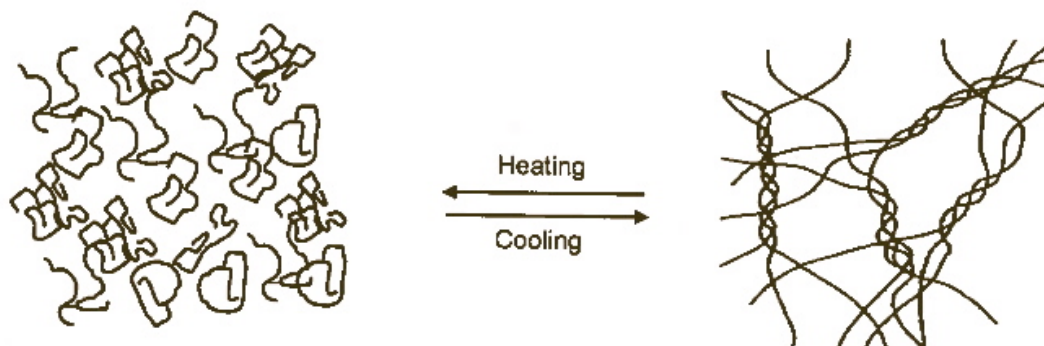


Figure 1.1. Thermo-reversible coil-helix transition of gelatin (Haug and Draget, 2009).

Once a gelatin gel network has set, further maturation of the gel occurs by two processes: Increasing order of the junctions in the molecular network and a general thickening of the network. The gel strength properties, such as the rigidity, will increase rapidly for several hours after setting of the gel and will continue to increase to a diminishing rate (Ward and Courts, 1977). This characteristic causes gelatin to form non-equilibrium gels, which increase in strength with time.

The Bloom strength of a specific gelatin is the rigidity of the gelatin gel, formed and measured under standard conditions. The Bloom is determined by the weight in grams required for depressing the surface of a 6.67 wt % gelatin gel 4 mm using a 12.7 mm diameter flat-bottomed cylindrical plunger under standard conditions (GMIA, 2006).

1.3 Emulsions

Conventional emulsions

An emulsion consists of two immiscible liquids, usually water and oil, where one liquid is uniformly dispersed as droplets throughout the other (McClements, 2005). Emulsions are usually prepared by a homogenizer, which breaks up and recoalesces the droplets (Norde, 2003). One can distinguish between coarse emulsion, having droplets larger than 1 μm , and colloidal emulsions with droplet size usually less than 1 μm (Schmidt and Lamprecht, 2009). Classification of emulsions is based on relative spatial distribution of the oil and water phases. An *oil-in water* (o/w) emulsion consists of oil droplets dispersed in an aqueous phase, while a *water-in-oil* (w/o) emulsion is the opposite with water droplets dispersed in an oil phase. The liquid phase is referred to as the *continuous* or *external* phase, while the droplets are called the *dispersed* or *internal* phase (McClements, 2005).

Double emulsions

In addition to the standard o/w and w/o emulsions already described, various types of multiple emulsions can be made. As previously mentioned, multiple emulsions are “emulsions of emulsions” with emulsions *water-in-oil-in-water* (w/o/w) and *oil-in-water-in-oil* (o/w/o) double emulsions being the two major types. Double emulsions are usually prepared by a two-step emulsifying procedure. For instance, a w/o/w emulsion is prepared by dispersing a pre-emulsified w/o emulsion into a continuous water phase. As mentioned previously, double emulsions have many potential applications particularly in food, pharmacology and cosmetics. Potential applications in pharmacology include the use of double emulsions as sustained and prolonged drug delivery systems, taste masking and enzyme delivery (Garti, 1997, Garti and Bisperink, 1998). The difference between conventional emulsions and multiple emulsions is illustrated in figure 1.2.

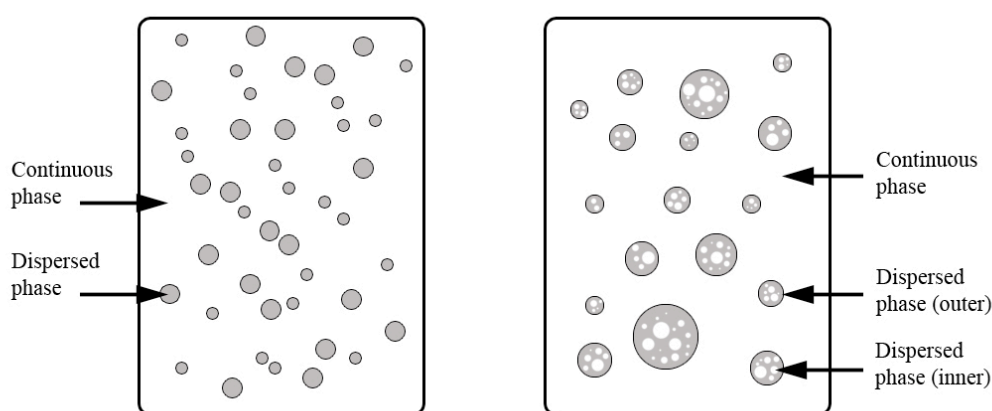


Figure 1.2. Schematic illustration of a conventional emulsion (left) and a double emulsion (right).

Emulsifiers and stabilizations

Emulsions are generally thermodynamically unstable, and tend to destabilize during storage. To achieve an appropriate shelf life, stabilizing agents are needed. Stabilizing agents may be classified into two main categories, texture modifiers and emulsifiers. A texture modifier acts by modifying the viscosity of the continuous phase, and can be divided into thickening agents and gelling agents (such as gelatin, used in the CCx technology). Emulsifiers are amphiphilic molecules that have the ability to adsorb to the oil-water interface, forming a protective film around the dispersed droplets and thereby protecting them from coalescence. The emulsifier additionally reduces the interfacial tension between the two phases. This may promote stability by making coalescence less energetically favorable and promotes dispersion of droplets during manufacture (Norde, 2003).

Emulsifiers are classified either as ionic or nonionic and stabilize emulsions primarily through electrostatic and sterical mechanisms. An HLB number, representing the hydrophile-lipophile balance of the agent, is used to predict the solubility of emulsifiers in the oil and/or aqueous phases (Aulton, 2007). Bancroft’s rule states that a water soluble emulsifier ($HLB > 7$) is used to prepare o/w emulsions while an oil soluble emulsifier ($HLB < 7$) is used for the preparation of w/o emulsions (Norde, 2003).

A surfactant is a small amphiphilic molecule that tends to adsorb to surfaces and interfaces, such as oil-water. As opposed to emulsifiers, a surfactant may not necessarily stabilize emulsions (Hasenhuettl and Hartel, 2008).

Destabilizing mechanisms

According to Aulton (2007), “an emulsion is considered as stable if the dispersed droplets retain their initial character and remain uniformly distributed throughout the continuous phase”. Different destabilizing mechanisms can lead to deviation from this ideal behavior. Physical destabilization leads to alternation in the spatial distribution and includes creaming, flocculation, coalescence, partial coalescence and phase inversion (Dickinson and Stainsby, 1982, McClements, 2005). Hydrolysis and oxidation are examples of chemical destabilization processes (McClements, 2005).

Flocculation occurs when two or more of the droplets in the dispersed phase aggregate. Each droplet retains its identity, but the aggregated droplets will physically act as a single unit (McClements, 2005, Aulton, 2007). Flocculation can reduce the shelf life of an emulsion, by speeding up the rate of gravitational separation of the two phases, resulting either in creaming or sedimentation (Luyten *et al.*, 1993). Flocculation increases the viscosity (Chanamai and McClements, 2000, Aulton, 2007) and tends to confer a shear-thinning behavior to the emulsions. At low shear rates, the flocs are aggregated, acting like particles of fixed shapes with a constant viscosity. At increased shear rate, the flocs disrupt and elongate with the shear field, which results in decreased viscosity (McClements, 2005).

Coalescence is the merging of individual droplets to form larger droplets. While flocculation can occur in minutes or hours after manufacturing of an emulsion, it might take weeks or months for coalescence to occur (Dickinson, 1989). Emulsions may be stabilized towards coalescence by addition of a suitable emulsifier that contributes to repulsion between dispersed droplets. In addition, maintaining a stable storage environment (e.g. avoidance of temperature fluctuation) will reduce the mobility of the droplets and hence prevent coalescence (McClements, 2005).

Destabilizing mechanisms in double emulsions

The two interfaces of double emulsions contributes to an increased complexity and is a driving force towards thermodynamic destabilization, and the systems usually have a strong tendency to undergo coalescence, flocculation and creaming (Garti, 1997, Benna-Zayani *et al.*, 2008). Coalescence is the main destabilization mechanism and includes coalescence of either inner or outer droplets or coalescence of inner droplets and the outer droplet interface (Dickinson, 2011). Efforts are being made to improve the stability of multiple emulsions, as they offer a great potential in pharmaceutical applications (Garti, 1997). In addition, shrinking or swelling of the inner droplets caused by transfer of materials may occur, and will contribute to emulsion destabilization (Dickinson, 2011).

Transport mechanisms in double emulsions

Effort has been made to investigate the release of substances initially entrapped in the inner water phase of w/o/w emulsions. Transport occurs mainly via reverse micellar transport or by direct diffusion through the thin lamella of surfactants that form in the oil layer, and is promoted by osmotic pressure (Kita *et al.*, 1978, Garti and Bisperink, 1998). The reverse micellar transport mechanism involves entrapment of molecules

inside a reversed micelle at one side of the oil-water interface, followed by diffusion through the oil layer and subsequent release of the content into the other water phase (Cheng *et al.*, 2006). In addition, the two interfaces may behave similarly to a dynamic lipid bilayer, where spontaneous formation of small holes can occur between the two interfaces, causing release of internally entrapped molecules (Paula *et al.*, 1996, Pays *et al.*, 2001).

1.4 The gastrointestinal system

The main function of the gastrointestinal system of humans is to process food into small molecules that can be absorbed into the internal environment of the body, where the energy of the molecules can be utilized. This break down processing of food, called digestion, is both a mechanical and enzymatic process. The digestive system consists of the gastrointestinal tract, the pancreas, the liver, and the gallbladder (Widmaier *et al.*, 2010).

Degradation in the stomach

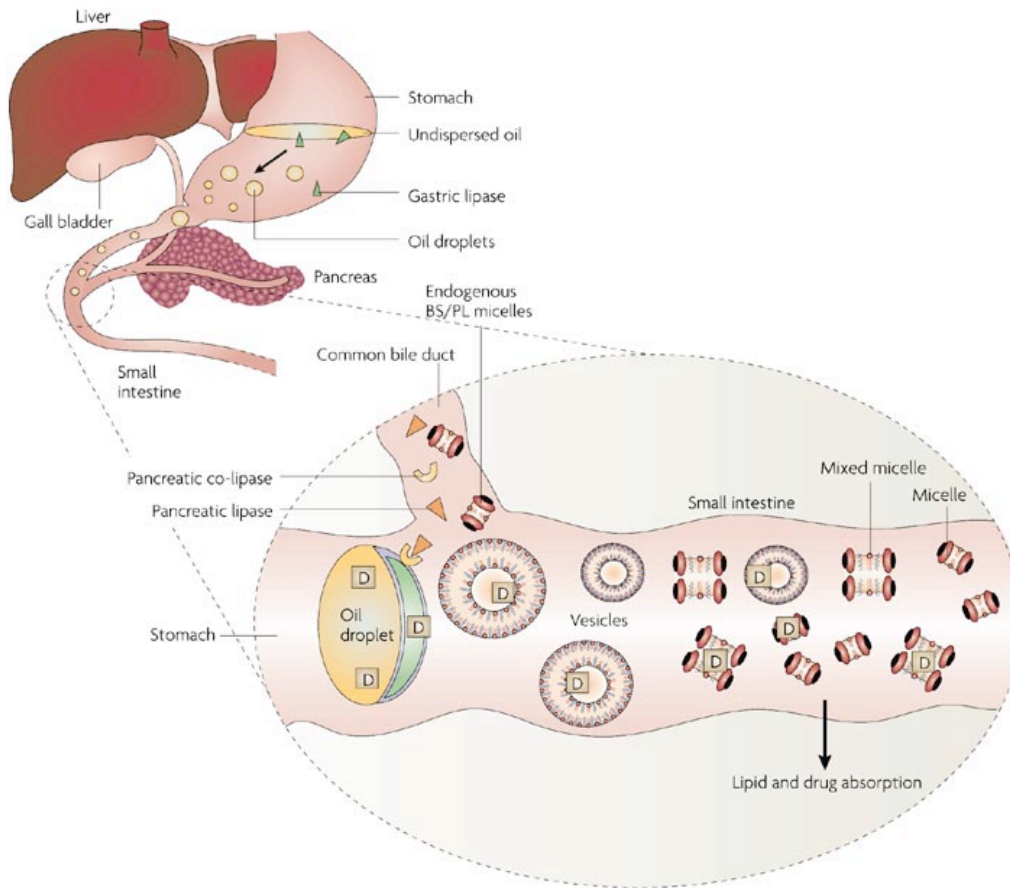
The stomach stores, dissolves, and partially digests food, before delivering it to the small intestine for further digestion and absorption. Glands in the stomach's wall secrete gastric acid and digestive enzymes, which contribute to the breakdown of food and pharmaceuticals by optimizing the pH and breaking down proteins and polysaccharides into shorter fragments, respectively. The gastric acid contributes to a low pH in the stomach, ranging from 1-3, depending of the fed state. The acidic environment alters the ionization of polar molecules, and the molecules are then partially digested by enzymes such as pepsin and amylase (Widmaier *et al.*, 2010).

Absorption in the small intestine

The process of absorption is almost completed in the upper part of the small intestine, and the rate of absorption is dependent on the rate of emptying of the stomach (Grahame-Smith and Aronson, 2002). Digestive enzymes are secreted from the pancreas and from the salivary glands in the intestinal wall. Amylases are cleaving starch and glycogen into disaccharides, and proteins are cleaved into shorter peptides and amino acid by proteases. Lipid digestive enzymes, the lipases, together with bile acids are needed to convert triglycerides into free fatty acids and monoglycerides (Sand *et al.*, 2006). The small intestine has a pH in the range of 6.0-7.5 (McClements and Li, 2010).

Lipid digestion

Lipid digestion occurs primarily in the small intestine. In addition some digestion of fat occur in the stomach. Gastric lipase facilitates lipid digestion in the stomach, whereas the lipases functioning in the small intestine are secreted from pancreas. Lipases carry out the digestion of fat at the interface between water and lipid. The rate of fat digestion is therefore controlled by the availability of the lipases to bind to the surface of oil droplets. The presence of co-lipase and surface-active bile acids are essential for optimal lipase activity in the small intestine. Together, bile acids and co-lipase facilitates the binding of lipases to lipid interfaces (Golding and Wooster, 2010). A schematic illustration of lipid digestion is presented in figure 1.3.



Nature Reviews | Drug Discovery

Figure 1.3. Lipid digestion in the small intestine (Porter et al., 2007).

1.5 Pharmaceuticals

The concept of drug therapy can be separated into four main processes (Grahame-Smith and Aronson, 2002):

- 1) The pharmaceutical process
- 2) The pharmacokinetic process
- 3) The pharmacodynamic process
- 4) The therapeutic process

The pharmaceutical process is concerned with drug formulation, route of absorption and patient compliance. In addition to the drug itself (the API), a medicine usually contains different excipients, manufacture impurities and occasionally degradants (Fox, 2007). The pharmacokinetic process includes absorption, distribution, metabolism and elimination of the drug. To study these processes, the concentration of the drug and metabolites are measured in body fluids over periods of time after administration. The pharmacodynamic process encompasses the pharmacological effects of the drug, both the one leading to a therapeutic effect as well as the adverse effects of a drug. The final therapeutic process determines whether the

pharmacological effect is transformed into the intended therapeutic effect (Aulton, 2007).

A drug's bioavailability is described by the proportion of the administered dose that reaches the systemic circulation intact, and thus is available for distribution to its site of action. Oral drug delivery involves the passage of drug across the gastrointestinal mucosa. After absorption, the drug has to pass the liver, where it has to avoid first-pass-metabolism, before it can reach the systemic circulation. Thus, when a drug is administered orally, a portion will reach the systemic circulation while another part of the dose will be metabolized and eliminated from the body. The bioavailability for orally delivered drugs is therefore less than 100% (Grahame-Smith and Aronson, 2002).

The most important reason why new pharmaceuticals are not approved is due to poor bioavailability and/or pharmacokinetic properties. To overcome these obstacles it is important to focus on the drug formulation to ensure that a new pharmaceutical has the basic qualities needed: The API must be able to be incorporated into a formula with other excipients and must perform the expected *in vivo* effect (Brewster, 2007, Tønnes *et al.*, 2008).

1.6 Rheological characterization

Rheology is the science of flow and deformation of matter, and materials are subjected to a range of deformations and flows in order to investigate rheological properties (Ross-Murphy, 1984, Smidsrød and Moe, 2008, Norde, 2003). A force has to be applied in order to deform a material, and the area of which the force acts on will influence the degree of deformation. The term *stress* (σ) is defined as force (F) per unit area (A) applied to a material (equation 1.1), and is a measure of the amount of deformation, often referred to as *strain* (γ), induced (Ross-Murphy, 1984). The deformation can be described as the ratio between the change in length of an object (ΔL) and its original length (L_0), described by equation 1.2.

$$\sigma = \frac{F}{A} \quad (1.1)$$

$$\gamma = \frac{\Delta L}{L_0} \quad (1.2)$$

Viscosity

Viscosity is defined as the ratio of stress to shear rate, and the common unit is Pascal seconds (Pa s) (McNaught and Wilkinson, 1997). Viscosity is the most important property affecting the flow of a fluid, and is related to the fluids resistance to flow (Doran, 2010). Two types of viscosities are known: Newtonian viscosity and non-Newtonian viscosity. A fluid is Newtonian if the shear force is proportional to the

shear velocity with the proportionality constant η , where η is the viscosity of the fluid. If η is not constant, the fluid is non-Newtonian. The viscosity for a non-Newtonian fluid is dependent on shear velocity and/or time. Types of non-Newtonian viscosities are given in table 1.6.1 (Smidsrød and Moe, 2008, Doran, 2010).

Table 1.6.1. Overview of non-Newtonian viscosities (Smidsrød and Moe, 2008).

Behavior by increasing:	Shear velocity	Time
Thinner	Shear thinning (Pseudoplastic)	Thixotropic
Thicker	Shear thickening (Dilatant)	Rheopectic

If the viscosity is a function of shear velocity, it will either increase or decrease with increased velocity, characterizing the material as shear thickening or shear thinning, respectively (Smidsrød and Moe, 2008).

Time dependent viscosity gives either thixotropic or rheopectic materials. Thixotropic properties are related to a materials ability to resume its original structure after structure breakdown. The viscosity of a thixotropic material decreases with time when exposed to shear, until a minimum is reached. Once the shear is removed, the viscosity recovers over time and the material is *reversible*. A rheoplastic material show opposite behavior to thixotropy, as the viscosity of a rheopectic material will increase with time (Doran, 2010).

Viscoelasticity

When an ideal elastic material is deformed, all the energy will be stored in the body, and when the deforming force is removed, the material will resume its original shape. Materials exhibiting both viscous and elastic properties at the same time are known as *viscoelastic*. Small strain oscillatory measurements can be performed in order to obtain information on the storage modulus (G'), the loss modulus (G''), and gelling – and melting temperatures (T_g and T_m) for viscoelastic materials (Ross-Murphy, 1984). The material to be examined is subjected to a harmonic oscillating deformation with an angular frequency (ω), while the force is measured. The material undergoes deformation (strain, γ), and responds with stress (σ), equation 1.3 and 1.4, respectively. The phase degree (δ) corresponds to the displacement between strain and stress, where γ_0 is the amplitude of the strain and σ_0 is the amplitude of the stress (Smidsrød and Moe, 2008).

$$\gamma = \gamma_0 \sin(\omega t) \quad (1.3)$$

$$\sigma = \sigma_0 \sin(\omega t + \delta) \quad (1.4)$$

The phase degree is a measure of the relation between the elastic and viscous properties of a material. For a perfect elastic material δ is equal to zero, and is completely in phase with the strain, while an ideal Newtonian fluid has δ equal to 90° . For all other materials the phase degree is between 0 and 90° .

The viscoelastic properties of a material are described by the storage and loss moduli, shown in equation 1.5 and 1.6, respectively.

$$G' = \frac{\sigma_0}{\gamma_0} \cos \delta \quad (1.5)$$

$$G'' = \frac{\sigma_0}{\gamma_0} \sin \delta \quad (1.6)$$

The relation between G' , G'' , δ and the corresponding viscoelastic behavior of a material is given in table 1.6.2.

Table 1.6.2. The relation between storage modulus (G'), loss modulus (G''), phase degree (δ) and viscoelastic behavior (Smidsrød and Moe, 2008).

Relation between G' and G''	Phase degree (δ)	Viscoelastic behaviour
$G' < G''$	$> 45^\circ$	Liquid
$G' = G''$	$= 45^\circ$	Transition state
$G' > G''$	$< 45^\circ$	Solid

1.7 Molecular weight distribution of biopolymers

The molecular weight of a biopolymer will have a significant effect on its physical properties. Different methods can be used to determine the molecular weight, and the most common ways to present the molecular weight is either as the average number (M_n) or as a weight average (M_w), shown in equation 1.7 and 1.8, respectively. If a biopolymer sample consists of molecules of equivalent weight, it is called monodisperse. The biopolymer is polydisperse if it consists of molecules of various weights. The polydispersity index (PI) is the ratio between the weight average and average number (equation 1.9), and if a biopolymer is monodisperse, PI is equal to one. The value of PI will increase as the degree of polydispersity increases (Smidsrød and Moe, 2008).

$$M_n = \frac{\sum_{i=1}^n n_i M_i}{\sum_{i=1}^n n_i} = \frac{\sum_{i=1}^n W_i}{\sum_{i=1}^n \frac{W_i}{M_i}} \quad (1.7)$$

$$M_w = \frac{\sum_{i=1}^n n_i M_i^2}{\sum_{i=1}^n n_i M_i} = \frac{\sum_{i=1}^n n_i M_i}{\sum_{i=1}^n n_i} \quad (1.8)$$

$$PI = \frac{M_w}{M_n} \quad (1.9)$$

2. MATERIALS AND METHODS

2.1 Materials

2.1.1 Gelatin

The Concordix matrices were prepared with pig skin gelatin, type A, and limed bovine bone gelatin, type B, with Bloom strength 160g, provided by GELITA® (Mannheim, Germany). Gelatin 226g Bloom type B, provided by DGF Stoess (Eberbach, Germany), was utilized for preparation of the double emulsions. Information about the different gelatins is given in table 2.1.1.

Table 2.1.1. Information on the gelatins used.

Type	Source	Bloom (g)	Batch number
A	Pig skin	160	629586
B	Limed bovine bone	160	630473
B	Cow hide	226	232635

2.1.2 Milli-Q water

Milli-Q (MQ) water was used in all experiments. The MQ water had an electrical conductivity of 18.2 mΩ (Millipore, Oslo, Norway).

2.1.3 Ingredients used to prepare Concordix matrices

Table 2.1.2 provides information on the different ingredients used together with gelatin and MQ water, in the preparation of Concordix matrices.

Table 2.1.2. Name and information on products used to prepare Concordix matrices.

Product	Information
Sorbitol	Food Innovation (Oslo, Norway) #4119307601, NV54006, Production date: 3/2012
Xylitol	Food Innovation (Oslo, Norway) #4351306443, NV54008, Production date: 3/2010
Sucralose	Sigma-Aldrich, CAS number 56038-13-2, lot number BCBD4344V
Citric acid	Food Innovation (Oslo, Norway)
Coffee flavour	Givaudan (Dubendorf, Switzerland), Batch number: D9000035130
Corn oil	Sigma-Aldrich

Sorbitol and xylitol are sugar alcohols and sucralose is an artificial sweetener, all three serving as sweeteners. Citric acid and coffee flavor improves the taste and aroma of the CCx. Corn oil is a vegetable oil consisting almost entirely of triglycerides, and was used to prepare O/W emulsions.

2.1.4 Artificial gastric acid

Dilute hydrochloric acid (0.1 M) was used as dissolution medium in the dissolution studies of Concordix matrices, in accordance with the European Pharmacopoeia (Pharmacopoeia, 2007).

2.1.5 Acetaminophen

Acetaminophen (Sigma-Aldrich, Steinheim, batch number 078K0032, $M_w = 151.17$ g/mol) was used as marker to determine the dissolution rate of Concordix matrices in the dissolution studies.

2.1.6 Trizma® base

Trizma® base (Sigma-Aldrich, USA, batch number 108K54151, $M_w = 121.14$ g/mol) has a buffering capacity in the pH range 7-9, and was used to increase the pH of Concordix matrices containing 30 wt% corn oil, to obtain a pH at approximately 8.5.

2.1.7 Tartrazine

Tartrazine (Sigma-Aldrich, USA, batch number 079K1462V, $M_w = 534.36$ g/mol, empirical formula $C_{16}H_9N_4Na_3O_9S_2$) is a water soluble, yellow dye, used in stability studies and *in vitro* lipolysis studies of double emulsions, described in more detail under *methods* section 2.2.8. The literature claims that fading of the color of tartrazine is accelerated in the presence of gelatin (Rowe *et al.*, 2009), but unpublished data has not detected this effect (Haug and Hattrem, 2010), and it was therefore chosen to use tartrazine as a marker. The molecular structure of tartrazine is illustrated in figure 2.1.

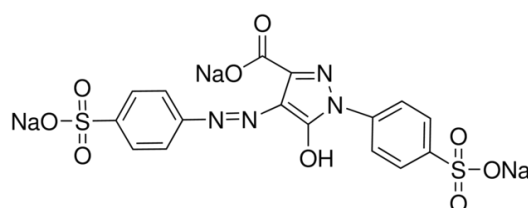


Figure 2.1. Molecular structure of tartrazine.

2.1.8 Polyglycerol Polyricinoleate (PGPR)

PGPR 90 Kosher (Grindsted, Denmark, batch number 4011576684) is an emulsifier used in the preparation of double emulsions.

2.1.9 Parabenes

Methyl 4-hydroxybenzoate sodium salt (Sigma-Aldrich, Japan, batch number BCBD5783V) and Propyl 4-hydroxybenzoate sodium salt (Sigma-Aldrich, Lot and filling code: 1432931 31209P03) were dissolved in MQ water and used as preservatives to increase the shelf-life of double emulsions during stability studies described in section 2.2.8.

2.1.10 Intestinal Digestion Fluid

Ingredients used to prepare the intestinal digestion fluid are presented in table 2.1.3. The products listed in the table were dissolved in MQ water to obtain the fluid, which was used as dissolution medium in *in vitro* lipolysis studies of double emulsions.

Table 2.1.3. Name and information on products used to prepare intestinal digestion fluid for *in vitro* lipolysis studies.

Product	Information
Trizma® maleate	Sigma-Aldrich, CAS number 72200-76-1, lot number 081M5447V, Mw: 237.21 g/mol
Bile extract porcine	Sigma-Aldrich, CAS number 8008-63-7, lot number 050M0133, Mw: 430 g/mol
Lecithin	The molecular formula was not given on the product, it was assumed that the formula was C ₄₀ H ₈₀ NO ₈ P (phosphatidylcholine lecithin), Mw: 734 g/mol
Calcium chloride dihydrate	Merck KGaA (Darmstadt, Germany) Mw: 147.02 g/mol
Sodium chloride	Merck KGaA (Darmstadt, Germany) Mw: 58.44 g/mol

Trizma® maleate was used as a buffering agent in the digestion fluid to obtain a pH of 7, which is in the range of the physiological pH in the small intestine. Bile extract porcine provided bile acids. Lecithins are fatty substances containing phospholipids found in both plants and humans. Bile acids and phospholipids are secreted into the intestinal lumen where they form mixed micelles and impact the activity of pancreatic lipases. Free fatty acids will inhibit pancreatic lipase activation. Calcium is known to form insoluble aggregates with free fatty acids and was added to the digestion fluid to prevent lipase inhibition (Larsen *et al.*, 2011).

2.1.11 Concentrated Pancreatic Lipase solution

Pancreatin, from porcine pancreas (Sigma-Aldrich, CAS number 8049-47-6, Lot number 061M1822V, USA) was utilized in preparation of concentrated Pancreatic Lipase Solution. Porcine pancreatin contains all enzymes secreted from the pancreas, with pancreatic triacylglyceride lipase, co-lipase, phospholipase A₂ and cholesterol esterase being the most important for lipid digestion (Larsen *et al.*, 2011).

2.2 Methods

2.2.1 SEC-MALLS

Size exclusion chromatography multi-angle laser light scattering (SEC-MALLS) analyses were performed for 160g Bloom gelatin type A and B, to determine the molecular weights and the molecular weight distribution of the two gelatins used to prepare Concordix matrices.

Theory

Size exclusion chromatography separates molecules based on size as they are flown through a column packed with porous beads. Smaller molecules tend to penetrate the pores to a larger extent than larger ones, leading to a longer retention time for the smaller particles, causing the larger particles to elute first from the column. A light scattering detector, detecting the scattered light for up to 18 angles simultaneously, detects the amount of light scattered, and a concentration sensitive detector measures the refractive index or absorbance. The molecular mass of the gelatin chains can be determined because the amount of light scattered is directly proportional to the molecular mass multiplied with the concentration (Christensen, 2010).

Procedure

Gelatin was dissolved in MQ water to obtain a concentration of 2 mg/mL and mixed with the eluting buffer (0.1 M Na₂SO₄, 0.02 M EDTA, 0.5 M Trizma base, pH 9), filtrated through a 1 µm filter (low protein binding) and stored at 4°C until analysis. A SEC-MALLS instrument (Wyatt Technology Corp, Santa Barbara, CA, USA) equipped with a packed column (TSK G-6000 + 5000 PWXL DAWN DSP / Optilab DSP, Supelco, Sigma Aldrich, Bellefonte, PA, USA), determined the molecular mass distribution, at a temperature of 40°C. The data was processed and analyzed using the computer software Astra (Version 4.90.07, Wyatt Technology Corp).

2.2.2 Preparation of Concordix matrices

Concordix matrices containing two different gelatins; 160g Bloom, type A and B, with various amounts of corn oil (0, 10, 30 and 50 wt%) were prepared and analyzed.

Preparation of Concordix without oil

The Concordix matrix without oil was made with the ingredients listed in table 2.2.2.1

Table 2.2.2.1. Concordix matrix with 0 wt % oil.

Product	Amount (wt %)
MQ water	38.11
Gelatin 160 Bloom	11.44
Sorbitol	14.66
Xylitol	34.21
Sucralose	0.43
Citric acid	0.42
Coffee flavor	0.74

The Concordix matrix was prepared by first dissolving gelatin (either type A or B) in MQ water at 65°C by stirring (100 rpm). Sorbitol and xylitol was then added and dissolved, thereafter sucralose and citric acid. The coffee flavor was added in the end. The liquid CCx was poured into small petri dishes (3.5 cm diameter), and stored in the refrigerator until use.

Preparation of Concordix with oil

Concordix matrices with different amounts of corn oil (10, 30 and 50 wt%) were prepared following the same procedure as for the matrix without oil, except that corn oil was added to the end. The Concordix were then homogenized using a VDI 12 homogenizer (VWR International GmbH, Darmstadt, Germany) equipped with a dispersing element (S12N-12S) with a dispersion speed of 27 800 rpm for approximately 4 minutes.

The amount of each ingredients used for preparation of CCx with 10, 30 and 50 wt% corn oil is given in table 2.2.2.2-4, respectively.

Table 2.2.2.2. Concordix matrix with 10 wt % corn oil.

Product	Amount (wt %)
MQ water	34.29
Gelatin 160 Bloom	10.29
Sorbitol	13.20
Xylitol	30.79
Sucralose	0.38
Citric acid	0.38
Coffee flavor	0.66
Corn oil	10.00

Table 2.2.2.3. Concordix matrix with 30 wt % corn oil.

Product	Amount (wt %)
MQ water	26.67
Gelatin 160 Bloom	8.01
Sorbitol	10.26
Xylitol	23.95
Sucralose	0.30
Citric acid	0.29
Coffee flavor	0.51
Corn oil	30.00

Table 2.2.2.4. Concordix matrix with 50 wt % corn oil.

Product	Amount (wt %)
MQ water	19.06
Gelatin 160 Bloom	5.72
Sorbitol	7.33
Xylitol	17.11
Sucralose	0.22
Citric acid	0.21
Coffee flavor	0.37
Corn oil	50.00

Preparation of Concordix matrices with acetaminophen

Acetaminophen was used as a marker in the dissolution studies of CCx matrices. Acetaminophen was added to a heated, liquid Concordix solution in such a quantity that 1.5 g of the final CCx gave a concentration of 0.1 mM acetaminophen after complete dissolution in 900 mL HCl (0.1 M). See appendix A, section A2, for calculation.

Samples (approximately 5 g) were poured into small petri dishes (d=3.5 cm) and allowed to gel at room temperature for 24 hours prior to use.

2.2.3 Mastersizer 3000

The emulsion droplet size of Concordix matrices with gelatin 160g Bloom (either type A or B) and different amounts of corn oil (10, 30 and 50 wt%) were measured using a Mastersizer 3000 (Malvern instruments, UK).

Theory

The Mastersizer 3000 is a laser diffraction instrument, comprised of a main optical unit, one or more dispersion units (wet or dry) and a measurement cell. The instrument transmits two sources of light, red (633 nm) and blue (466 nm), through a sample and records the beam that is diffracted off of the particles to be measured, and returned to the detectors. The light scattering pattern obtained by the particles is interpreted by the Mastersizer software, which provides accurate volume-based particle size information (Malvern, 2011).

The instrument is equipped with a stirrer that prevents sedimentation of the particles in the beaker, and an ultrasonic probe. The manufacturer recommends an obscuration above 5 % in order to obtain a significant signal, but the obscuration should not exceed 15 % (Ryzak and Bieganowski, 2011, Malvern, 2011).

Procedure

The heated, liquid Concordix matrix to be analyzed was first diluted 1:10 in MQ water. Approximately 3 droplets of the diluted CCx were added to the Mastersizer 3000 beaker (a wet dispersion unit, Hydro LV / MV), to an obscuration in the range of 5 to 9 %. For each sample, 5 replicates were measured in series and the instrument software provided an analysis report based on the average. Information on the analysis report is found in appendix C.

2.2.4 Viscosity measurements

The shear viscosity of Concordix matrices with gelatin 160g Bloom (either type A or B) and different amounts of corn oil (0, 10, 30 and 50 wt %) were measured with a StressTech Rheometer (Reologica, Lund, Sweden) set up with a cone / plate geometry (cone = 4°, d = 40 mm). A zero gap was performed prior to addition of sample with gap size 150 µm. Heated, liquid CCx (approximately 1.5 mL) was then applied to the plate, and covered with silicone oil (Dow Corning®, 200/10cS fluid, UK) to prevent evaporation during the measurement. A pre-shear (2 1/s, 300 s) was applied to obtain temperature equilibrium prior to viscosity measurements. Measurements were performed at 0.6, 0.8, 1, 2, 4, 7, 10, 20, 40, 60, 80 and 100 1/s, at 60°C.

2.2.5 Small strain oscillatory measurements

Small strain oscillatory measurements were performed on Concordix matrices with gelatin 160g Bloom (either type A or B) and different amounts of corn oil (0,10, 30 and 50 wt %) in a StressTech Rheometer (Reologica, Lund, Sweden). The rheometer was set up with a cone / plate geometry (cone = 4°, d = 40 mm) and a zero gap was performed prior to addition of sample using a gap size of 150 µm. The sample (approximately 1.5 mL) was applied to the plate, and covered with silicone oil (Dow Corning®, 200/10cS fluid, UK) to prevent evaporation during the measurement. For samples containing 0, 10, and 30 wt % oil, the start and end temperature was 60°C, and for the Concordix with 50 wt % the start and end temperature was 70°C. Cooling and heating rate was 2°C/minute. The curing temperature was at 20°C, and holding time was 15 minutes. Measurements were performed at a constant frequency of 1 Hz. Additional information on the small strain oscillatory measurements are provided in appendix E.

2.2.6 Longitudial deformations

Concordix matrices were prepared as described in section 2.2.2 and liquid CCx were casted in steel wells (NTNU workshop), as illustrated in figure 2.2. It is important to add enough Concordix to give positive meniscus: The top plate will exert pressure and ensure equal gel height for all cylinders. The casted matrix were stored at room temperature and allowed to gel for 24 hours prior to measurement. The wells were lubricated with liquid fat (Akofine sp01, slip melting point 45°C, Aarhus, Karlshamn) prior to sample addition, to ensure that the gels could easily be removed from the wells. The wells used are giving a gel cylindrical gel shape with diameter of approximately 16 mm, and height of approximately 18 mm.



Figure 2.2. Steel wells utilized for casting of Concordix gels. Each cylinder (6 cylinders are shown between the bottom and top plate) has an interior height=18 cm and diameter=16 cm. The top plate is exerting a press, to ensure equal gel height.

The gels were removed from the wells after 24 hours, and the diameter and height of each gel were measured using a digital caliper, to ensure correct measurements. The size of each gel is presented in appendix F.

Compression measurements were performed in order to determine Young's modulus, force and strain at break with a texture analyzer (TA.XT.-Plus Texture Analyser,

Stable Micro Systems, Surrey, UK) for Concordix gels with gelatin 160g Bloom (either type A or B), containing varying amounts of corn oil (0, 10 and 30 wt%).

Young's modulus

Theory

Young's modulus, E , is a parameter used to characterize the stiffness of an elastic material, and is commonly known as the elastic modulus. It is defined as the constant ratio of stress over strain in the region where Hooke's law is valid (Goodwin and Hughes, 2000). Hooke's law is presented in equation 2.1 and Young's modulus in equation 2.2.

$$\sigma = E\gamma \quad (2.1)$$

$$E = \frac{\sigma}{\gamma} = \frac{\frac{F}{A}}{\frac{\Delta L}{L_0}} = \frac{FL_0}{A\Delta L} \quad (2.2)$$

Equation 2.2 is used to determine Young's modulus (N/m^2), when force (F) is exerted on the object during compression. A is the original cross-sectional area of the object, and L_0 is the original length. The force is applied, and the change in length (ΔL) is measured. Figure 2.3 presents a schematic force-distance curve for a gelatin gel, subjected to force to obtain Young's modulus. The initial linear region (red line on the figure) represents the viscoelastic region from which Young's modulus is determined.

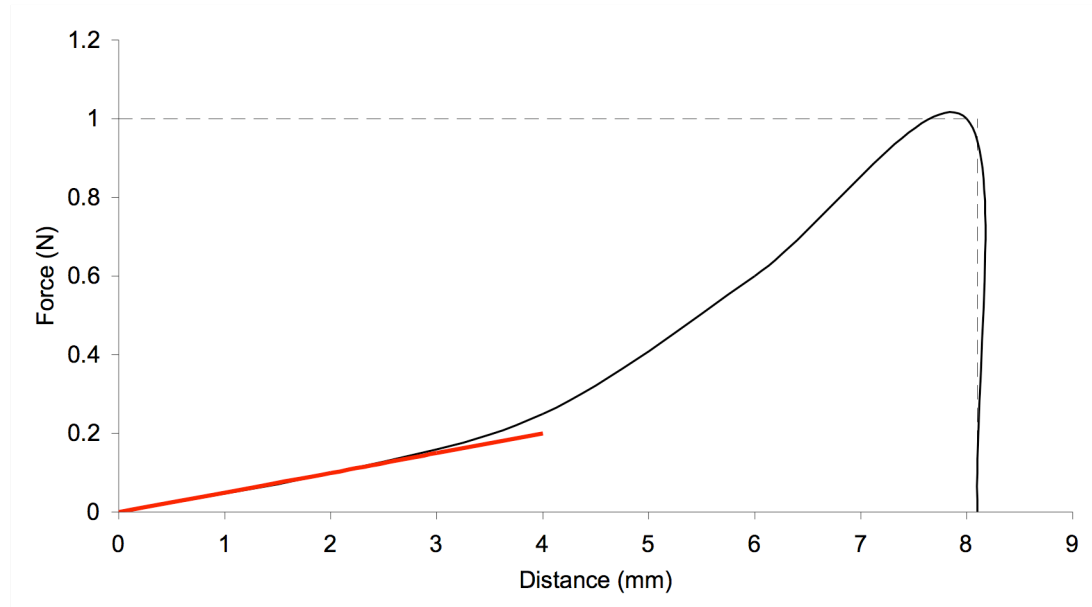


Figure 2.3. Force-distance curve for a gelatin gel subjected to force (N). The peak is where fracture occurs, and the dotted grey lines marks force at break and distance at break at y-axis and x-axis, respectively. The red line represents the viscoelastic region of the gelatin gel, used for calculation of Young's modulus and force and strain at break for Concordix gels.

Procedure

Young's modulus was found by compression measurements of Concordix gels, casted as illustrated in figure 2.2. The gel was placed in the centre of the texture analyzer, and a compression of 2 mm was performed with a probe (p/50, 50 mm diameter cylindrical) at 0.1 mm/s using a load cell of 5 kg. The results were analyzed with the software "Exponent" that was coupled to the instrument. Young's module was found by determining the slope in the region 0.10-0.15 mm of the force-distance curve obtained from the software. Linear regression was performed to ensure that the region was linear and measurements with R^2 (the Coefficient of Determination) values below 0.98 were excluded.

Force and strain at break

After measuring Young's modulus, the probe was exchanged with a smaller probe (p/2, 2 mm diameter stainless) and the measurements were repeated on the same gels. Compression measurements were performed with a speed at 0.1 mm/s until break was achieved, using a 5 kg load cell. The software was used to determine force at break as the first peak obtained from the force-distance curve, which corresponds to the first break in the gel. Strain at break was found by dividing the distance at break by the original height of the gel.

2.2.7 Dissolution studies

Theory

Dissolution of drug molecules from a solid formulation involves replacement of the drug released by solvent molecules, and is determined by the relative affinity of the molecules involved. The rate of dissolution is determined by the rate-limiting step, which is commonly the diffusion of dissolved solute through the static liquid layer that exists at the solid/liquid interface. For some occasions, the release of molecules from the solid into the solution is the rate-limiting step, followed by fast transport across the static layer. The rate of diffusion will follow Fick's Law of diffusion, which states that the rate of concentration change of dissolved material is proportional to the concentration difference between the two sides of the diffusion layer (Aulton, 2007). However, the rate-limiting step for dissolution of Concordix matrices is considered to be the break down of the gelatin network and Fick's law does therefore not apply for these studies.

Procedure

In order to measure the dissolution profiles of Concordix matrices with gelatin 160g Bloom (either type A or B) and different amounts of corn oil (0, 10, 30 and 50 wt%), dissolution studies were performed in a dissolution unit (SOTAX USP 1,2,5,6 Manual). Two independent studies were performed, each with two replicates of every matrix type, giving four replicates altogether. Gelled CCx matrices containing acetaminophen as marker, prepared as described in section 2.2.2, were cut out in similar sized pieces (1.50 g) and placed in their respective baskets inside the beakers in the dissolution unit, see figure 2.4.



Figure 2.4. The interior of the dissolution unit (SOTAX USP): Three glass beakers are shown (with three additional beakers behind the ones seen), each containing a metal basket, where the gel is placed. Samples are extracted directly from the beaker with a syringe, which is connected to the small metal tube that is seen to the right for the rod holding the basket.

Each basket was filled with 900 mL artificial gastric acid (0.1 M HCl). The temperature was held constant at 37 °C, and the agitation was 75 rpm. Samples (approximately 4 mL) were withdrawn at specific times (see table 2.2.7 for an overview of gel types and corresponding sampling times) using a syringe.

Table 2.2.7. Matrix types and corresponding sampling times (min) for dissolution studies of the CCx matrices with various amounts of corn oil (0, 10, 30 and 50 wt %).

Gel types	Sampling times (min)
160 Bloom A and B 0 wt % oil	1, 6, 11, 16, 21, 26, 36, 46, 56, 66
160 Bloom A and B 10 wt % oil	2, 6, 10, 14, 18, 23, 28, 38, 48, 58
160 Bloom A and B 30 wt % oil	2, 6, 10, 14, 18, 23, 28, 38, 48, 58, 68
160 Bloom A and B 50 wt % oil	2, 7, 12, 17, 22, 27, 37, 47, 57, 67, 127, 187, 247

After complete dissolution, the samples were filtrated two times through “low protein binding” filters (first through a 1.2 µm-filter and then through a 0.2 µm-filter) to remove oil droplets. The samples were then analyzed by spectrometry (Lambda 25 UV/VIS spectrophotometer, Perkin Elmer Instruments) at 243.3 nm, the known absorption maximum for acetaminophen. Artificial gastric acid was used as blank sample. The results obtained were compared to a standard of known concentration of acetaminophen.

In order to measure the absorbance of the excipients in the CCx-formulation, a sample of gelatin, sucralose and coffee flavor dissolved in HCl (0.1 M) were prepared for each gel type. The absorbance was measured at 243.3 nm, and subtracted from the absorbance of each sample to prevent them from affecting the results.

2.2.8 Double emulsions

Preparation of Double Emulsions: Method I

Double emulsions containing the same amount of tartrazine in either inner or outer water phase (serving as control and negative control, respectively) were prepared. The double emulsions were stabilized by either gelatin 226g Bloom type B or tween80, giving a total of four emulsions. In order to achieve this, two primary w/o emulsions (PE) were made. The ingredients used to prepare PE1 and PE2 are listed in table 2.2.8.1 and 2.2.8.2, respectively.

Table 2.2.8.1. Primary emulsion #1 (PE1).

Product	Amount (wt %)
PGPR 90	10.0
Tartrazine (2 wt %)	20.0
Corn oil	70.0

Table 2.2.8.2. Primary emulsion #2 (PE2).

Product	Amount (wt%)
PGPR 90	10.0
MQ water	20.0
Corn oil	70.0

PGPR was mixed with corn oil and the respective aqueous phase (see table 2.2.8.1 and 2.2.8.2) was added at a rate of approximately 20 mL/min while homogenizing with a VDI 12 homogenizer (VWR International GmbH, Darmstadt, Germany) at 27 800 rpm for approximately 5 minutes.

The external water phases (WP) were prepared next. Gelatin or tween80 was mixed with the respective ingredients given in table 2.2.8.3.

Table 2.2.8.3. The four water phases used to prepare double emulsions. The amount of each ingredient is given as weight percentage (wt %) of the total water phase.

Water phase 1		Water phase 2		Water phase 3		Water phase 4	
Gelatin	10.0	Gelatin	10.0	Tween80	2.5	Tween80	2.5
226 Bloom Type B		226 Bloom Type B					
MQ water w/parabene stock solution	90.0	MQ water w/parabene stock solution	85.0	MQ water w/parabene stock solution	97.5	MQ water w/parabene stock solution	92.5
		Tartrazine (2 wt %)	5.0			Tartrazine (2 wt %)	5.0

Four double emulsions (DEs) were made by homogenizing 20 % primary emulsion and 80 % water phase using a VDI 12 homogenizer at 5000 rpm for approximately 3 minutes. Table 2.2.8.4 shows how the PEs and WPs were combined to obtain the four different DEs.

Table 2.2.8.4. The four double emulsions (DE1, 2, 3 and 4) consisting of primary emulsion (20 %) and water phase (80 %).

Double emulsion	DE1	DE2	DE3	DE4
Primary emulsion	PE1	PE2	PE1	PE2
Water phase	WP1	WP2	WP3	WP4

Preparation of Double Emulsions: Method II

Due to observed physical instability of the double emulsion produced following *method I* described above, a new production procedure was made. Double emulsions containing the same amount of tartrazine in either inner or outer water phase (serving as control and negative control, respectively) were prepared, as for *method I*.

Two primary emulsions were made, identical to those made following *method I* above. Then DE1 and DE2 were made with the ingredients listed in table 2.2.8.5. DE3 and DE4 were made following the procedure described in *method I*.

Table 2.2.8.5. Double emulsion 1 and 2, prepared by method II. The amount of each ingredient is given as percentage (%) of the total double emulsion.

DE1		DE 2	
MQ water w/parabenes	70.0	MQ water w/parabenes	66.0
Gum Arabicum Type 8013, MVW 0800193	2.0	Gum Arabicum Type 8013, MVW 0800193	2.0
		Tartrazine (2 wt %)	4.0
PE1	20.0	PE2	20.0
Gelatin 226 Bloom Type B	8.0	Gelatin 226 Bloom Type B	8.0

Gum arabicum was dissolved in MQ water containing parabenes, at room temperature for approximately 30 min under stirring (100 rpm). The primary emulsion was added, and the emulsion was homogenized with VDI 12 at 5000 rpm for 1.5 minutes. The mixtures were placed in a water bath at 55°C before adding the gelatin, which was dissolved by stirring (100 rpm). Samples (approximately 5 g) were poured into small petri dishes (d=3.5 cm) and allowed to gel at room temperature.

The double emulsions were stored in the dark at room temperature. While the emulsions with gelatin were stored in a gelled state, the emulsions with tween80 remained in a liquid state.

Stability study with double emulsions using tartrazine as marker

Four different double emulsions were made, as described above. Two of them with 10 wt % gelatin type B, 226g Bloom, where the first (DE1) contained a total of 4 wt % of tartrazine in the inner water phase, whereas the second (DE2), serving as a negative control, contained a total of 4 wt % in the outer water phase. For comparison two double emulsions were made with 2.5 wt % tween80: One with tartrazine in the inner water phase (DE3), and the other in the outer phase (DE4), serving as a negative control. The total amount of tartrazine in the double emulsions with tween80 was 4 wt % as well.

The stability studies were performed to examine the long term stability for the double emulsions. The amount of tartrazine released from the inner water phase of DE1 and DE3 was compared to the negative controls (DE2 and DE4, respectively). The measurements were taken at day 0, 8, 15, 29, 43, 57 and 78 for all the four emulsions. At each day of measurement, 1.50 grams of the double emulsions was dissolved in 50.00 grams of MQ water at 37°C by stirring (100 rpm) until the gelled emulsions were dissolved (approximately 10 min). Next, the samples were filtrated through two low protein binding filters, first a 1.2 µm-filter followed by a 0.2 µm-filter, to remove oil droplets. To avoid high oil concentrations, the dissolved samples were allowed to cream prior to filtration.

The measurements were performed using a Lambda 25 UV/VIS spectrophotometer at 435 nm, the known absorption maximum for tartrazine. The negative controls were used as references for 100 % tartrazine in outer phase, and the amount released from the inner to outer water phase was found by dividing the absorbance for the DE1 by DE2, and DE3 oby DE4.

Microscopic examination of double emulsions

The double emulsions used for the stability study were also examined by microscopy at the same days as the amounts of tartrazine were measured (day 0, 8, 15, 29, 43, 57 and 78). A Nikon Eclipse TS100 microscope was used, equipped with a camera (Nikon digital sight UBS (H) EXT. 1/0), and pictures were taken at a 400x magnification. The camera was connected to a computer and the software NIS-Element F 3.0 was used to edit the images.

In vitro lipid digestion of double emulsions

Double emulsions with gelatin 226g Bloom, type B, containing tartrazine as marker, were prepared as described above, following *method II*. The emulsions were subjected to *in vitro* lipolysis experiments to simulate the digestion in the small intestine. Several *in vitro* lipolysis models are described in the literature and Larsen and co-workers (2011) review those most commonly used in studies of lipid- and surfactant-based drug delivery systems. One of the methods described in the review, “Monash” (Cuine *et al.*, 2008, Kaukonen *et al.*, 2004a, Kaukonen *et al.*, 2004b), was used as a basis for the method in this study.

Intestinal Digestion Fluid was prepared by dissolving the ingredients given in table 2.2.8.6 in MQ water. The pH was adjusted to approximately 7 by addition of NaOH (1 M).

Table 2.2.8.6. Intestinal digestion fluid.

Product	Concentration (mM)
<i>Trizma® maleate</i>	50
<i>Bile extract porcine</i>	10
<i>Lecithin</i>	2.5
CaCl ₂ x 2 H ₂ O	5
Sodium chloride	150

Concentrated Pancreatic Lipase solution was made by dissolving 2.5 g porcine pancreatic lipase in 12.5 g intestinal digestion fluid, while stirring for 15 min at approximately 300 rpm, followed by centrifugation at 4000 rpm and 5°C for 15 min. The supernatant was collected and stored on ice until use.

DE1 and DE2 (1.50 g) were dissolved in Intestinal Digestion Fluid (45.0 mL) for 10 minutes at 37°C while stirred at 100 rpm. After 10 minutes the double emulsions were completely dissolved and concentrated pancreatic solution (4.5 mL) was added to each dissolved emulsion solution. The study was conducted two times, to obtain two independent replicates. Table 2.2.8.7 presents the sampling times for the two studies.

Table 2.2.8.7. Sampling times (min) for the two replications of in vitro lipolysis of double emulsions.

Replicate	Sampling times (min)
1	10 ¹ , 15, 20, 25, 30, 40 and 50
2	10 ² , 10 ¹ , 13, 16, 19, 25, 30 and 40

¹Immediately after addition of lipases

²Just prior to lipase addition

Samples were extracted according to table 2.2.8.7 and added directly to centrifugation tubes containing 0.5 mL HCl (2 M) to immediately stop the reaction. The tubes were centrifuged at 4000 rpm and 20°C for 10 min. The supernatant was collected and filtrated using 1.0 µm and 0.1 µm filters. The samples were analyzed on a Lambda 25 UV/VIS spectrophotometer at 435 nm. The negative control (DE2) was used as reference for 100 % tartrazine in the outer phase, and the amount of released tartrazine was determined by dividing the absorbance value obtained for the DE1 by DE2.

The method used for inhibition of the lipolysis reaction differs from the Monach-method reviewed by Larsen *et al.* (2011). It was chosen to stop the reaction by lowering the pH to approximately 1 by addition of HCl. This is far from the pH in the small intestine (6-7.5) and it was presumed that the reduction in pH would cause immediate inactivation of the lipases, thereby stopping the reaction. The HCl additionally causes the bile acids to precipitate, which simplified the centrifugation and filtration steps.

3. RESULTS AND DISCUSSION

3.1 SEC-MALLS

Size Exclusion Chromatography – Multi-Angle Laser Light Scattering (SEC-MALLS) analysis was performed for 160g Bloom gelatin type A and B, to determine the molecular weights and the molecular weight distributions of the two gelatins used in all studies of the Concordix matrices.

The molecular weight distribution of 160g Bloom gelatin, type A and B is presented in figure 3.1. The concentration ($\mu\text{g/mL}$) is plotted against the molecular weight (kg/mol) and the values of M_w , M_n and PI are given in table 3.1. Appendix B provides the summary reports obtained from Astra and the raw data are found on the attached CD.

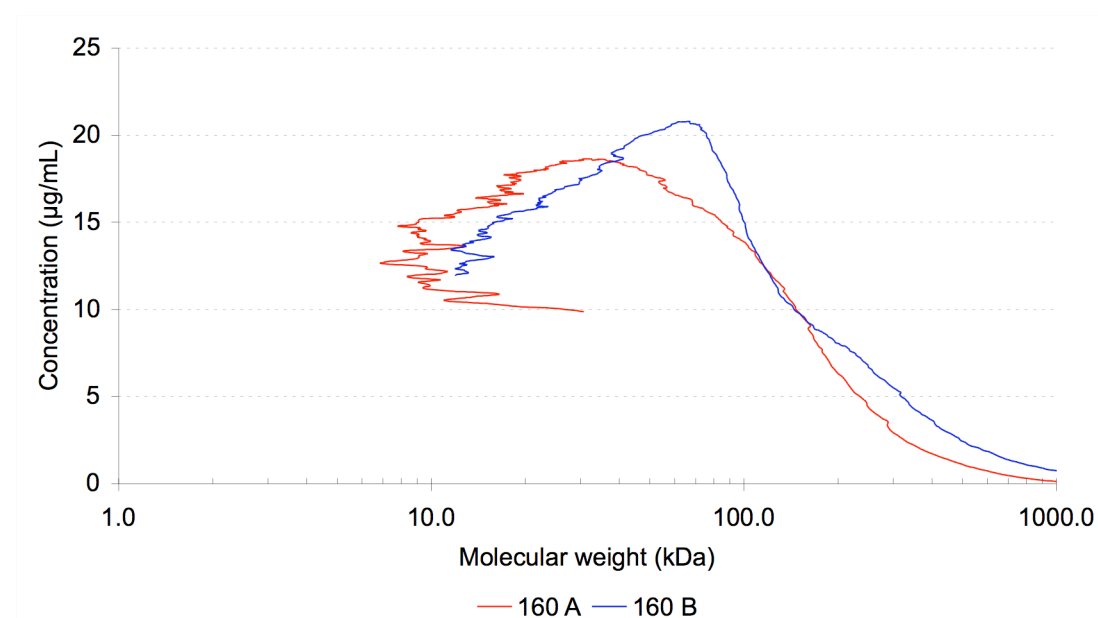


Figure 3.1. Molecular weight distribution for gelatin 160g Bloom, type A and B, with concentration ($\mu\text{g/mL}$) as function of molecular weight (kDa). The data were obtained from SEC-MALLS analyses of the two gelatins.

Table 3.1. M_w , M_n and PI obtained from SEC-MALLS for 160g Bloom gelatin, type A and B.

Gelatin 160g Bloom	M_w (kDa)	M_n (kDa)	PI
A	68 900	27 390	2.515
B	153 700	39 160	3.925

Figure 3.1 shows a broad molecular weight distribution, both for type A and B gelatin. Table 3.1 shows that type B has a higher weight average molecular weight than type A gelatin, and also a higher polydispersity index, which was also seen from the graph; the type B curve has a bigger shoulder of chain aggregates compared to type A. The molecular weight distribution is determined by the type and intensity of the hydrolysis process used during partially hydrolysis of the parent collagen to obtain gelatin (Schrieber and Gareis, 2007). The broad distribution observed is therefore due to the manufacturing procedure of the gelatins. Hydrolysis of α -chains results in sub- α chains, while covalently linked α -chains gives chains above 100 kDa. The figure showed a characteristic peak for the type B gelatin at 100 kDa, which is the size of one α -chain. There was also seen a peak at 200 kDa, representing the β -chains. For the type A gelatin a peak was observed at approximately 30 kDa, in the sub- α region. Shoulders representing γ -chains and other gelatin aggregates were seen in the curves for both gelatin types.

For type B gelatin, a major part of the molecular weight fraction usually corresponds to the size of the α -chain, while the type A gelatin does not have a pronounced peak for α -chains, but rather a broader weight distribution (Schrieber and Gareis, 2007). Figure 3.1 fits well with the literature in regards to the α -chain peak, which was only observed for type B. The two curves showed equivalent widths, indicating a similar molecular weight distribution.

3.2 Droplet size determination of Concordix matrices

Concordix matrices with varying amounts of corn oil (10, 30 and 50 wt %) and 160g Bloom gelatin, either type A or B, were dissolved in MQ water and analyzed using a Mastersizer 3000 to determine the droplet sizes of the dispersed oil droplets. The results are presented in figure 3.2. The analysis reports obtained from the Mastersizer software are provided in appendix C. Raw data files are found one the attached CD.

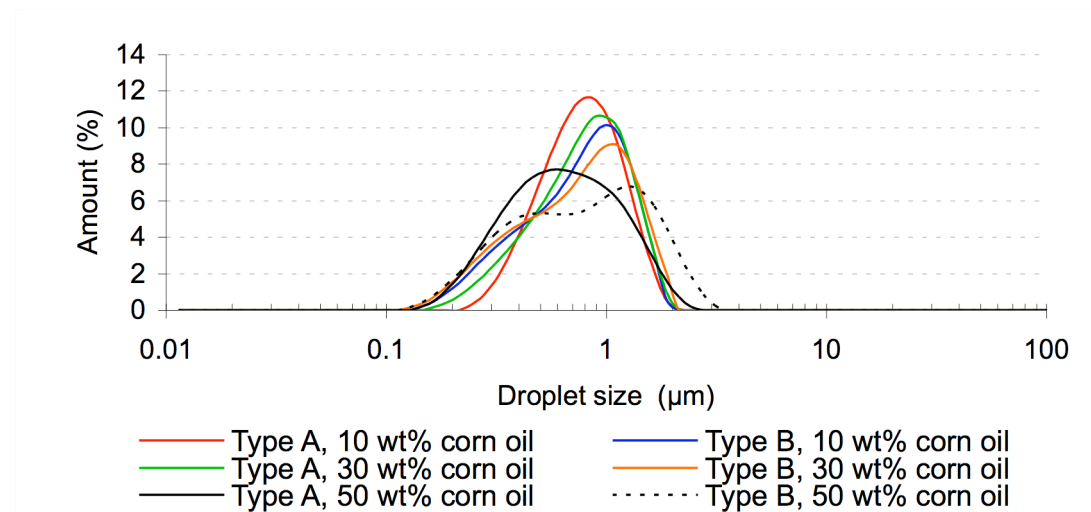


Figure 3.2. Amount (%) of each droplet size (diameter) fraction of the dispersed oil droplets in Concordix matrices with 160g Bloom gelatin (type A or B), and various amounts of corn oil (10, 30 and 50 wt %).

From the results shown in figure 3.2, there was seen a droplet size peak at approximately 1 μm for the Concordix matrices with 10 and 30 wt % corn oil, for both type A and B gelatins. The distribution of the CCx matrix with 50 wt % oil and type A gelatin showed a slight shift to the left, with a peak at approximately 0.6 μm. Two peaks were observed for the CCx matrix with 50 wt % oil and type B gelatin, at approximately 0.5 and 1.5 μm. The relatively small difference in the measured droplet diameters may have been due to the high-velocity homogenization procedure during matrix manufacturing (section 2.2.2), which is likely to give similar droplet sizes regardless of the amount of oil and gelatin type.

The volume weighted mean diameter (μm) together with the width of distribution for each matrix type is given in table 3.2.

Table 3.2. Volume weighted mean diameter ($D[3.2]$, μm) and width of distribution (span) for the dispersed oil droplets in Concordix matrices with 160g Bloom gelatin (type A or B), and different amounts of corn oil (10, 30 and 50 wt %). The data are based on an average result, automatically calculated from 5 replicates by the Malvern software. Raw data for each replicate are provided on the attached CD. The standard deviations were negligible and were not included in the table.

Sample	10 wt %	10 wt %	30 wt %	30 wt %	50 wt %	50 wt %
	Type A	Type B	Type A	Type B	Type A	Type B
D[3.2] (μm)	0.742	0.642	0.707	0.616	0.570	0.619
Span	1.100	1.325	1.217	1.470	1.680	1.925

The span provides information on the polydispersity of the sample. A broad span indicates a polydisperse size distribution of the oil droplets. Table 3.2 shows a broader size distribution, represented by span, for type B gelatin matrices compared to type A, regardless of oil content. A broader size distribution was also obtained with increased amounts of oil. The volume weighted mean droplet diameter was similar for all the matrix types, ranging from 0.570-0.742 μm , and the observed trend was a slight decrease in volume with increasing oil content, except for type B, which showed approximately the same volume when containing 30 or 50 wt % oil.

An increased viscosity was observed for the CCx matrices with high oil content (the viscosity results are presented in the next section; 3.3). A higher viscosity gave reduced mobility of the oil droplets, which made it difficult to evenly mix the emulsions during preparation, and may thus have contributed to a less homogeneous droplet size distribution for matrices with 50 wt % oil. This may also explain the two peaks observed for the CCx matrices with type B gelatin and 50 wt % oil.

3.3 Viscosity measurements of Concordix matrices

The shear viscosity of the Concordix matrices with 160g Bloom gelatin (either type A or B) containing varying amounts of corn oil (0, 10, 30 and 50 wt %) was measured in a rheometer (StressTech) with increasing shear (0.6-100 1/s) at 60°C. Raw data related to this section are provided in appendix D.

Figure 3.3.1 compares the viscosity of the various Concordix matrices at shear rate of 10 1/s.

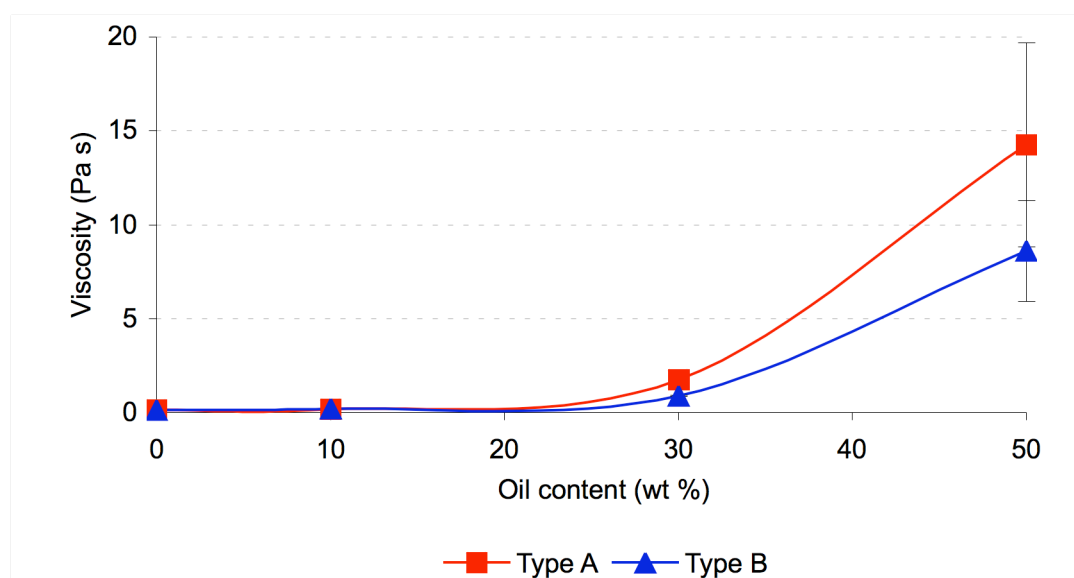


Figure 3.3.1. The viscosity (Pa s) for Concordix matrices with 160g Bloom gelatin, type A and B, and different amounts of corn oil (0, 10, 30 or 50 wt %) at shear rate of 10 1/s and 60°C ($N=3$, average \pm S.D.).

Figure 3.3.1 shows that the viscosity clearly increased with increasing oil content, in both type A and B matrices, but a larger increase was observed for type A. The observed viscosity increase upon oil addition was in accordance with experiments described in the literature, which also found that oil addition to the continuous phase of emulsions will increase overall emulsion viscosity (van Aken *et al.*, 2011). The increase in viscosity is due to the dissipation of energy in the presence of oil droplets, which increases with the fraction of the dispersed phase (McClements, 2005).

Figures 3.3.2 and 3.3.3 show viscosity as a function of increasing shear rate (from 0.6 to 100 1/s) for Concordix matrices with gelatin type A and B, respectively.

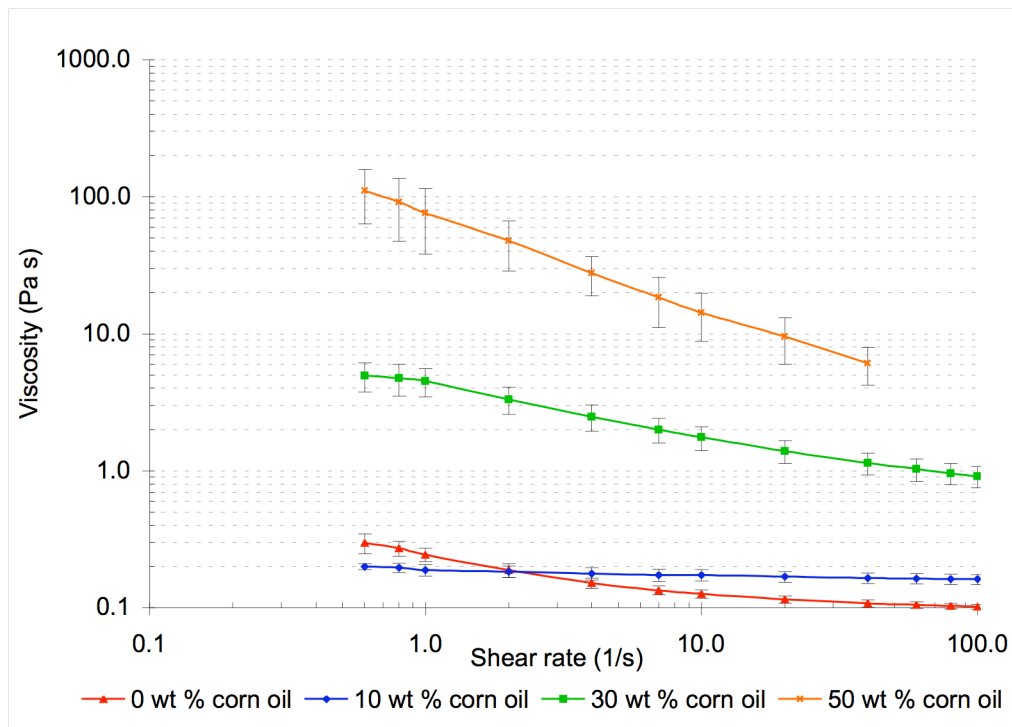


Figure 3.3.2. The viscosity (Pa s) as a function of shear rate (1/s) for the CCx matrices containing 0, 10, 30 or 50 wt % corn oil and 160g Bloom gelatin, type A. Measurements were performed at 60°C (N=3, average \pm S.D.). Raw data are found in appendix D1.

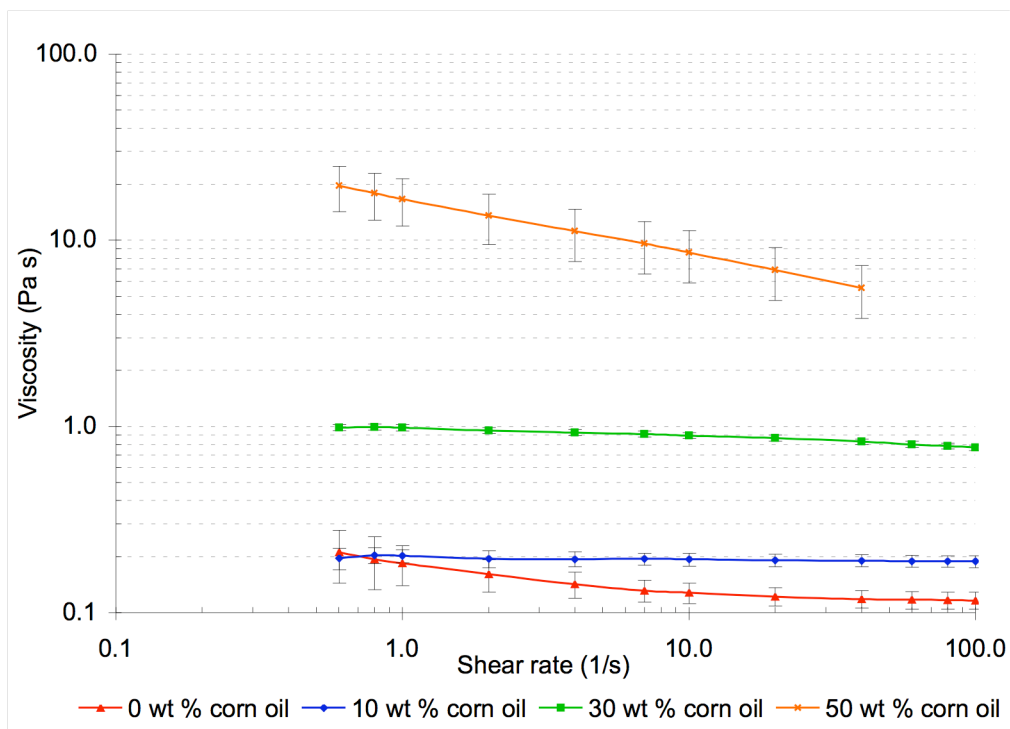


Figure 3.3.3. The viscosity (Pa s) as a function of shear rate (1/s) for the CCx matrices containing 0, 10, 30 or 50 wt % corn oil and 160g Bloom gelatin, type B. Measurements were performed at 60°C (N=3, average \pm S.D.). Raw data are found in appendix D1.

Figures 3.3.2 and 3.3.3 show almost Newtonian behavior of matrices containing 10 wt % oil. For matrices without oil a slight shear thinning behavior was observed. This was an unexpected result: It was expected that the systems without oil would behave more like Newtonian fluids, and that the systems would become more shear thinning upon oil addition, as emulsions are known to exhibit shear thinning behavior when the concentration of the dispersed phase increases (Pal, 2000). When the oil content was increased above 10 wt %, a shear thinning behavior was observed for both type A and B gelatin matrices, but the effect was more pronounced for type A. For instance for matrices containing 50 wt % oil, the viscosity decreased from approximately 110 to 6 Pa s and from 20 to 5 Pa s for type A and B gelatin, respectively.

For matrices with 50 wt % oil, it is likely that the oil droplets were densely packed. Upon shear, they will elongate with the field and disrupt (McClements, 2005). The shear thinning effect was observed already at 30 wt % oil, and to a greater extent for type A gelatin matrices compared to type B. This may have indicated flocculation between the droplets, which dispersed as the shear rate increased. Shear thinning behavior is often seen in flocculated emulsions, as mentioned in the introduction. Since the shear thinning was more pronounced for type A gelatin matrices than type B, it indicated that the gelatin was interacting with the oil in some way that caused flocculation.

Electrostatic interactions

Droplet interactions are strongly affected by the nature of the adsorbed polymer on the droplet surfaces and droplet aggregation may occur due to electrostatic polymer interactions (Norde, 2003). One hypothesis was that the observed shear thinning behavior of the CCx matrices was due to flocculation caused by electrostatic interactions between gelatin molecules at the droplet interfaces. To test the hypothesis different CCx systems with 30 wt % oil were made, two containing 250 mM NaCl (type A and B gelatin), and the others were adjusted to obtain pH of approximately 7.5 (type A and B gelatin) and 8.5 (type A and B gelatin) by addition of NaOH and trizma buffer, respectively (the pH of the original Concordix matrices with 30 wt % oil was 4.5 and 4.2 for type A and B gelatin, respectively). The attempt was to see if the salt and/or change in pH would screen the charges, and thereby reduce the attraction between the droplets, leading to dispersion instead of flocculation.

Figures 3.3.4 and 3.3.5 present the viscosity as a function of shear rate for the Concordix matrices with 250 mM NaCl and pH of 7.5 and 8.5, stabilized by gelatin type A and B, respectively.

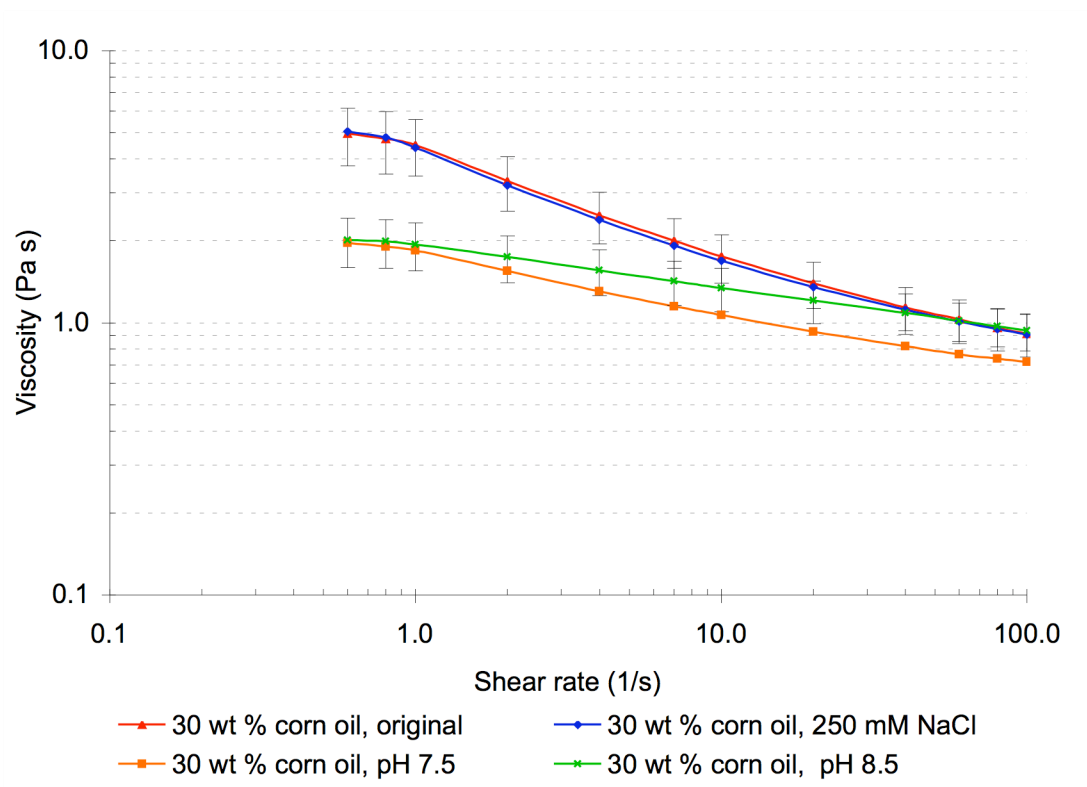


Figure 3.3.4. The viscosity (Pa s) as a function of shear rate (1/s) for the CCx matrices containing 30 wt % corn oil. The original matrix (N=3, average \pm S.D.) was compared to the same matrices with addition of 250 mM NaCl (N=1) or with increased pH to 7.5 (N=2, average) or 8.5 (N=3, average \pm S.D.). All the systems contained 160g Bloom gelatin type A, and the measurements were performed at 60°C. Raw data are found in appendix D2.

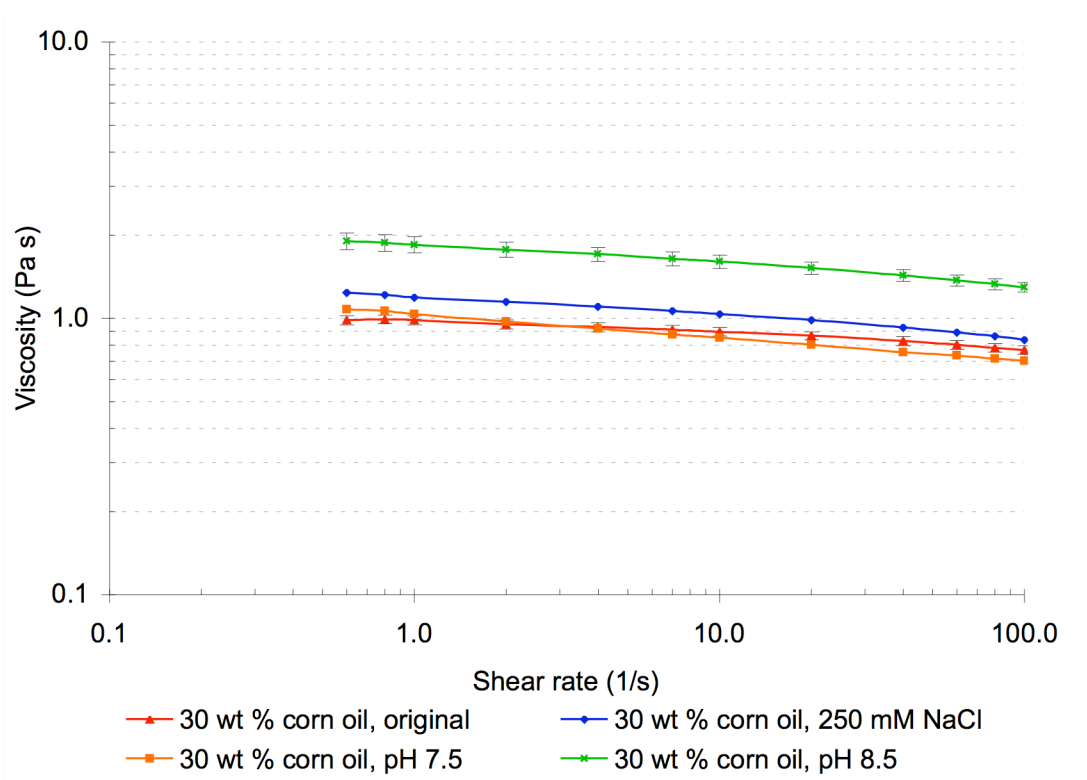


Figure 3.3.5. The viscosity (Pa s) as a function of shear rate (1/s) for the CCx matrices containing 30 wt % corn oil. The original matrix ($N=3$, average \pm S.D.) was compared to the same matrix with addition of 250 mM NaCl ($N=1$) or with increased pH to 7.5 ($N=2$, average) or 8.5 ($N=3$, average \pm S.D.). All the systems contained 160g Bloom gelatin type B, and the measurements were performed at 60°C. Raw data are found in appendix D2.

No effect on the shear thinning behavior was observed from figures 3.3.4 and 3.3.5 upon addition of 250 mM NaCl to the Concordix matrices, and it was therefore unlikely that the flocculation was caused by electrostatic interactions. A slight increase in viscosity for the matrix with type B gelatin was observed when salt was added, compared to the original matrix, although the shear thinning behavior did not change. It is known from the literature that addition of 0.1 M NaCl is sufficient to effectively screen electrostatic interactions (Vu *et al.*, 2001, Lootens *et al.*, 2003) so the addition of 250 mM NaCl should thus ensure complete screening.

The increase in pH gave a decrease in the shear thinning behavior of matrices with gelatin A, compared to the original matrix (figure 3.3.4). The shear thinning behavior of gelatin B matrices was not affected much, although the increase in pH to 8.5 seemed to increase the overall viscosity of the type B gelatin matrix (figure 3.3.5). The pH of the original Concordix matrices were, as previously mentioned, 4.5 and 4.2 for type A and B gelatin, respectively. For the matrix with gelatin B, the pH was almost in the range of the isoelectric point of type B gelatin, but for the type A gelatin matrix, the pH was far away from the IEP. By increasing the pH to 7.5 and 8.5, a pH in the range of the IEP of gelatin A was obtained. Since electrostatic interactions already were excluded, the differences in the viscosity and shear thinning behavior for

matrices stabilized by type A and B gelatin had to be explained by other variations between the two gelatin types.

SEC-MALLS analysis (section 3.1) found that type B gelatin had a higher molecular weight average than type A gelatin, and also a higher degree of high molecular weight aggregates. It was predicted that an increased amount of high molecular weight fractions would increase the viscosity, so the molecular weight difference between gelatin type A and B did not correlate to the rheological behavior observed. Droplet size determination (section 3.2) did not show any significant difference between type A and B gelatin, and could not explain the different viscosity behaviors.

The remaining difference between type A and B gelatins is their different isoelectric point. The IEP of type B gelatin (pH 4.8-5.5) is lower than for type A gelatin (pH 7-9.4), because of the alkaline pre-treatment of type B, which converts asparagine and glutamine into their carboxyl forms. One hypothesis was that the lack of asparagines and glutamines in type B gelatin could explain the different rheological properties of type A and B gelatin matrices. Both asparagines and glutamines have weak polar side chains consisting of a non-ionizable amide group, which can both accept and donate hydrogen bonds (Weichenberger and Sippl, 2006, Haug and Draget, 2009). The amide group of asparagine can form efficient hydrogen bonds with peptide backbones. Glutamine does not have this ability, because of its extra methylene group, which increases the conformational entropy (Wishart, 2012). Although asparagines only constitute for approximately 2 % of the gelatin, (Rose, 1987), it is possible that hydrogen bonding between asparagines and the gelatin protein backbone facilitates flocculation between adjacent oil droplets. One suggestion is that the observed variation in shear thinning behavior of Concordix matrices stabilized by type A and B gelatin was due to a stronger initial flocculation of type A, caused by asparagines, which disrupted as the shear rate increased.

Unpublished data by Dalbakk (2012), did not show a similar shear thinning behavior for emulsion matrices stabilized by 200g Bloom gelatin type A without sugar alcohols. An increased protein-protein interaction and flocculation of protein stabilized emulsions upon sugar addition is also reported in the literature (van Aken, 2006). This may indicate that asparagines facilitate protein interactions to a higher degree in the presence of sugar alcohols, which may cause a dependency on the shear thinning behavior on the addition of sugar alcohols to the emulsion.

Non-Newtonian viscosity

Non-Newtonian materials can have both time dependent and independent viscosity. Viscosity sweeps were performed in order to examine the viscosity properties of Concordix matrices containing 30 wt % corn oil, with 160g Bloom gelatin, type A and B. The matrices were subjected to increasing shear rates (from 0.6 1/s to 60 1/s) followed by a rate decrease in opposite direction. The results from these experiments are presented in figure 3.3.6.

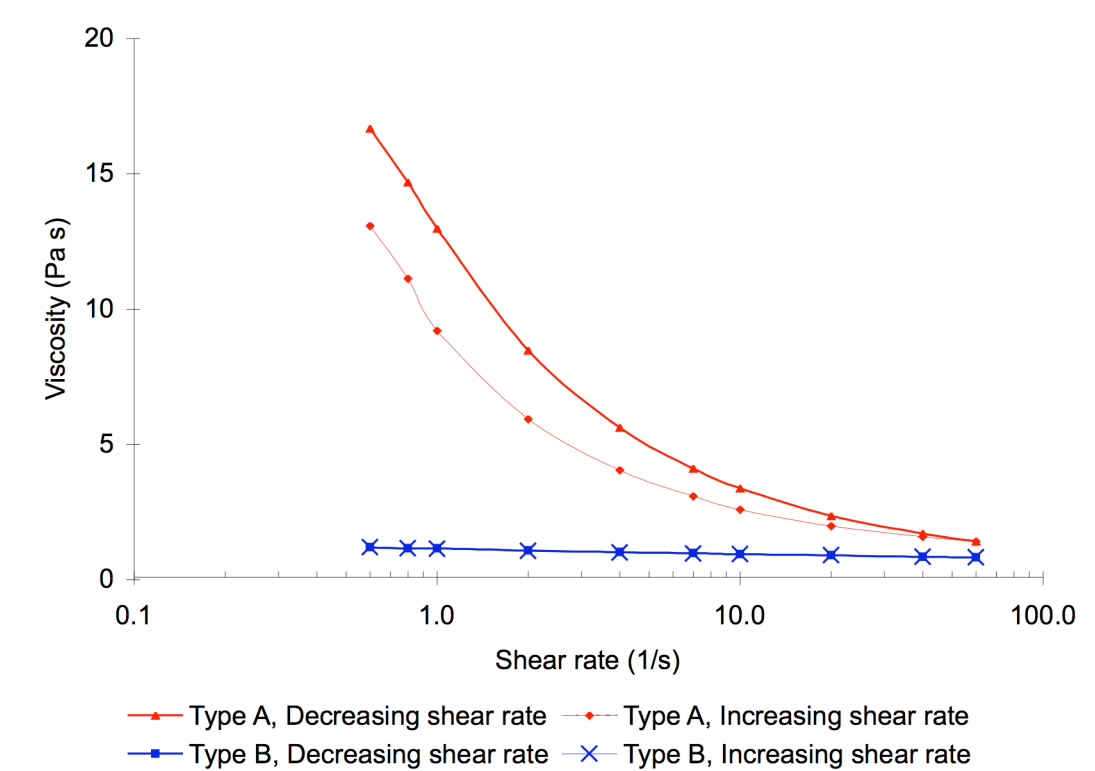


Figure 3.3.6. The viscosity (Pa s) as a function of shear rate (1/s) for the CCx matrices containing 30 wt % corn oil and 160g Bloom gelatin, type A and B ($N=2$, average). Raw data are presented in appendix D3.

Figure 3.3.6 shows an almost Newtonian behavior for the Concordix matrix stabilized by type B gelatin. There was, however, seen a slight shear thinning behavior, as the curve showed a weak decrease in viscosity upon increased shear rate. The matrix resumed its initial viscosity value upon reversed shear rate. Hence, the viscosity of the CCx matrix with type B gelatin was dependent on shear rate, and seemed to slightly exhibit pseudoplastic properties. The viscosity was not time dependent.

The type A matrix did exceed its original viscosity when the shear rate was decreased back to the initial rate, indicating a time dependent behavior. Although, the lower initial viscosity may have been due to the pre shear with rate of 2 1/s performed just prior to the first measurement. Some structure breakdown may already have occurred, and measurement taken at shear rates below 2 1/s may thus have been incorrect. To further investigate if the type A matrix has time dependent viscosity, the experiment was repeated by performing the same shear sweep twice, with a 15 minutes break in between the two sweeps, to allow structure regeneration. The result is presented in figure 3.3.7.

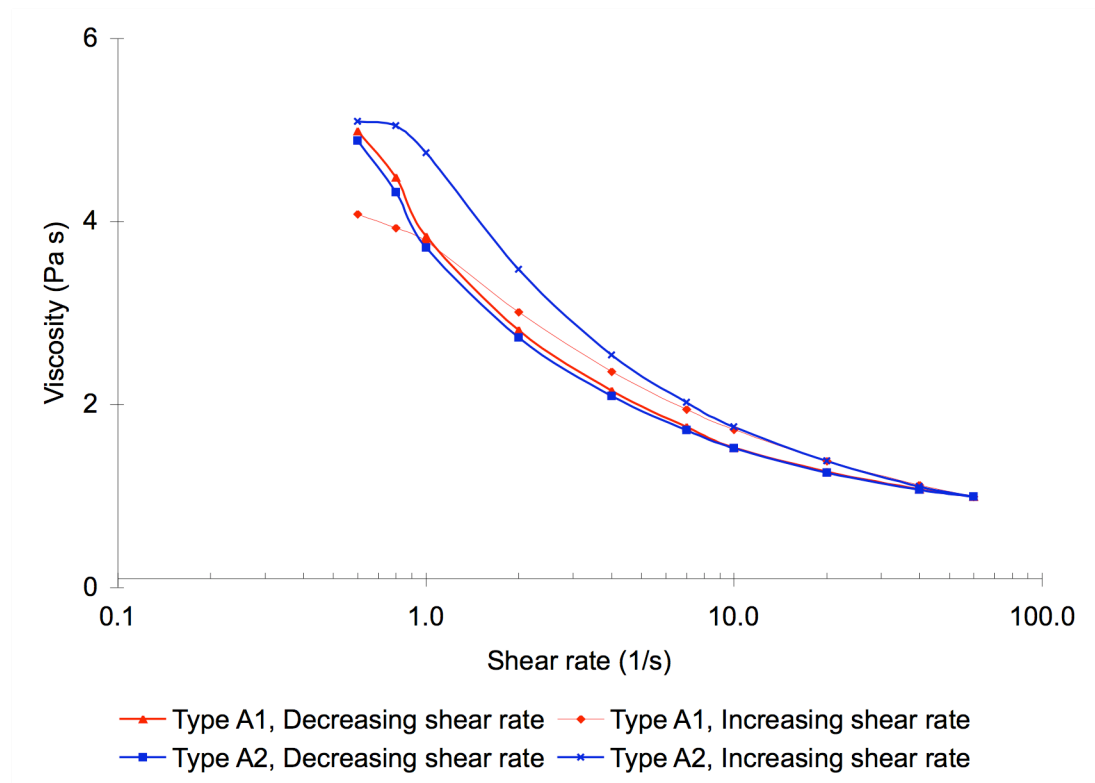


Figure 3.3.7. The viscosity (Pa s) as a function of shear rate (1/s) for the CCx matrices containing 30 wt % corn oil and 160g Bloom gelatin, type A and B (N=1). A1 and A2 are the same sample, but correspond to shear rate sweep number 1 and 2, respectively. A break time of 15 min was applied before the second shear rate sweep was performed. Raw data are found in appendix D3, table D3.3.

Figure 3.3.7 shows that structure breakdown occurred upon increasing shear, and that the structure was resumed when the shear rate was reversed. However, the structure was not completely resumed as the rate of structure breakdown exceeded the rate of structure reformation. The figure also shows that some structure reinforcement occurred during the break, as there was seen a slight increase in viscosity between the last measurement for sweep 1 and the first measurement of sweep 2. This result indicated that the type A gelatin matrix exhibited time dependent viscosity, with time dependent structure reinforcement after structure breakdown, which indicated that it was a thixotropic material.

A low initial viscosity was observed for the first sweep, compared to the other measurements at the same rate (0.6 1/s). This was likely due to the pre shear rate of 2 1/s performed prior to measurements. The first measurement was taken immediately after the pre shear, and since the pre shear rate exceeded the rate of the first measurement, some structure breakdown may already have occurred, as discussed previously. It is therefore possible that the thixotropic behavior observed from figure 3.3.7 was deceptive, and that the observed behavior was due to structure breakdown prior to measurement. For further studies it is highly recommended to use the same pre shear rate as the first measure point, to avoid this uncertainty.

The viscosity at high shear rate was approximately 1 Pa s for type A gelatin matrices in both figures 3.3.6 and 3.3.7, indicating that a complete structure breakdown had occurred at 60 1/s. However, the initial viscosity varied between the two independent experiments. An initial viscosity of 13 and 4 Pa 1/s was observed for type A gelatin matrices in figures 3.3.6 and 3.3.7, respectively. Although the Concordix matrices are supposed to have a homogeneous distribution of oil droplets in the continuous phase, this is rarely entirely achieved due to for instance, emulsion destabilizations such as flocculation or insufficient homogenization of the two phases during matrix preparation. Thus variation between the samples may have caused the observed variations in initial viscosity. Although the result indicated that type A gelatin matrices undergo structural reinforcement with time, there are still many unknown parameters, such as the time needed for reinforcement to occur. In addition storage conditions such as temperature and the number of melting and gelling cycles, may influence the matrix structure. To obtain a complete understanding of the viscosity, it is important to keep time and other kinetic parameters constant between independent experiments.

3.4 Rheological characterization of Concordix matrices

3.4.1 Small strain oscillatory measurements of Concordix matrices

In addition to the viscosity measurements, rheological data were also obtained by small strain oscillating measurements of the Concordix matrices with 160g Bloom gelatin (either type A or B) and different amounts of corn oil (0, 10, 30 and 50 wt %). The measurements were performed using a rheometer (StressTech), and the storage modulus (G'), gelling temperature (T_g) and melting temperature (T_m) were determined, giving information about the elastic properties of the matrices.

Statistical analyses were performed with Minitab 16 on the results obtained, by a two-sample t-test comparison of the values for G' , T_g and T_m for the different Concordix matrices. The p-values are presented in appendix J1.

Effect of oil content on the storage modulus of Concordix matrices

The storage modulus is presented in figure 3.4.1.1 Information on calculations and raw data are found in appendix E1.

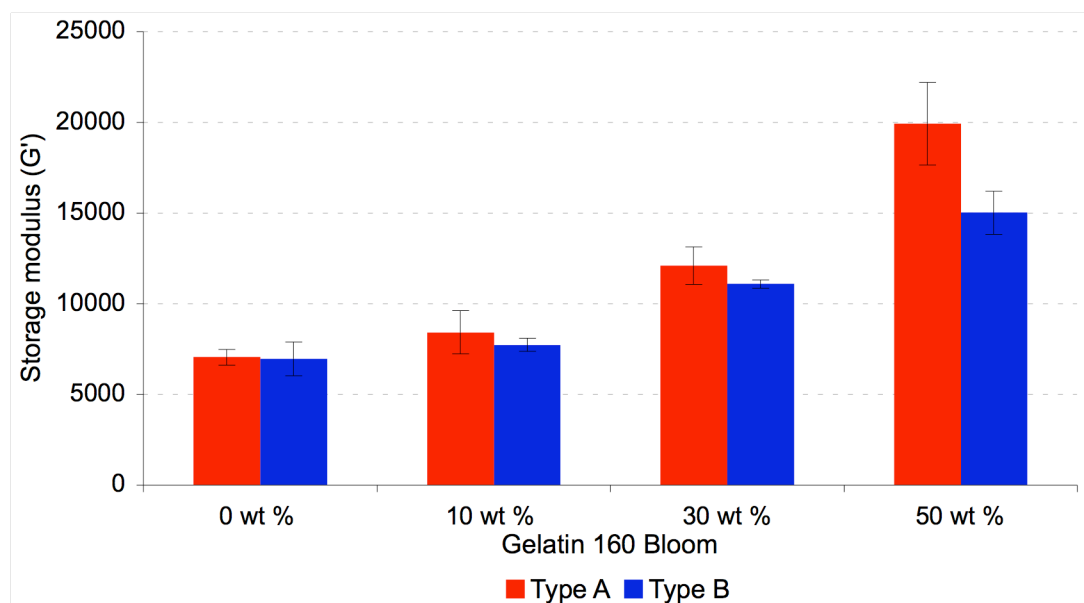


Figure 3.4.1.1. Storage modulus (G') for Concordix matrices containing 0, 10, 30 or 50 wt % corn oil and 160g Bloom gelatin, type A and B ($N=6$, average \pm S.D.).

An increase in storage modulus was observed with increased oil content for both type A and B gelatin matrices. For type A matrices there was found a significant increase in G' ($p < 0.05$) when oil was added to the matrix, for all three oil contents (appendix J1, table J.1). For type B matrices the increase was significant at oil content of 30 and 50 wt %. This result was in accordance with previous studies performed on Concordix matrices with 260g Bloom gelatin: An increased G' with increasing oil content was obtained, with a higher value of G' for type A gelatin with high oil content (Wold, 2011).

Filler substances like oil droplets may affect the physical properties of filled gels (Matsumura *et al.*, 1993). A previous study by Matsumura and co-workers has shown that oil droplets may lead to increased gel strength. This effect can be explained by interactions between the oil droplets and the protein network, and depending of the nature of the interaction, will either weaken or enhance the gel strength. Oil droplets tend to increase the gel strength if the network protein can absorb to the oil-water interface, reinforcing the structure by attractive interactions between the oil droplets and the protein network (McClements *et al.*, 1993). Since gelatin is a network protein and has the ability to absorb to oil interfaces, it is likely that the oil droplets act as active fillers in the CCx matrices, causing increased gel strength as observed from figure 3.4.1.1.

From figure 3.4.1.1 it was also seen a trend of higher G' for type A gelatin matrices compared to type B gelatin at same oil contents, and there was a significant difference between the matrices with 50 wt% oil, as shown in table J.1, appendix J1.

The observed difference between matrices with gelatin type A and B may have been due to a higher degree of flocculation in type A, as discussed previously in section 3.3. Flocculation causes reinforcement of the gel structure and may therefore explain the increased gel strength observed for type A gelatin matrices.

Effect of oil content on gelling and melting temperatures of Concordix matrices

Gelling and melting temperatures are presented in figures 3.4.1.2 and 3.4.1.3, respectively. Calculations and raw data are found in appendix E2 and E3.

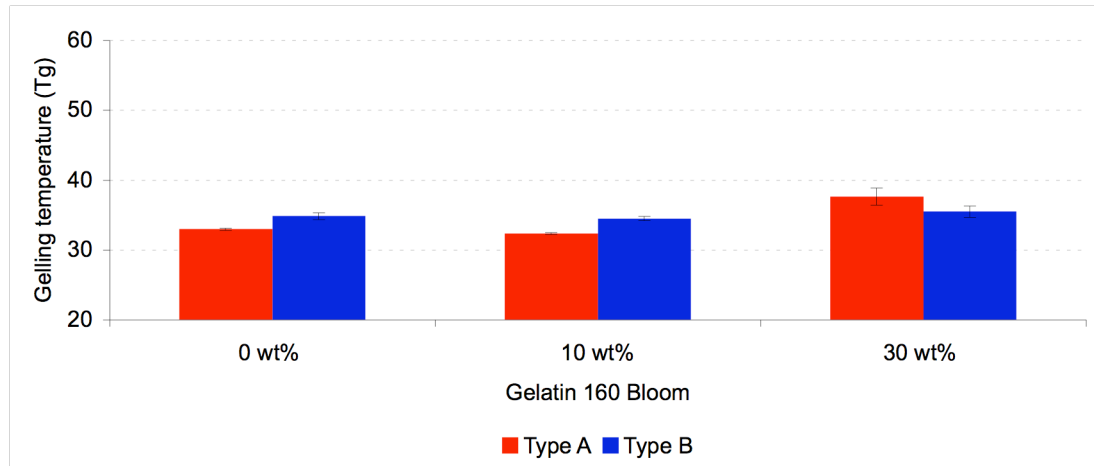


Figure 3.4.1.2. Gelling temperatures (T_g) for the CCx matrices containing 0, 10 or 30 wt % corn oil and 160g Bloom gelatin, type A and B ($N=6$, average \pm S.D.).

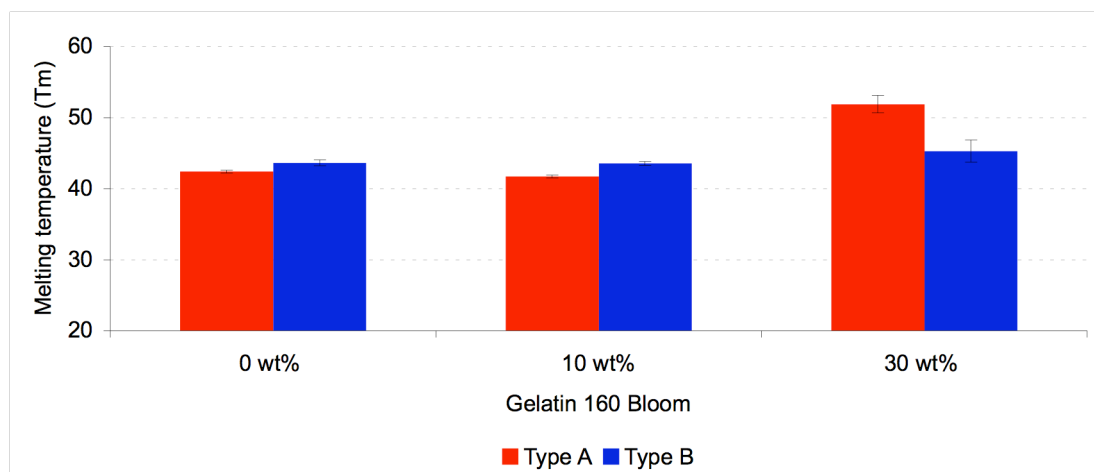


Figure 3.4.1.3. Melting temperatures (T_m) for the CCx matrices containing 0, 10 or 30 wt % corn oil and 160g Bloom gelatin, type A and B ($N=6$, average \pm S.D.).

The amount of oil did not seem to influence the gelling and melting temperatures to the same extents as the storage modulus. However, matrices with 30 wt % oil, stabilized by type A gelatin had a significantly increased temperature for both gelling and melting, as shown in appendix J1. This can be explained by the same two factors as discussed above for the storage modulus: Oil droplets acting as active fillers that reinforce the gel structure, and increased flocculation in type A gelatin matrices.

The gelling and melting temperature was not found for the CCx matrices containing 50 wt % corn oil due to the lack of a phase degree of 45°. The matrices were in a solid state at all temperatures (20-60°C) as the phase degree was constantly above 45°, which indicated a higher degree of structure in matrices with 50 wt % oil.

3.4.2 Longitudinal deformation of Concordix gels

Gelled Concordix matrices containing 0, 10 and 30 wt % corn oil and 160g Bloom gelatin, type A and B, were studied using a texture analyzer (TA.XT.-Plus Texture Analyser, Stable Micro System, Surrey, UK). The Concordix matrices containing 50 wt % corn oil were excluded due to their highly viscous nature that complicated the molding process. The matrices were prepared as described in methods, section 2.2.2, and the molding procedure is described in methods section 2.2.5. The parameters examined were Young's modulus (E), force at break (N) and strain at break (%). Appendix F provides additional information on the instrument settings, data and calculations.

Statistic analyses were performed with Minitab 16 on the obtained results, by a two-sample t-test comparison of the values for E and force and strain at break for the different Concordix gels. The p-values are presented in appendix J2.

Young's modulus

Figure 3.4.2.1 presents Young's modulus (E) for Concordix gels with 160g Bloom gelatin, type A and B, and different corn oil contents. The respective values of E (kPa), together with information about the Concordix gel, and number of replicates (N) are listed in table 3.4.2.1. Calculations are shown in appendix F (section F.3.1).

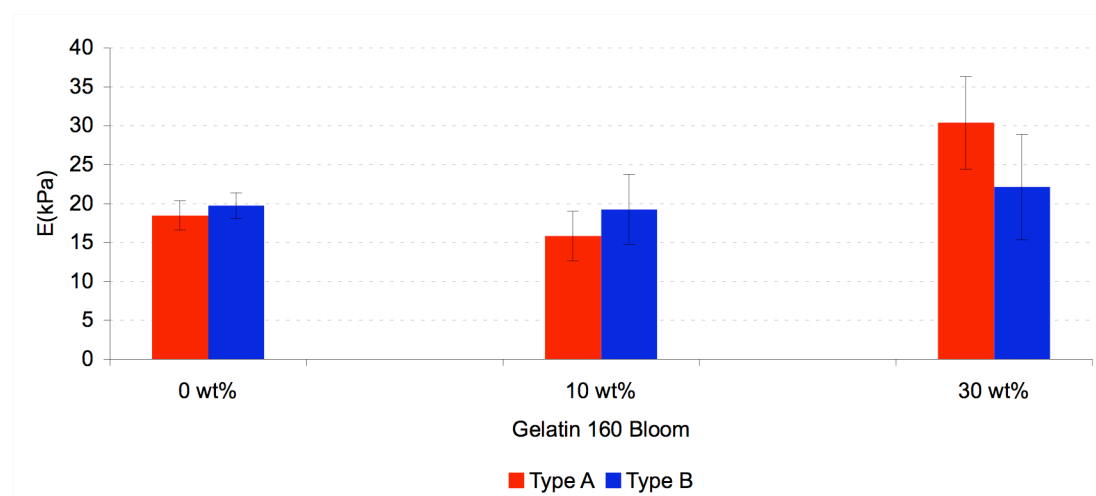


Figure 3.4.2.1. Young's modulus (E(kPa)) for the Concordix gels containing 0, 10 and 30 wt % corn oil and 160g Bloom gelatin type A and B (average \pm S.D.). The number of replicates is found in table 3.4.2.1.

Table 3.4.2.1. Young's modulus (E) for Concordix gels with 160g Bloom gelatin, type A and B and 0, 10 and 30 wt % corn oil (average \pm S.D. and number of replicates).

Gelatin Type	Oil content (wt %)	Average E (kPa)	\pm S.D.	N
A	0	18.5	1.9	4
A	10	15.9	3.2	8
A	30	30.4	5.9	8
B	0	19.7	1.7	7
B	10	19.3	4.5	7
B	30	22.1	6.8	8

Figure 3.4.2.1 and table 3.4.2.1 show a weak trend of increased Young's modulus upon oil addition, although similar values of E were seen for gels containing 0 and 10 wt % corn oil. For the CCx matrices containing 30 wt % corn oil, there was seen a pronounced increase of E, indicating that a higher oil content contributes to a more rigid gel. This increase was only significant for type A gels; shown in appendix J2, table J.4. The results correlated with the data obtained for G' for the same matrices, which showed a significant increase in storage modulus upon oil addition.

There is a correlation between Young's modulus and storage modulus. Ideally the value of E equals 3 times G' for an elastic material (Moe, 1992). The relation is found from the following equation: $E = 2(1+\mu)G$, where μ is the Poisson's ratio (the ratio of transverse to longitudinal strains). For elastic materials μ is approximately 0.5, giving $E=3G$. However, this ratio of 3 only applies for a homogeneous isotropic material (Markidou *et al.*, 2005, ASM-International, 2005). The value of G' and E for Concordix matrices with 160g Bloom gelatin, either type A or B, and various amounts of oil (0, 10 and 30 wt %), together with the ratio, is presented in table 3.4.2.2.

Table 3.4.2.2. The correlation between storage modulus and Young's modulus for Concordix matrices with 160g Bloom gelatin, type A and B, and various amounts of corn oil (0, 10 and 30 wt %).

Gel type (gelatin type and wt % oil)	Average G' (Pa)	Average E (Pa)	$\frac{E}{G'}$
A, 0 wt %	7061	18500	2.6
A 10 wt %	8427	15900	1.9
A 30 wt %	12113	30400	2.5
B 0 wt %	6957	19700	2.8
B 10 wt %	7735	19300	2.5
B 30 wt %	11097	22100	2.0

Table 3.4.2.2 shows that the value of E was in the range of 1.9 to 2.8 times the value of G' for the Concordix matrices investigated. This is slightly below the claimed value of 3, which may have been due to heterogeneous regions in the matrices. In addition, G' was measured by small oscillatory measurements while E was found by compression measurement. Differences in how force was applied may also have given variation of the Poisson's ratio for the two distinct measurement types, causing deviation from the ratio of 3.

Force at break

Force at break (N) for Concordix gels with 160g Bloom gelatin, A and B, and different corn oil contents (0, 10 and 30 wt %) is presented in figure 3.4.2.2. The respective values of N, together with information about the Concordix gel, and number of replicates are listed in table 3.4.2.3. Data are presented in appendix F4.

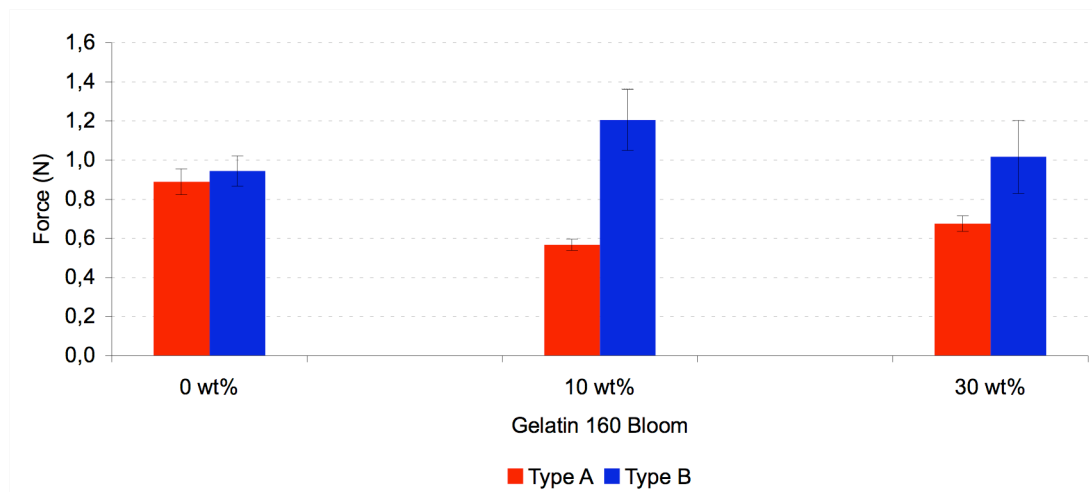


Figure 3.4.2.2. Force (N) at break for the Concordix gels containing 0, 10 and 30 wt % corn oil and 160g Bloom gelatin type A or B (\pm S.D.). The number of replicates is listed in table 3.4.2.3

Table 3.4.2.3 Force at break (N) for Concordix gels with 160g Bloom gelatin, type A and B and 0, 10 and 30 wt % corn oil (average \pm S.D. and number of replicates).

Gelatin Type	Oil content (wt %)	Average Force (N)	\pm S.D.	N
A	0	0.89	0.07	4
A	10	0.57	0.03	8
A	30	0.68	0.04	8
B	0	0.95	0.08	7
B	10	1.21	0.16	8
B	30	1.02	0.19	8

Figure 3.4.2.2 shows that break occur at a lower force in gels stabilized with type A gelatin, compared to type B, which was significant for gels with 10 and 30 wt % oil ($p < 0.05$), appendix J2, table J.5. Similar studies performed on Concordix gels stabilized by 260g Bloom gelatin showed a decrease in force at break when oil was added (Wold, 2011). This trend was not observed from figure 3.4.2.2. In the presented study, the gels were generally weaker, indicated by the lower Bloom value of 160g. This indicated that the variation in oil content has a lower impact on the force at break when the gel is initially weak.

Strain at break

Figure 3.4.2.3 shows the strain at break (%) for Concordix gels with 160g Bloom gelatin, type A and B, and different corn oil content (0, 10 and 30 wt %). The respective values of strain, together with information about the Concordix gel, and number of replications are listed in table 3.4.2.4. Calculations are provided in appendix F3.2.

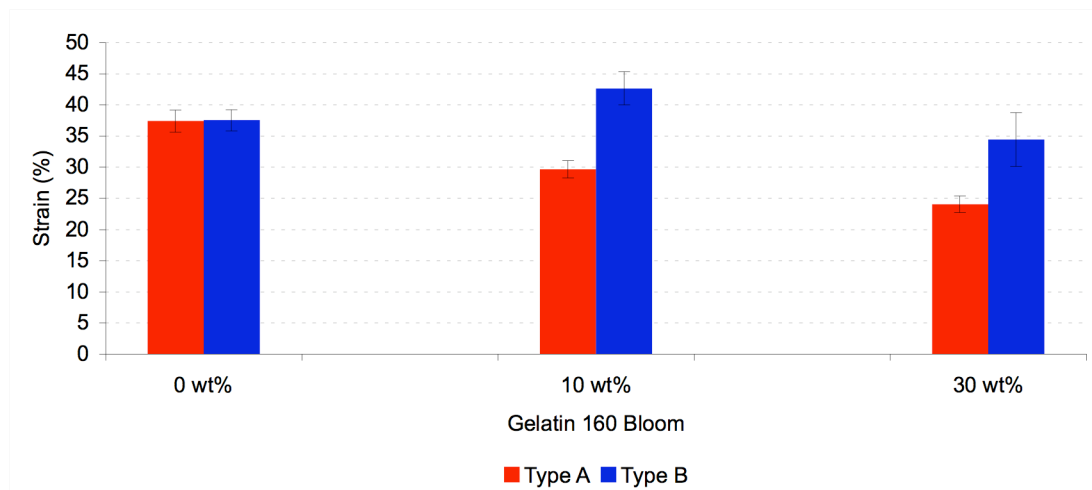


Figure 3.4.2.3. Strain (%) at break for the Concordix gels containing 0, 10 and 30 wt % corn oil and 160g Bloom gelatin type A or B (\pm S.D.). The number of replicates is listed in table 3.4.2.4.

Table 3.4.2.4. Strain at break (%) for Concordix gels with 160g Bloom gelatin, type A and B and 0, 10 and 30 wt % corn oil (average \pm S.D. and number of replicates).

Gelatin Type	Oil content (wt %)	Average Strain (%)	\pm S.D.	N
A	0	37.4	1.8	4
A	10	29.7	1.4	8
A	30	24.1	1.3	8
B	0	37.6	1.7	7
B	10	42.7	2.7	8
B	30	34.5	4.3	8

Figure 3.4.2.3 shows a lower strain at break for gels with type A gelatin, compared to type B gelatin, which was in accordance with the force (N) at break (figure 3.4.2.2). These results indicated that the stiffness of the Concordix gels with gelatin type B was higher than for gels with gelatin A.

For the gels with type A gelatin, figure 3.4.2.3 and table 3.4.2.4 showed that break was obtained at a significantly lower strain when corn oil was added to the gel, shown in appendix J2, table J.6. This result was also supported by the literature. Sala (2007) states that the fracture behavior of emulsion-filled gels is influenced by the oil content. Oil droplets acts as concentrated stress areas, resulting in decreased fracture strain, supporting the observed decrease in strain upon oil addition for gels with type A gelatin. No major trend was observed for type B gelatin gels. However, high standard deviations between the replicates conferred uncertainty to the results. The deviations may have been due to air bubbles at the gel surface, creating possible propagation zones and hence a lowering of the strain at break. In addition, elements of anisotropy in the gels could also have caused variations between the replicates.

3.5 *In vitro* dissolution study of Concordix matrices

In vitro dissolution studies were performed on Concordix matrices in simulated gastric fluid (0.1 M HCl). This was done in order to see if the gelatin type (A or B) and/or variation in the amount of corn oil (0, 10, 30 and 50 wt %) influenced the dissolution rate of the matrix. Acetaminophen was used as a marker to measure the dissolution rate, and it was assumed that the amount of acetaminophen released from the Concordix matrix corresponded to the dissolution of the matrix itself. The dissolution studies were performed as described in methods section 2.2.7. Raw data, standard curves and calculations are presented in appendix G.

Figures 3.5.1-3.5.4 show the dissolution profiles for the Concordix matrices with 160g Bloom gelatin (type A or B) and varying amounts of corn oil (0, 10, 30 and 50 wt%).

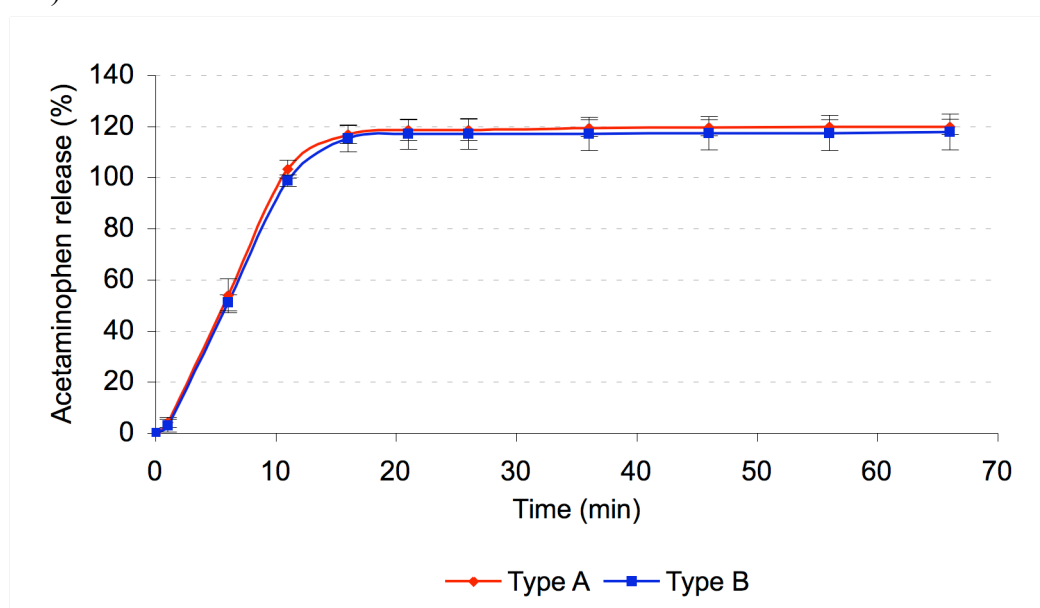


Figure 3.5.1. The amount of acetaminophen released as a function of time, measured by dissolution of CCx matrices containing 0 wt % corn oil and 160g Bloom gelatin, type A and B, in artificial gastric acid in a dissolution unit ($N=4$, average \pm S.D.). Calculations are shown in appendix G1.1.

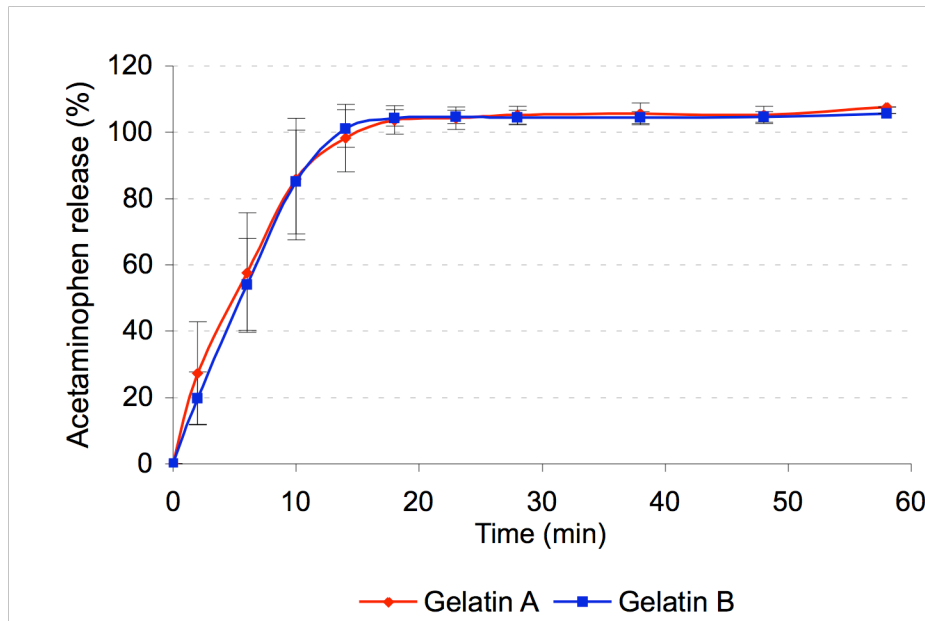


Figure 3.5.2. The amount of acetaminophen released as a function of time, measured by dissolution of CCx matrices containing 10 wt % corn oil and 160g Bloom gelatin, type A and B, in artificial gastric acid in a dissolution unit (N=4, average \pm S.D.). Calculations are shown in appendix G1.2.

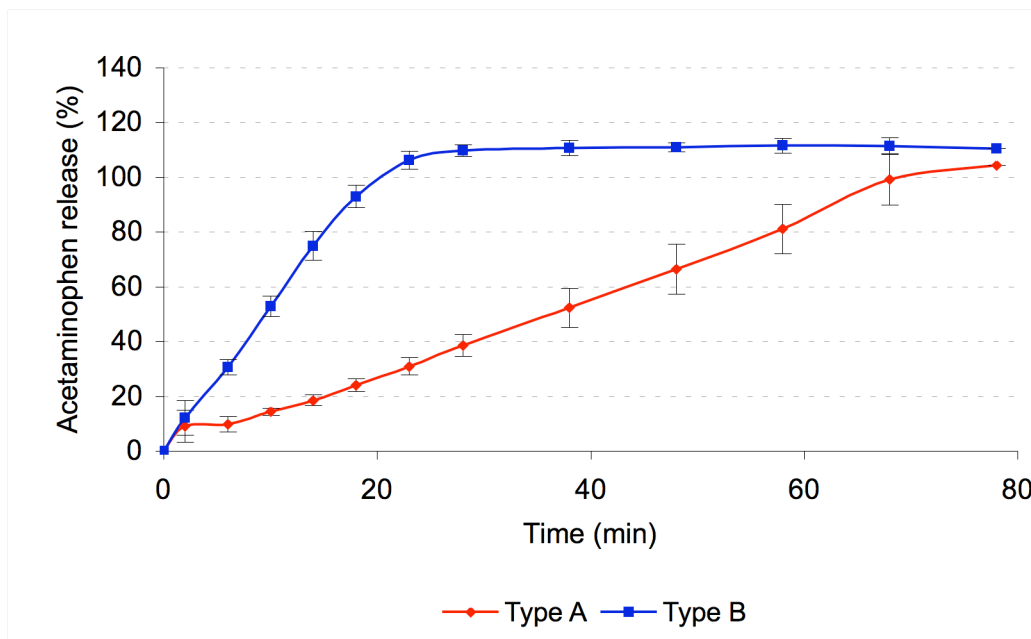


Figure 3.5.3. The amount of acetaminophen released as a function of time, measured by dissolution of CCx matrices containing 30 wt % corn oil and 160g Bloom gelatin, type A and B, in artificial gastric acid in a dissolution unit (N=4, average \pm S.D.). Calculations are shown in appendix G1.3.

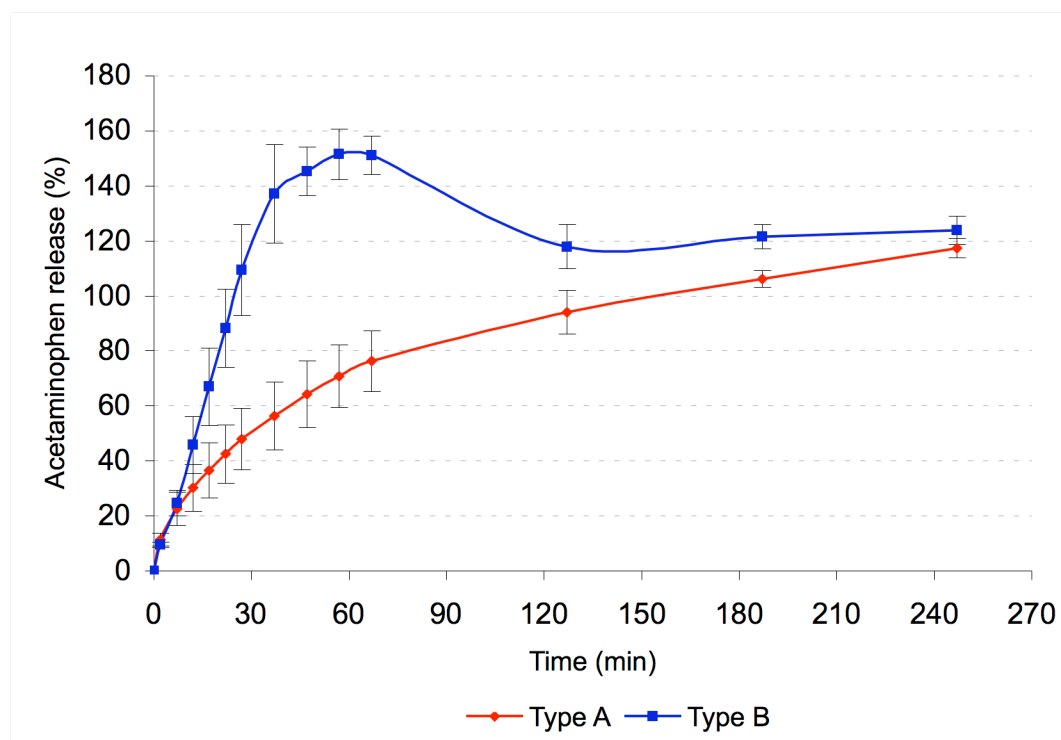


Figure 3.5.4. The amount of acetaminophen released as a function of time, measured by dissolution of CCx matrices containing 50 wt % corn oil and 160g Bloom gelatin, type A and B, in artificial gastric acid in a dissolution unit ($N=4$, average \pm S.D.). Calculations are shown in appendix G1.4.

Figures 3.5.1-4 show a faster dissolution for CCx gels stabilized with type B gelatin, compared to type A for the two highest oil contents (30 and 50 wt%). Similar dissolution profiles were observed for the two gelatin types with low amounts of oil (0 and 10 wt %). The dissolution profile of the CCx matrices with gelatin type B and 50 wt % oil differed from the others. A top was observed at around 70 minutes, followed by a decline in dissolution at around two hours, and then a slight release. This result was unexpected and was most likely an artifact, caused by a change of filters before the three last measurement points. The filters used up to the last three samples were likely clogged at the end, and thus the extra pressure applied to be able to filter the samples, may have caused bursting of oil droplets causing an increased marker concentration in the filtrated samples.

To interpret the results, linear regression was performed on the initial linear regions of the slopes from figures 3.5.1-4. The initial dissolution rate (dm/dt), determined by the linear regression, is presented in table 3.5.1.

Table 3.5.1. Dissolution rates for Concordix matrices with 0, 10, 30 and 50 wt % corn oil and 160g Bloom gelatin (either type A or B), obtained by linear regression of the initial linear regions of the eight curves in figures 3.5.1-3.5.4. The time gradients, corresponding to the linear region used to obtain the dissolution rate, are listed. Calculations are provided in appendix G2.

Oil content	Gelatin type A dm/dt (% / min)	Gelatin type B dm/dt (% / min)	Gradient (min)
0 wt %	9.9	9.6	1 - 11
10 wt %	7.3	8.2	2 - 10
30 wt %	1.1	5.5	6 - 14
50 wt %	1.9	3.6	2 - 12

Table 3.5.1 shows a decrease in initial dissolution rate with increased oil content, both for gelatin type A and B matrices. The decline was more prominent for gelatin type A than B. One exception was the slightly higher dissolution rate for type A gelatin gels with 30 wt % oil compared to 50 wt % oil, but this was likely due to the different time gradient. These results indicated a faster dissolution of the matrices stabilized by type B gelatin, compared to those stabilized by type A. For instance, for the matrices containing 50 wt % oil, the dissolution rate for gelatin type B matrices was almost 2 times faster than for the matrices with type A gelatin.

All dissolution profiles in figures 3.5.1-3.5.4 show acetaminophen released above 100 percent. This overshoot may have been caused by a combination of present oil droplets and loss of fluid both during preparation and measurements. A better estimation for the time needed to completely release the marker was where the curves in figures 3.5.1-4 level off. It was observed from the figures that a total release was obtained after approximately 20 minutes for CCx with 0 and 10 wt % oil, both for type A and B gelatin matrices. For CCx with 30 wt % oil, the entire marker was released at approximately 30 minutes for type B gelatin matrices, but for type A gelatin a complete release was not obtained during the 80 minutes of dissolution. The curve just started to level off around 80 minutes. For CCx matrices with 50 wt % oil and type B gelatin, a 100 % release was obtained after approximately 70 minutes, while a complete release was not obtained for matrices with 50 wt % oil and type A gelatin during the 4 hours of dissolution.

The increase in dissolution time in line with increased oil content for both matrices stabilized by type A and B gelatin, but to a greater extend for type A, should be seen in accordance with the gel properties previously investigated:

First, the viscosity was also increasing when oil was added to the matrices, with a more prominent increase for type A than B (figures 3.3.1 and 3.3.2). An increased viscosity is likely to increase the dissolution time of the matrix, since a more viscous material is more resistant towards flow. The possibility that the CCx matrices stabilized by type A gelatin are more prone to flocculation compared to type B due to asparagines, as discussed in section 3.3, may also help explain the prolonged dissolution rate observed for type A gelatin gels compared to type B. The increase in storage modulus and gelling and melting temperatures with increasing oil content (section 3.4.1) also supports the prolonged dissolution rates for Concordix gels containing 30 and 50 wt % corn oil, as the oil may act as an active filler substance which reinforces the gel. A higher G' for Concordix matrices with type A gelatin

compared to type B, also corresponded well to the results from the dissolution studies. The longitudinal deformations showed a significant increase in Young's modulus when addition of 30 wt % oil to type A gels (see table J.4, ($p < 0.05$)). Thus, the increased stiffness also corresponded well to the prolonged dissolution rate seen for type A gels compared to type B at high oil contents.

When considering the use of Concordix matrices as a delivery vehicle for pharmaceuticals, the studies performed have showed that both gel strength properties and dissolution rate are influenced by the gelatin type used to stabilize the matrices, as well as the oil content. These are important parameters when considering the use of CCx matrices as delivery systems for APIs. The gel strength will influence the mouth feel and how chewable the matrix is. The dissolution time is important in terms of delivery location of a pharmaceutical in the body. It is therefore possible to tailor the Concordix matrix to fit the requirements for optimal delivery of any pharmaceutical. Although the dissolution studies were performed in artificial gastric acid, the dissolution medium did not contain any enzymes, e.g. gastric lipase. It is important to keep in mind that the dissolution profiles obtained in the present study will most likely differ to some degree from *in vivo* dissolution.

3.6 Stability study with Double Emulsions stabilized by Gelatin versus Tween80

Double emulsions prepared by method #1

W/o/w double emulsions (DEs) were prepared according to the procedure described in methods section 2.2.8. The aim was to examine the long-term stability of the double emulsions by measuring the amount of tartrazine released from the inner to outer water phase by time. The goal was to optimize a stable double emulsion system that can be used for the delivery of APIs, as double emulsions have the potential to serve as a highly controllable delivery system for sustained drug release. Comparison of DEs stabilized with 226g Bloom gelatin type B and DEs stabilized with tween80 was performed.

Calculations related to this section are provided in appendix H.

Tartrazine release

The double emulsions were studied over 78 days. The amounts of tartrazine in controls and negative controls were detected using a spectrophotometer. It was assumed that the negative control corresponded to a 100% release, which was used to find the percent released at each day of measurement. The result is presented in figure 3.6.1. The long-term stability of the negative controls was also examined to determine if tartrazine was a suitable marker for this experiment.

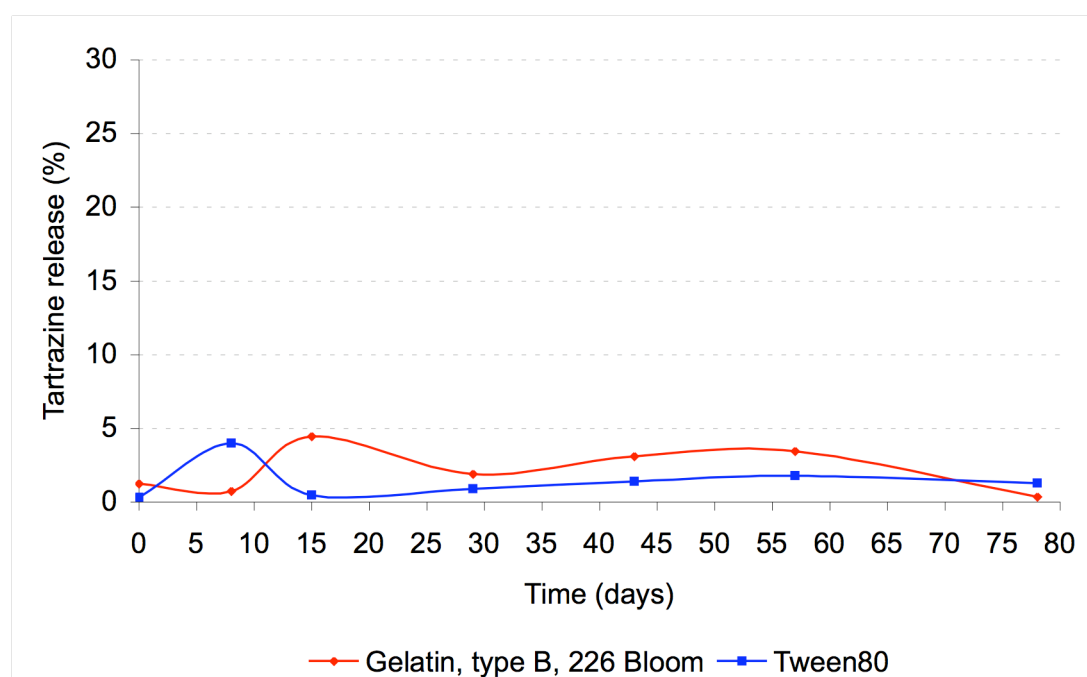


Figure 3.6.1. The amount of tartrazine (%) released from inner to outer water phase of w/o/w double emulsions stabilized by 226g Bloom gelatin type B or tween80, as a function of time (days).

Figure 3.6.1 shows that both double emulsions stabilized by gelatin and tween80 were stable during the 78 days of measurement.

Although the double emulsions seemed stable over the time span of the stability study, there were seen small variations in between the measurements. The most obvious error was the filtrating procedure. Oil droplets may have bursted/divided due to the pressure applied during filtration, leading to some release of tartrazine. To avoid this problem, the dissolved double emulsions were left for creaming before filtration, which made extraction of the water phase easier. However, it is likely that the filtration caused a small error. One possibility to avoid these errors is to centrifuge the samples prior to filtration, to completely separate the phases.

Figure 3.6.2 shows the absorbance of tartrazine in the negative controls as a function of time.

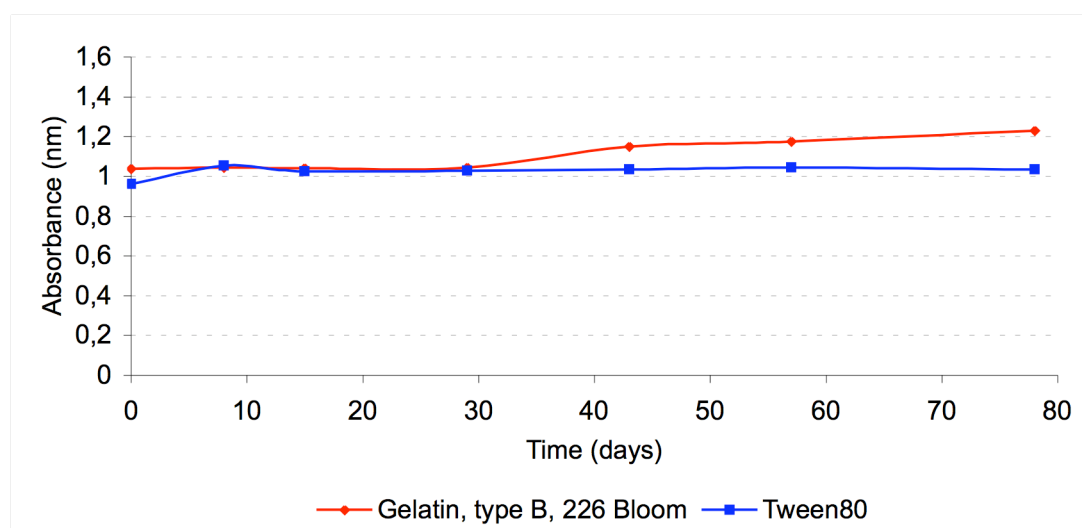


Figure 3.6.2. Amount of tartrazine measured as absorbance (nm) as a function of time (days) of w/o/w double emulsions stabilized by 226g Bloom gelatin type B or tween80, containing tartrazine in outer water phase, serving as negative controls.

Figure 3.6.2 shows that the concentration of tartrazine in the outer water phase was relatively stable over time, indicating that tartrazine is a suitable marker for the given experiment. A small increase in absorbance was observed for emulsions stabilized by gelatin after day 30. As mentioned in the materials (section 2.1.7), fading of tartrazine has been observed in presence of gelatin (Rowe *et al.*, 2009), but this was not observed in this study.

Microscopic examination of double emulsions prepared by method #1

The physical stability of the double emulsions was also determined by microscopic examination of both controls and negative controls for the two emulsion types (gelatin and tween80). Pictures are presented in figures 3.6.3 to 3.6.6.

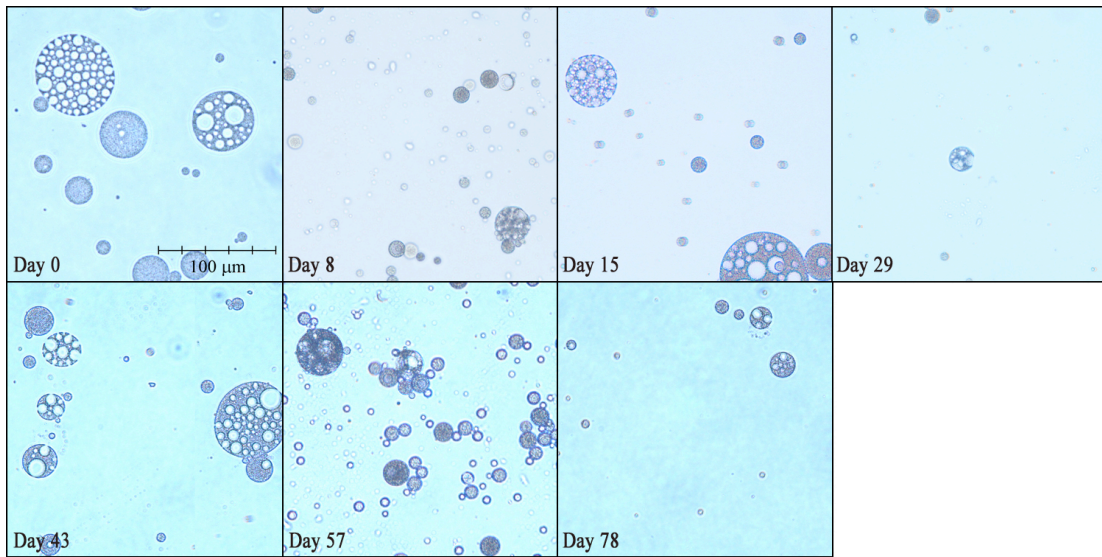


Figure 3.6.3 Pictures of the double emulsion made with gelatin type B, 226g Bloom, with tartrazine in the inner water phase. The magnification is 400x. The same scale bar applies for all pictures.

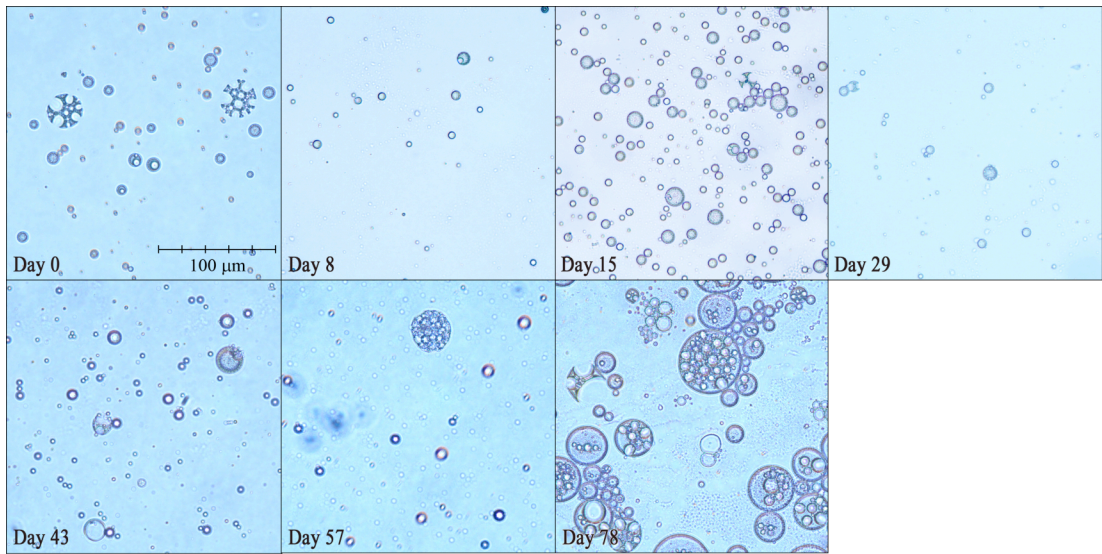


Figure 3.6.4 Pictures of the double emulsion made with gelatin type B, 226g Bloom, with tartrazine in the outer water phase, serving as negative control. The magnification is 400x. The same scale bar applies for all pictures.

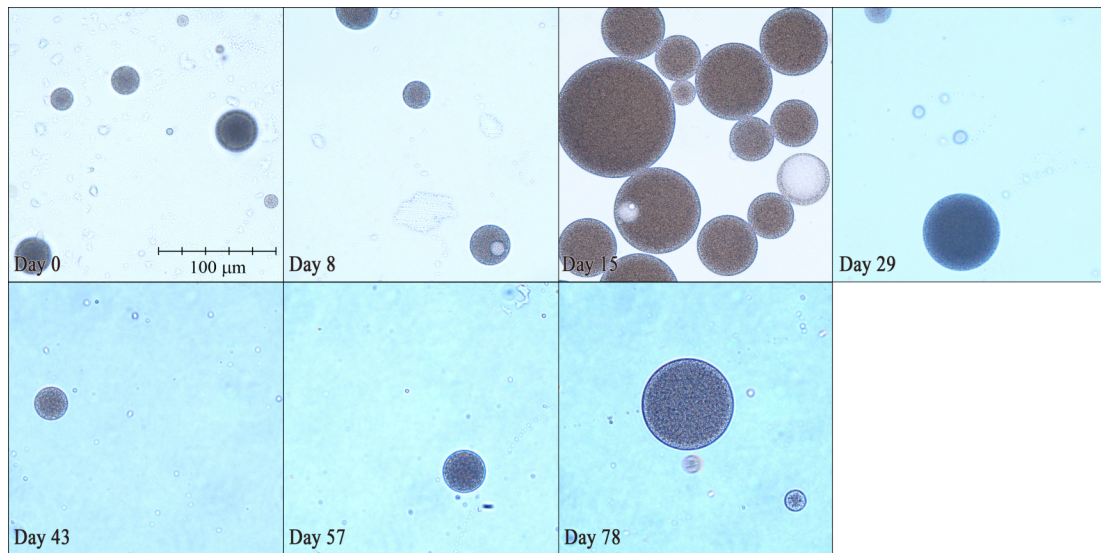


Figure 3.6.5. Pictures of the double emulsions made with tween80, with tartrazine in the inner water phase. The magnification is 400x. The same scale bar applies for all pictures.

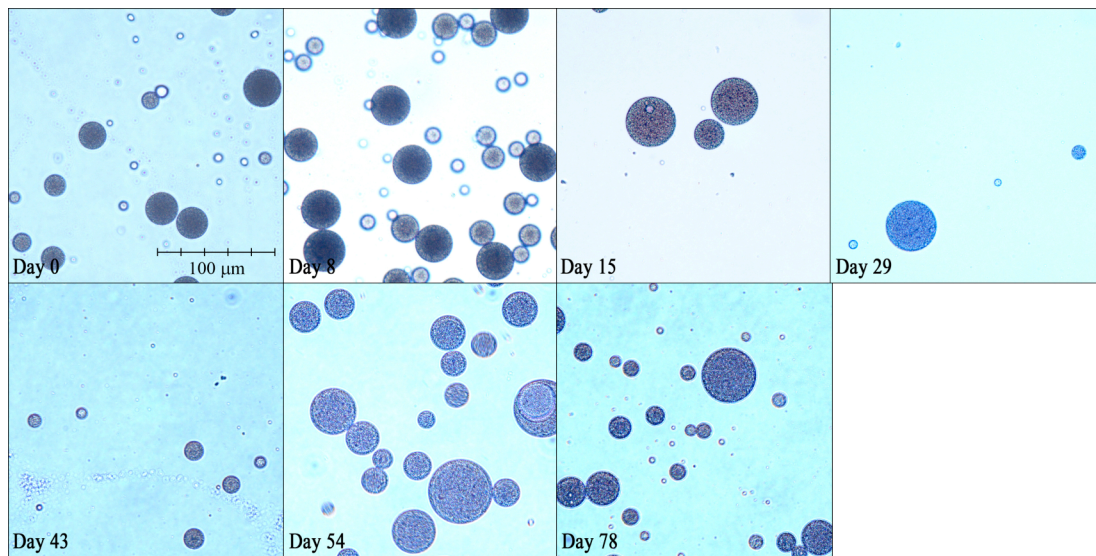


Figure 3.6.6. Pictures of the double emulsions made with tween80, with tartrazine in the outer water phase, serving as negative control. The magnification is 400x. The same scale bar applies for all pictures.

All the four double emulsions shown in figures 3.6.3-6 were very polydisperse, with a droplet size in the range of 5 to 80 μm . They were profoundly bigger than the droplet size for the conventional emulsions, having a mean size of approximately 1 μm (section 3.1).

Figures 3.6.3 and 3.6.4 show initial coalescence of the dispersed inner water droplets in the double emulsions with gelatin, both for the control (figure 3.6.3) and the negative control (figure 3.6.4). It is known from the literature that increased viscosity in the external water phase of w/o/w emulsions complicates the manufacturing procedure because it tends to cause breaking of the oil droplets (Benna-Zayani *et al.*, 2008). The coalescence in figures 3.6.3 and 3.6.4 was observed already at day 0 (the day of emulsion preparation). This may have been caused by destabilization of the oil

droplets due to the viscous continuous phase during emulsion preparation, which is likely to influence the inner water phase as well. Despite the initial coalescence, the emulsions seemed to remain stable during the time span of the study. The higher viscosity of the double emulsions stabilized by gelatin, compared to tween80, can explain why coalescence was nearly absent in the double emulsions with tween80 in figures 3.6.5 and 3.6.6. Both the control and negative control appear stable. Some flocculation is observed for all four double emulsions.

Although the double emulsions stabilized by tween80 were more stable than emulsions stabilized by gelatin, the gelatin is more suitable for pharmacological applications due to its ability to form chewable, gelled vehicles. In addition, the safety of gelatin is well established for medical use.

Double emulsions prepared by method #2

As the objective was to make stable double emulsions suitable for use in delivery of pharmaceuticals, it was desirable to make physically stable emulsions. The double emulsions showed stability in terms of low tartrazine release (figure 3.6.1), but the system was not ideal in terms of physical stability. It was therefore chosen to use a new manufacturing procedure for the double emulsions, which was *method II*, as previously described. This was performed in order to reduce the coalescence of the inner dispersed water droplets during manufacturing, and to see how it would influence the stability of the double emulsions. Instead of dissolving the gelatin in the external water phase *before* mixing the two water phases, the gelatin was added after preparation of the double emulsions, in order to decrease the viscosity of the continuous phase. The double emulsions contained the same amounts of ingredients, although the new procedure also included the emulsifier Gum Arabicum in the external water phase. The emulsions containing tween80 were identical to the previous experiment.

Tartrazine release

The tartrazine release was determined by the same procedure as described above for double emulsions prepared by method I. Figure 3.6.7 shows the release of tartrazine from inner to outer water phase as a function of time.

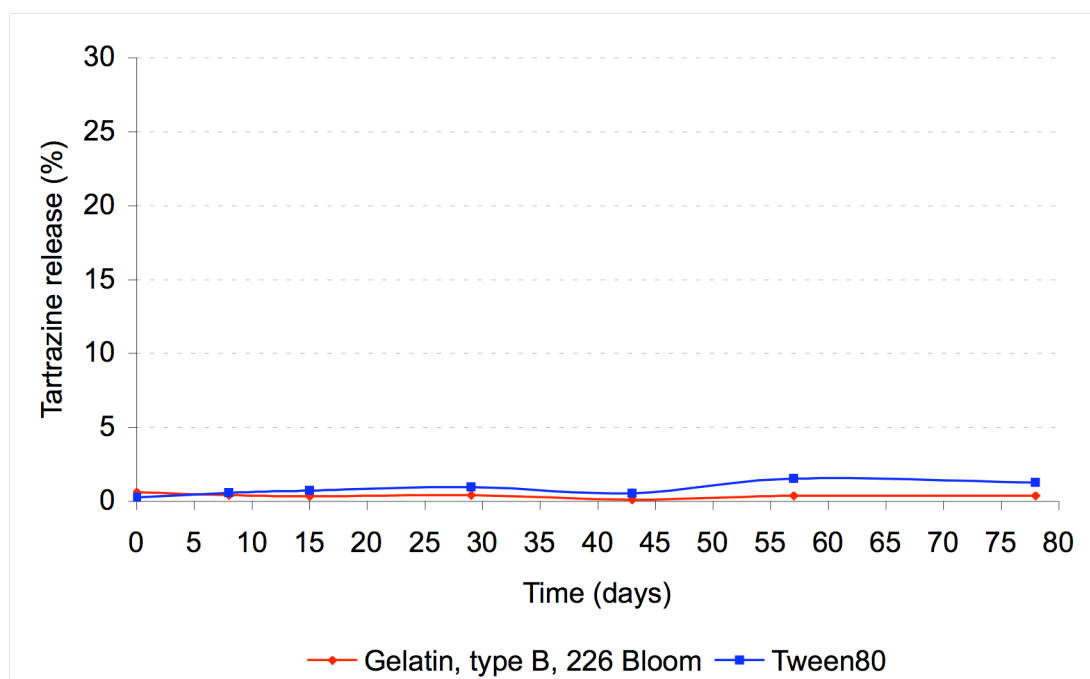


Figure 3.6.7. The amount of tartrazine (%) released from inner to outer water phase of w/o/w double emulsions stabilized by 226g Bloom gelatin type B or tween80 (prepared by method II), as a function of time (days).

Figure 3.6.7 shows almost no release of tartrazine from inner to outer water phase. Both the emulsions stabilized by tween80 and gelatin appeared to be stable over the time span of the study. The amount of tartrazine released was lower compared to the results seen in figure 3.6.1, indicating that the new preparation method gave an increased stability to the emulsions. PGPR was used as an emulsifier, stabilizing the inner dispersed phase in the double emulsions (see methods section 2.2.8). Studies by Graber (2010) showed that addition of NaCl to a w/o emulsion stabilized by PGPR gave a further decrease of interfacial tension than achieved by the emulsifier alone. Graber proposed that this effect was probably a result of reduced solubility of the PGPR in water caused by NaCl, increasing its absorption at the interface, and thereby reducing the interfacial tension. Tartrazine is an ionic molecule and may function in the same way as NaCl, by reducing the interfacial tension, contributing to stabilization of w/o emulsions in the presence of PGPR. As mentioned in the introduction, transport of materials across the lipid layer in w/o/w double emulsions may occur by different mechanisms. Cheng *et al.* (2006) found that transport of ions through the oil film in w/o/w double emulsions mainly occurs by reversed micelles, and ions with smaller Pauling radius are transported faster than larger ones, due to easier entrapment into the reversed micelle. Tartrazine is a relatively large molecule with several ionic groups, and it is therefore expected that its transport by reversed micelles is slow. In addition, the ionic groups of tartrazine will reduce its oil solubility, which should prevent direct diffusion through the oil layer. It seems that the properties of the marker itself will greatly affect the degree of transport through the double emulsion, and if this study was performed with another marker than tartrazine, other results might have been observed.

Figure 3.6.8 shows the concentration of tartrazine in the outer water phase as a function of time for the double emulsions prepared with method II.

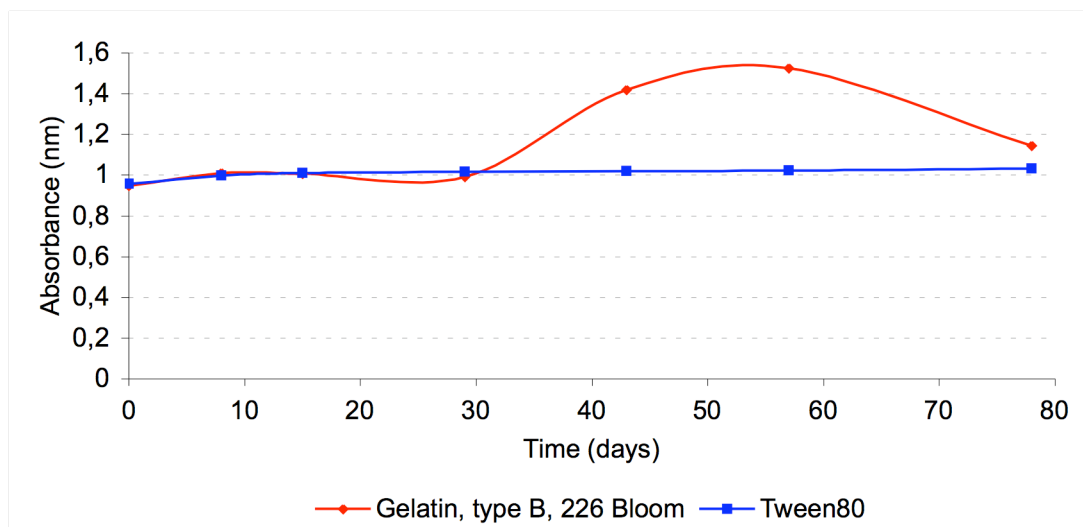


Figure 3.6.8. . Amount of tartrazine measured as absorbance (nm) as a function of time (days) of w/o/w double emulsions stabilized by 226g Bloom gelatin type B or tween80 (prepared by method II), containing tartrazine in outer water phase, serving as negative controls.

Figure 3.6.8 shows that the amount of tartrazine in the negative control with tween80 was stable during the 78 days of the trial. The negative control with gelatin appeared to undergo destabilization after day 30. However, at the last day of measurement the amount of tartrazine was in the same range as the initial state. One possible explanation for this result was the storage conditions of the emulsions. After preparation at day 0, the gelatin-stabilized emulsions were stored in small petri dishes in darkness at room temperature until use, as described in methods section 2.2.8, and a new dish was used to cut out a new gel sample at each day of measuring. After approximately 30 days it was observed that the gels had undergone various degrees of water loss and drying. This may have led to a higher concentration of tartrazine in the remaining gel, causing increased absorbance and thereby fluctuations in the measurements due to the condition of the gel sample used. This highlights the importance of proper storage of the emulsion. It is extremely important to tightly close the petri dishes with parafilm under the lid.

Microscopic examination of double emulsions prepared by method #2

The physical stability of the new emulsions was also examined by microscopy. The pictures are presented in figures 3.6.9 to 3.6.10.

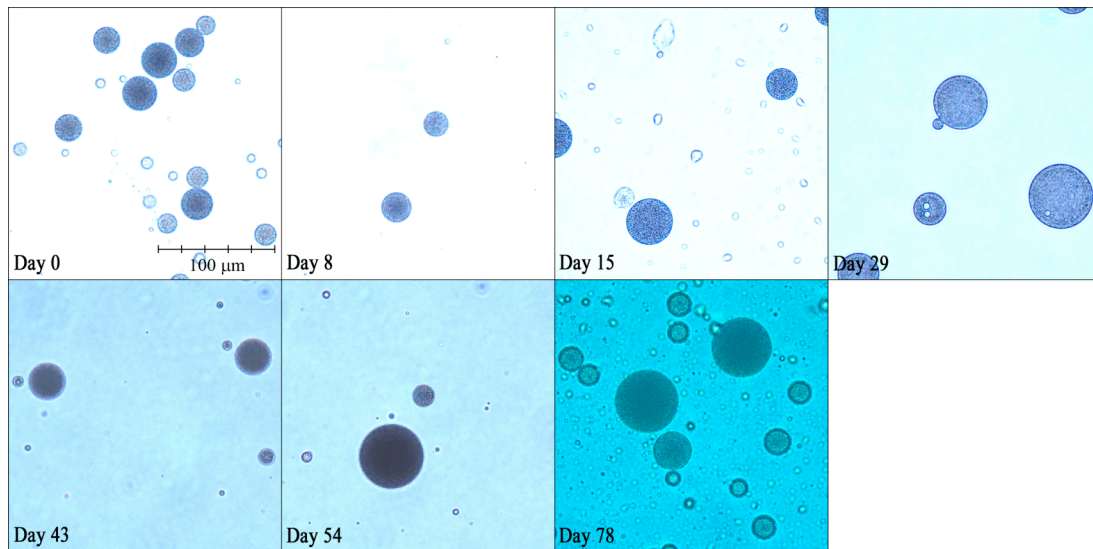


Figure 3.6.9. Pictures of the double emulsion made with gelatin type B, 226g Bloom, with tartrazine in the inner water phase. The emulsions were made using method II (section 2.2.8). The magnification is 400x. The same scale bar applies for all pictures.

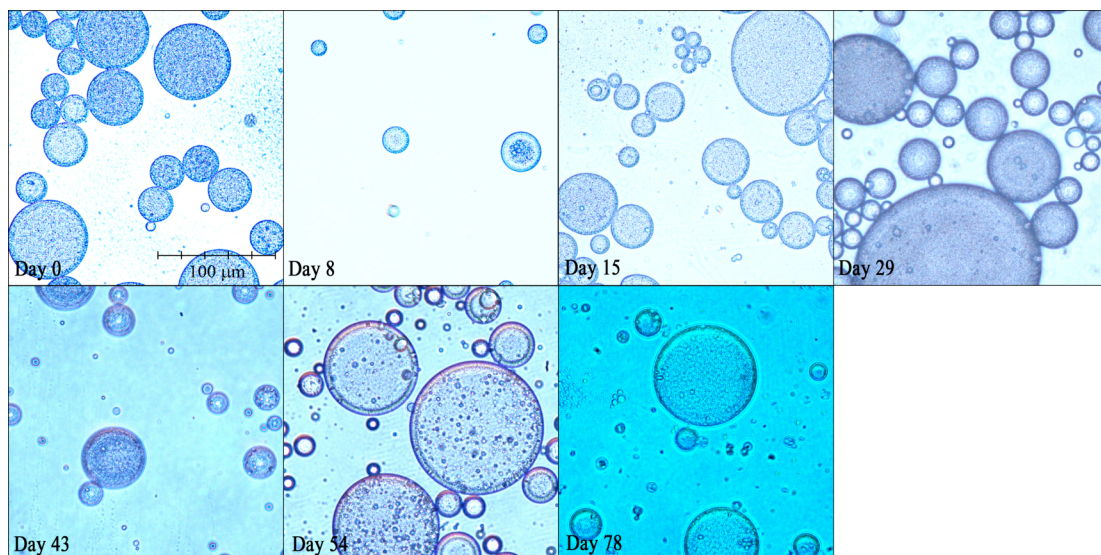


Figure 3.6.10. Pictures of the double emulsion made with gelatin type B, 226g Bloom, with tartrazine in the outer water phase, serving as negative control. The emulsions were made using method II (section 2.2.8). The magnification is 400x. The same scale bar applies for all pictures.

The double emulsions prepared by method II were also very polydisperse, with droplet size in the range of 5 to 100 μm. The oil droplets of the control (figure 3.6.9) were generally smaller than those of the negative control (figure 3.6.10), and appeared more stable overall. The emulsifier PGPR may, as previously discussed, have increased the emulsion stability in the presence of tartrazine (Graber, 2010). If the presence of tartrazine in the inner water phase of the control causes an increased stabilization of the inner w/o emulsion by PGPR, it can explain the higher stability observed for the control (figure 3.6.9) compared to the negative control (figure 3.6.10) where all the tartrazine was in the external water phase and thus did not interact with PGPR.

The double emulsions shown in figures 3.6.9 and 3.6.10 appeared more stable compared to the emulsions previously made using the first method of preparation, shown in figures 3.6.3 and 3.6.4. Less coalescence was observed for the inner water droplets, both for the control and negative control. Since gelatin was added after preparation of the w/o/w emulsion, the external water phase was less viscous during preparation, likely causing less destabilization of the oil droplets. It was assumed that less destabilization of oil droplets would provide increased stability of the inner water phase, and thus less coalescence.

Both the decrease in tartrazine release (figure 3.6.7 versus 3.6.1) and the increased physical stability (figures 3.6.9 and 3.6.10 versus figures 3.6.3 and 3.6.4) confirmed that the double emulsions prepared by the second method were more stable than double emulsions prepared by the first method.

Double emulsions dissolved at day 0

The double emulsions dissolved at day 0 were kept throughout the study trial, and measurements and pictures were taken as for the other double emulsions previously described. This study was performed with double emulsions prepared by method II. The emulsions were dissolved in a paraben-containing dissolution medium to increase the shelf-lives of the dissolved emulsions.

Figure 3.6.11 shows the release of tartrazine from inner to outer water phase as a function of time for the double emulsions dissolved at day 0.

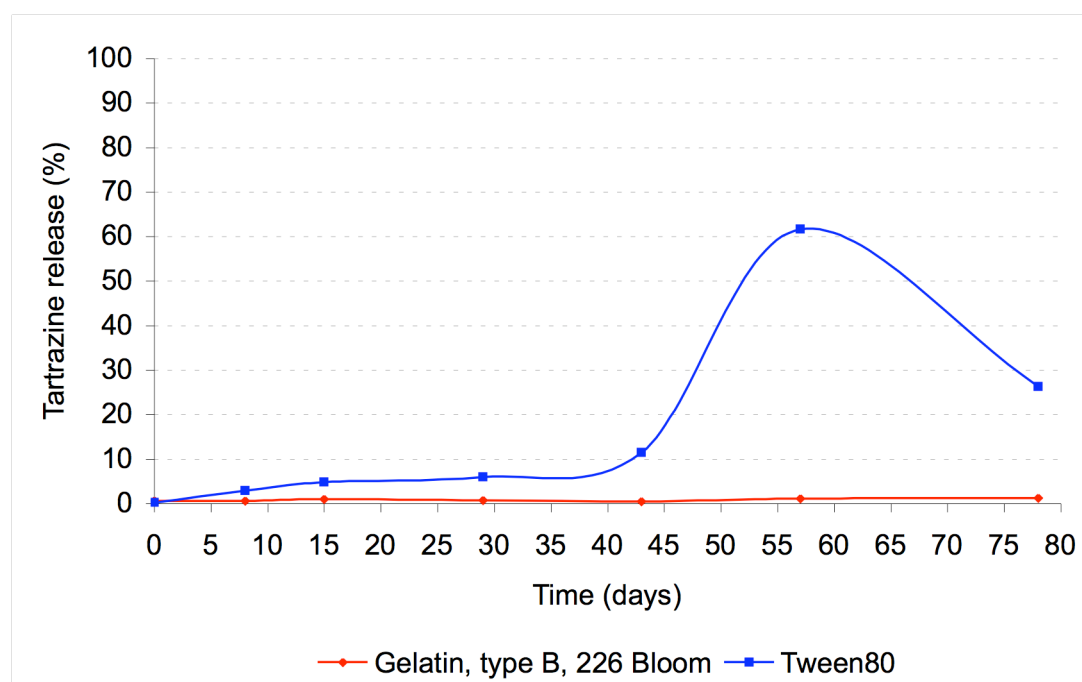


Figure 3.6.11. The amount of tartrazine (%) released from inner to outer water phase was measured as a function of time for double emulsions with gelatin 226g Bloom, type B and tween80. The emulsions were dissolved in MQ water containing parabens at day 0 and the dissolved emulsions were stored throughout the study trial.

From figure 3.6.11 it was seen that the gelatin emulsion was stable in the dissolved state throughout the 78 days of the study, while the emulsion containing tween80 was

less stable. It must be taken into consideration that the emulsions were diluted (1:33) in the dissolved state, which caused a reduction of the excessive of surfactants. The destabilization observed for the double emulsions with tween80 may have been due to the lower amount of emulsifier present. The result therefore indicated that the emulsion stability in a dissolved state is dependent on the stabilizing agent.

3.7. In vitro Lipolysis of Double Emulsions

Acid stability of double emulsions with gelatin

For double emulsions to be utilized as a delivery system for APIs, it is essential to characterize the release of API from the double emulsion in the gastrointestinal tract. The stability of w/o/w double emulsions stabilized by gelatin 226g Bloom type B, containing tartrazine in the inner water phase (prepared by method II described in section 2.2.8) was examined under gastric conditions. The double emulsions were dissolved in artificial gastric fluid (0.1 M HCl) or MQ water for 24 hours and the dissolved samples were thereafter examined visually and by microscopy. Absorbance measurements were not performed due to filtration complications, as tartrazine seemed to adhere to the filter at low pH. In figures 3.7.1-3.7.5, double emulsions dissolved in MQ water and gastric fluid are compared. Both double emulsions dissolved in MQ water and gastric fluid seemed stable during the 24 hours of dissolution. Based on these pictures, together with unpublished data by Hattrem (2012), the double emulsions were found to be stable under acidic conditions. It must be kept in mind that the artificial gastric fluid did not contain gastric lipases, and that the double emulsions might therefore be less stable *in vivo*. However, it was assumed that the double emulsions are not totally dissolved in the stomach, although some destabilization may occur *in vivo*, and that they will be transported more or less intact through the stomach and reach the small intestine. It was therefore appropriate to further study the behavior of the double emulsion in the gastrointestinal tract through *in vitro* lipolysis studies.

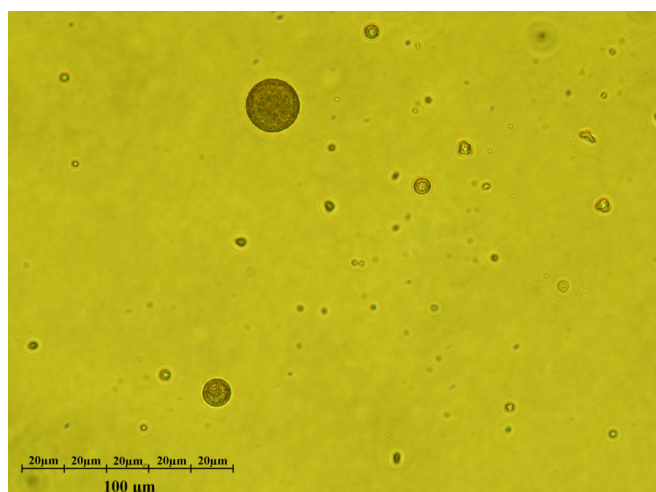


Figure 3.7.1. W/o/w double emulsion stabilized by gelatin 226g Bloom, type B dissolved in artificial gastric fluid (0.1 M HCl) for 3 hours. The magnification is 400x.

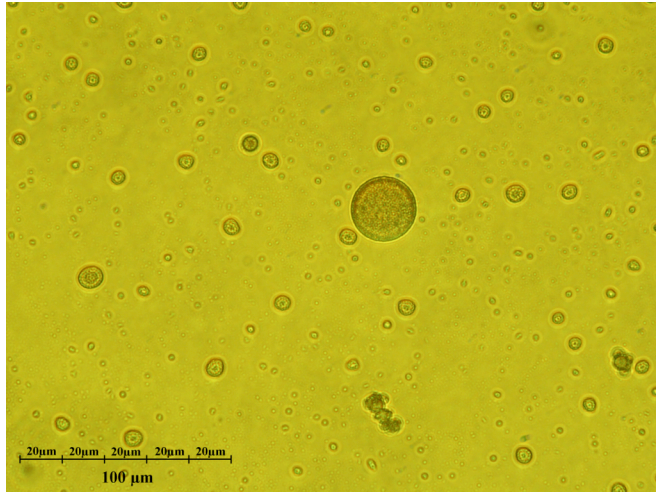


Figure 3.7.2. W/o/w double emulsion stabilized by gelatin 226g Bloom, type B dissolved in artificial gastric fluid (0.1 M HCl) for 24 hours. The magnification is 400x.

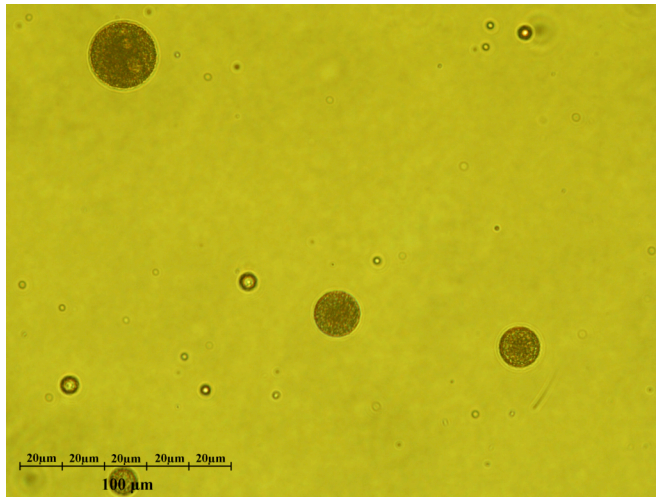


Figure 3.7.3. W/o/w double emulsion stabilized by gelatin 226g Bloom, type B dissolved in MQ water for 3 hours. The magnification is 400x.

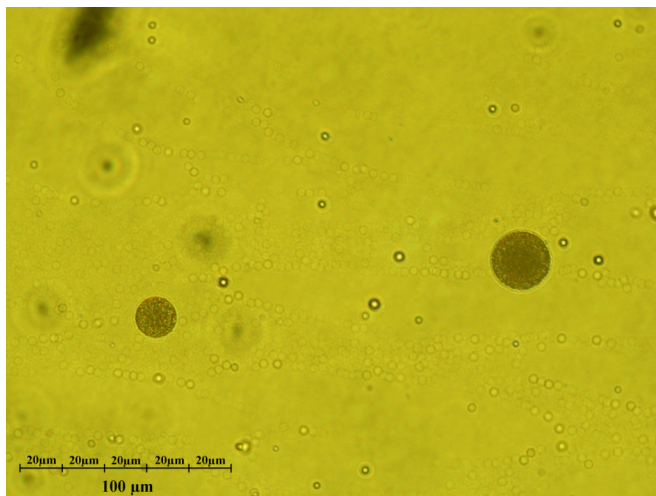


Figure 3.7.4. W/o/w double emulsion stabilized by gelatin 226g Bloom, type B dissolved in MQ water for 24 hours. The magnification is 400x.



Figure 3.7.5. W/o/w double emulsions stabilized by gelatin 226g Bloom, type B dissolved in artificial gastric fluid (0.1 M HCl, right) and MQ water (left). The emulsions were dissolved for 3 hours while stirring (100 rpm), and then allowed to cream before the picture was taken.

In vitro lipolysis of double emulsions with gelatin

Double emulsions were prepared according to *method II* described in section 2.2.8. Two emulsions stabilized with gelatin 226g Bloom, type B were made, a control (DE1) with tartrazine in inner water phase and a negative control (DE2) with tartrazine in outer water phase. *In vitro* lipolysis was performed according to the method described in section 2.2.8 to determine the release of tartrazine under intestinal conditions.

The intention was to study the release of an inner marker from the double emulsion under intestinal conditions. This was performed with the use of tartrazine as a marker by measuring its absorbance in both the control and the negative control. The negative control corresponded to a 100 % release, and the amount released was found by dividing the absorbance measured for the control by the negative control.

The result of the study is presented in figure 3.7.6. Data and calculations are shown in appendix I.

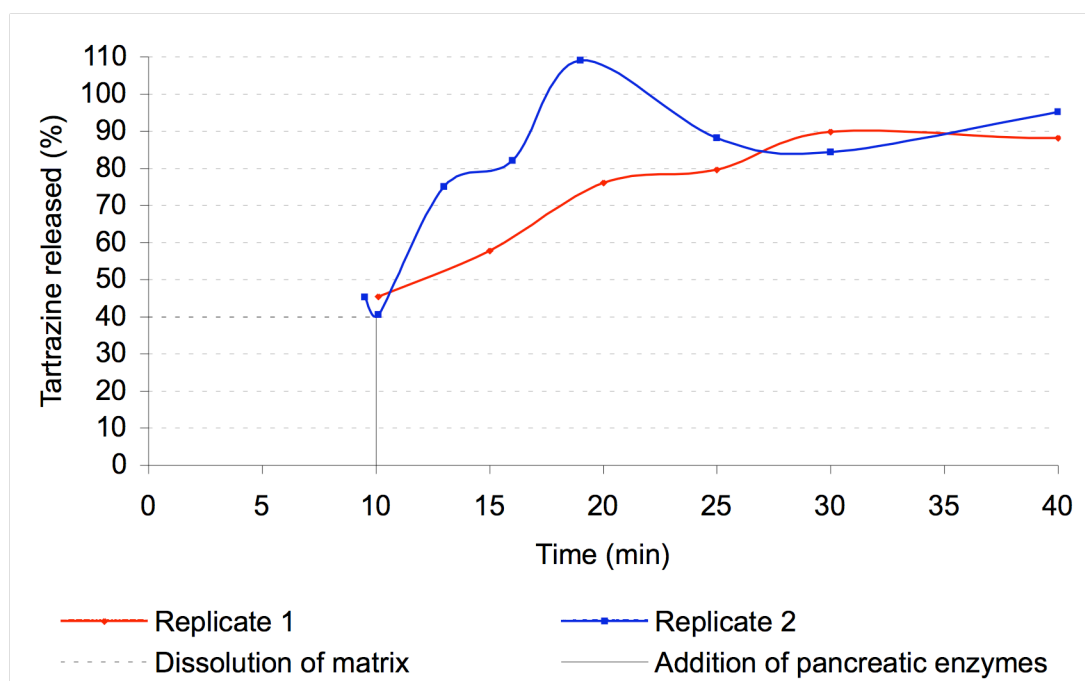


Figure 3.7.6. The amount of tartrazine (%) released from the inner water phase of w/o/w emulsions with 226g Bloom gelatin type B, from two independent replicates. The gel matrices were subjected to dissolution in intestinal digestion fluid for 10 minutes prior to addition of concentrated pancreatic solution, followed by sampling.

Figure 3.7.6 shows that a total release of tartrazine occurred under intestinal conditions. A total release was assumed to be obtained when the curves leveled off. The release profile varied somehow between the two replications, but a total release was obtained after approximately 30 and 20 minutes for replicate 1 and 2, respectively. For the first replicate, approximately 45 percent of the tartrazine was released immediately after addition of pancreatic solution to the dissolved emulsion. It was therefore extracted a sample of the second replicate just prior to addition of the pancreatic solution. The graph shows that 45 percent tartrazine also was released without the presence of lipases. This result indicated that release of tartrazine also occurs in absence of the pancreatic solution. The fact that the marker was released under the intestinal conditions indicated that the double emulsion might be suitable for delivery of gastric unstable pharmaceuticals that needs to be delivered to the intestine in order to have an effect. The emulsion was previously shown to be stable under gastric conditions, and thus the internal marker would first be released when the double emulsion has reached the small intestine. However, it cannot be excluded that some release will occur *in vivo* in the stomach due to gastric lipases.

It was necessary to perform control experiments to determine what caused the release of tartrazine in the absence of lipases. The first approach was to investigate the stability of the double emulsion in the presence of the salt buffer and when acid was added, but in the absence of both bile extracts and the pancreatic solution. Intestinal digestion fluid was prepared without porcine bile extracts, but otherwise equal to the digestion fluid used for the previous dissolutions. The double emulsions (control and negative control) were dissolved according to the procedure described in methods section 2.2.8. The release of tartrazine in the presence of salt and acid was found to be

less than 1 % and the double emulsions were therefore considered as stable under these conditions (Calculations are presented in appendix I, table 1.3).

The intestinal digestion fluid contained bile extracts, which may have influenced the stability of the emulsions, causing a release of tartrazine in the absence of lipases. To test this hypothesis, *in vitro* dissolution was performed in the absence of concentrated pancreatic solution, but with an otherwise equal protocol as the experiments given in figure 3.7.6. The result is presented in figure 3.7.7, together with the curves from figure 3.7.6.

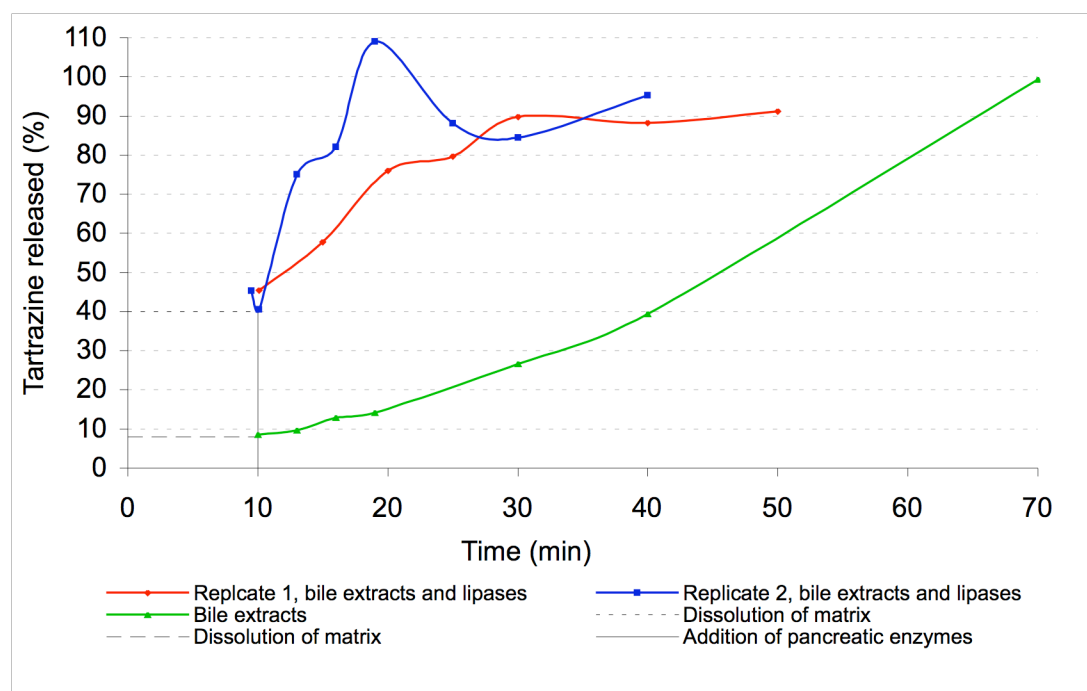


Figure 3.7.7. The amount of tartrazine (%) released from the inner water phase of w/o/w emulsions with gelatin 226g Bloom, type B. The gel matrices were dissolved in digestion fluid, in presence of either bile extracts or bile extracts and lipases. The matrices were subjected to dissolution in the intestinal digestion fluid for 10 minutes prior to sampling.

Figure 3.7.7 shows that the bile extracts was sufficient to break down the emulsion and completely release the marker within 70 minutes.

The destabilization of the double emulsions by bile extract could be explained by the surface-active properties of the bile acids. The gelatin, which interacts at oil-water interfaces, was probably replaced by bile acids. This is likely to have resulted in a thinner lamella between the two water phases, which may have contributed to increased transport of tartrazine across the membrane. To prevent this form of destabilization, one possibility is to make a more surface stable emulsion. The same dissolution study can be performed with double emulsions stabilized by other emulsifiers, such as tween80. This would tell if other emulsifiers are more suitable than gelatin, or if the same replacement happens independently of the nature of the emulsifier.

The overall observation was that release, possibly followed by absorption, would happen in the intestine, although the mechanism is still not completely known.

It must be pointed out that these experiments were performed based on a new method. One disadvantage of the method might have been the lack of information on the enzymatic activity of the pancreatic lipase. For further studies it is recommended to examine the enzyme activity, and it may be advantageous to use purified lipases instead to obtain better control of the reaction. In addition, the dissolution medium contained substances that are naturally not present to the same extent in the gastrointestinal tract. For instance, CaCl was added to prevent accumulation of fatty acids, however it is not present in the same extent in the digestion fluid in the

3.8 Prospective research

More extensive viscosity measurements of Concordix matrices should be performed in order to investigate the thixotropic behavior observed for type A gelatin matrices. More replicates should be included, and Concordix matrices with other gelatin types and oil amounts should also be investigated. It is highly recommended that the pre shear rate is the same as the rate at the first measurement point, or alternatively not use pre shear at all, to avoid structure change prior to measurements.

The dissolution studies in simulated gastric fluid could be optimized to better represent the *in vivo* environment by the addition of gastric lipases. Another option regarding dissolution studies of Concordix matrices is to tag the various ingredients in the matrix with a fluorescent marker, and investigate the release in artificial gastric fluid by scanning laser confocal microscope.

Dissolution studies of double emulsions should be performed in more detail to investigate their stability in gastric conditions. Due to time shortcoming, only visually examination of double emulsions under gastric conditions was performed in this study. In order to obtain a better representation of *in vivo* behavior, gastric lipases should be added to the dissolution medium and absorbance measurements should be performed. The method used for the lipolysis experiments should be further optimized. For further studies it is recommended to investigate the enzymatic activity of the pancreatic lipases. The activity can for instance be expressed in terms of tributyrin units, as reported by (Sek *et al.*, 2001).

4. Concluding remarks

Investigation of Concordix matrices with 160g Bloom gelatins and various amounts of corn oil showed that both gelatin type and oil content influenced the matrix properties. An increase in matrix strength and viscosity was observed upon oil addition, and the increase was more pronounced for matrices with type A gelatin compared to type B. The oil droplets were proposed to function as active fillers, which reinforced the matrices. An increased *in vitro* dissolution time under gastric conditions was also observed when oil was added to the matrices, with prolonged dissolution time for matrices with type A gelatin compared to type B. The ability to adjust rheological properties and dissolution time by varying the gelatin type and/or oil content offers a great advantage for Concordix matrices as delivery systems for various pharmaceuticals. The matrix can be tailored for both immediate and controlled release, depending on the mechanism of action of the pharmaceutical to be delivered.

Stability studies of w/o/w double emulsions stabilized by either gelatin or tween80 showed long-term emulsion stability in terms of low release of an entrapped marker, tartrazine, from the inner to outer water phase. The w/o/w double emulsions were also stable under gastric conditions. The internal marker was released during *in vitro* lipolysis of the double emulsions under intestinal conditions. This property offers great advantage for the use of double emulsions as delivery vehicles of gastric unstable pharmaceuticals, to avoid degradation in the stomach, but rather obtain controlled release in the small intestine. In addition, double emulsions have the potential to simultaneously deliver multiple pharmaceuticals with distinct properties. Lipid soluble drugs can be entrapped in the dispersed oil phase, while the dispersed inner water phase can simultaneously contain water-soluble drugs.

References

- ALBERTS, B., JOHNSON, A., LEWIS, J., RAFF, M., ROBERTS, K. & WALTER, P. 2008. *Molecular Biology of The Cell*, New York, Garland Science.
- ANDERSEN, O., ZWEIDOEFF, O. K., HJELDE, T. & RØDLAND, E. A. 1995. Problems when swallowing tablets. A questionnaire study from general practice. *Tidsskrift for Den Norske Lægeforening*, 115, 947-949.
- ASM-INTERNATIONAL 2005. *Mechanics and Mechanisms of Fracture: An Introduction (#06954G)*. Ohio: ASM International®.
- AULTON, M. E. 2007. *The design and manufacture of medicines*, Churchill Livingstone, Elsevier.
- BENNA-ZAYANI, M., KBIR-ARIGUIB, N., TRABELSI-AYADI, M. & GROSSIORD, J. L. 2008. Stabilisation of W/O/W double emulsion by polysaccharides as weak gels. *Colloids and Surfaces A: Physicochemical and Engineering Aspects*, 316, 46-54.
- BREWSTER, M. 2007. Physical form and formulation needs in contemporary drug pipelines. *M3: Molecules, Materials and Medicine*. Reykjavik, Iceland.
- CHANAMAI, R. & MCCLEMENTS, D. J. 2000. Creaming stability of flocculated monodisperse oil-in-water emulsions. *Journal of Colloid and Interface Science*, 225, 214-218.
- CHENG, J. F., C. J., ZHAO, M., LUO, Q., WEN, L. X. & PAPADOPOULOS, K. D. 2006. Transport of ions through the oil phase of W1/O/W2 double emulsions. *Journal of Colloid and Interface Science*, 305, 175-182.
- CHRISTENSEN, B. E. 2010. SEC-MALLS, compendium in TBT4135 Biopolymer chemistry. NTNU.
- CUINE, J. F., MCEVOY, C. L., CHARMAN, W. N., POUTON, C. W., EDWARDS, G. A., BENAMEUR, H. & PORTER, C. J. H. 2008. Evaluation of the impact of surfactant digestion on the bioavailability of danazol after oral administration of lipidic self-emulsifying formulations to dogs. *Journal of Pharmaceutical Sciences*, 97, 995-1012.
- DALBAKK, G. 2012. Unpublished work, master thesis 2012. NTNU, Trondheim.
- DICKINSON, E. 1989. FOOD COLLOIDS - AN OVERVIEW. *Colloids and Surfaces*, 42, 191-204.
- DICKINSON, E. 2011. Double Emulsions Stabilized by Food Biopolymers. *Food Biophysics*, 6, 1-11.
- DICKINSON, E. & STAINSBY, G. 1982. *Colloids in foods*, London, Elsevier.
- DORAN, P. M. 2010. *Bioprocess Engineering Principles*, London, Academic Press.
- FOX, A. W. 2007. *Pharmaceutics. Principles and Practice of Pharmaceutical Medicine*. Chichester: Wiley.
- GARTI, N. 1997. Double emulsions - Scope, limitations and new achievements. *Colloids and Surfaces a-Physicochemical and Engineering Aspects*, 123, 233-246.
- GARTI, N. & BISPERINK, C. 1998. Double emulsions: progress and applications. *Current Opinion in Colloid & Interface Science*, 3, 657-667.
- GILSENAN, P. M. & ROSS-MURPHY, S. B. 2000. Viscoelasticity of thermoreversible gelatin gels from mammalian and piscine collagens. *Journal of Rheology*, 44, 871-883.

- GMIA 2006. Gelatin Manufacturers Institute of America, Inc. Standard methods for testing of edible gelatins.
- GOLDING, M. & WOOSTER, T. J. 2010. The influence of emulsion structure and stability on lipid digestion. *Current Opinion in Colloid & Interface Science*, 15, 90-101.
- GOODWIN, J. W. & HUGHES, R. W. 2000. *Rheology of chemists - An introduction* Cambridge, UK, The Royal Society of Chemistry.
- GRABER, M. 2010. *Transport Phenomena in Rotating Membrane Processed W/O/W Emulsions*. Dr.ing. thesis, ETH Zurich.
- GRAHAME-SMITH, D. G. & ARONSON, J. K. 2002. *Clinical pharmacology and drug therapy*, Oxford, Oxford University Press.
- HASENTHUETTL, G. L. & HARTEL, R. W. 2008. *Food emulsifiers and their applications: Secound edition*, New York, Springer Science+Business Media, LLC.
- HATTREM, M. N. 2012. Unpublished work, dr.ing thesis. NTNU.
- HAUG, I. J. 2003. *Physical and Rheological Characterisation of Fish Gelatin and Mixtures of Fish Gelatin and kappa-Carrageenan*. Dr.-ing thesis, NTNU.
- HAUG, I. J. & DRAGET, K. I. 2009. *Handbook of hydrocolloids*, Cambridge, Woodhead Publishing Limited.
- HAUG, I. J. & HATTREM, M. N. 2010. Unpublished results Trondheim.
- HAUG, I. J., SAGMO, L. B., ZEISS, D., OLSEN, I. C., DRAGET, K. I. & SETERNES, T. 2011. Bioavailability of EPA and DHA delivered by gelled emulsions and soft gel capsules. *European Journal of Lipid Science and Technology*, 113, 137-145.
- KAUKONEN, A. M., BOYD, B. J., CHARMAN, W. N. & PORTER, C. J. H. 2004a. Drug solubilization behavior during in vitro digestion of suspension formulations of poorly water-soluble drugs in triglyceride lipids. *Pharmaceutical Research*, 21, 254-260.
- KAUKONEN, A. M., BOYD, B. J., PORTER, C. J. H. & CHARMAN, W. N. 2004b. Drug solubilization behavior during in vitro digestion of simple triglyceride lipid solution formulations. *Pharmaceutical Research*, 21, 245-253.
- KITA, Y., MATSUMOTO, S. & YONEZAWA, D. 1978. Permeation of Water through Oil Layer in W-O-W-Type Multiple-Phase Emulsions. *Nippon Kagaku Kaishi*, 11-14.
- LARSEN, A. T., SASSENE, P. & MÜLLERTZ, A. 2011. In vitro lipolysis models as tool for the characterization of oral lipid and surfactant based drug delivery systems. *International Journal of Pharmaceutics*, 417, 245-255.
- LOOTENS, D., CAPEL, F. O., DURAND, D., NICOLAI, T., BOULENGUER, P. & LANGENDORFF, V. 2003. Influence of pH, Ca concentration, temperature and amidation on the gelation of low methoxyl pectin. *Food Hydrocolloids*, 17, 237-244.
- LUYTEN, H., JONKMAN, M., KLOEK, W. & VAN VILET, T. 1993. *Creaming bbehaviour of dispersed particles in dilute xanthan solutions*, Cambridge, Royal Society of Chemistry.
- MALVERN 2011. Mastersizer 3000 - User manual. Worcestershire, UK: Malvern Instruments.
- MARKIDOU, A., SHIH, W. Y. & SHIH, W. H. 2005. Soft-materials elastic and shear moduli measurement using piezoelectric cantilevers. *Review of Scientific Instruments*, 76.

- MATSUMURA, Y., KANG, I. J., SAKAMOTO, H., MOTOKI, M. & MORI, T. 1993. Filler Effects of Oil Droplets on the Viscoelastic Properties of Emulsion Gels. *Food Hydrocolloids*, 7, 227-240.
- MCCLEMENTS, D. J. 2005. *Food emulsions: principles, practice, and techniques*, Florida, CRC Press.
- MCCLEMENTS, D. J. & LI, Y. 2010. Structured emulsion-based delivery systems: Controlling the digestion and release of lipophilic food components. *Advances in Colloid and Interface Science*, 159, 213-228.
- MCCLEMENTS, D. J., MONAHAN, F. J. & KINSELLA, J. E. 1993. Effect of Emulsion Droplets on the Rheology of Whey-Protein Isolate Gels. *Journal of Texture Studies*, 24, 411-422.
- MCNAUGHT, A. D. & WILKINSON, A. 1997. *Compendium of Chemical Terminology*, Oxford, Blackwell Scientific Publications.
- MOE, S. T. 1992. *Superswelling alginate gels - Preparation and some physical properties*. Dr.ing. thesis, NTNU.
- NORDE, W. 2003. *Colloids and interfaces in life sciences*, Monticello, N.Y., Marcel Dekker.
- NORLAND, R. E. 1990. *FISH GELATIN*, Lancaster, Technomic Publ Co.
- PAL, R. 2000. Shear Viscosity Behavior of Emulsions of Two Immiscible Liquids. *Journal of Colloid and Interface Science*, 225, 359-366.
- PAULA, S., VOLKOV, A. G., VANHOEK, A. N., HAINES, T. H. & DEAMER, D. W. 1996. Permeation of protons, potassium ions, and small polar molecules through phospholipid bilayers as a function of membrane thickness. *Biophysical Journal*, 70, 339-348.
- PAYS, K., GIEMANSKA-KAHN, J., POULIGNY, B., BIBETTE, J. & LEAL-CALDERON, F. 2001. Double emulsions: how do release occur? *Journal of controlled release*, 79, 193-205.
- PHARMACOPOEIA, E. 2007. *European Pharmacopoeia*, Strasbourg, France, European Directorate for the Quality of Medicines and Health Care.
- PORTER, C. J. H., TREVASKIS, N. L. & CHARMAN, W. N. 2007. Lipids and lipid-based formulations: optimizing the oral delivery of lipophilic drugs. *Nature Reviews Drug Discovery*, 6, 231-248.
- ROSE, P. I. 1987. Gelatine. *Encyclopedia of Polymer Science and Engineering*. New York: Wiley and Sons.
- ROSS-MURPHY, S. B. 1984. Rheological methods. In: CHAN, H. W.-S. (ed.) *Biophysical Methods in Food Research*. London: Blackwell Scientific Publications.
- ROWE, R. C., SHESKEY, P. J. & QUINN, M. E. 2009. *Handbook of Pharmaceutical Excipients*, London, Pharmaceutical Press.
- RYZAK, M. & BIEGANOWSKI, A. 2011. Methodological aspects of determining soil particle-size distribution using the laser diffraction method. *Journal of Plant Nutrition and Soil Science*, 174, 624-633.
- SALA, G. 2007. *Food gels filled with emulsion droplets - Linking large deformation properties to sensory perception*. PhD, Wageningen.
- SAND, O., SJAASTAD, Ø. V., HAUG, E. & BJÅLIE, J. G. 2006. *Menneskekroppen*, Oslo, Gyldendal Akademisk.
- SCHMIDT, C. & LAMPRECHT, A. 2009. Nanocarriers in drug delivery - Design, Manufacture and Physicochemical properties. *Nanotherapeutics -Drug delivery concepts in Nanoscience*. Singapore: Pan Stanford Publishing Pte. Ltd.

- SCHRIEBER, R. & GAREIS, H. 2007. *Gelatine Handbook - Theory and Industrial Practice*, Weinheim, Wiley-VCH.
- SEK, L., PORTER, C. J. H. & CHARMAN, W. N. 2001. Characterisation and quantification of medium chain and long chain triglycerides and their in vitro digestion products, by HPTLC coupled with in situ densitometric analysis. *Journal of Pharmaceutical and Biomedical Analysis*, 25, 651-661.
- SETERNES, T., DRAGET, K. I. & HAUG, I. J. 2009. *Chewable Gelled Emulsions*. 13/123,163.
- SMIDSRØD, O. & MOE, S. T. 2008. *Biopolymer chemistry*, Trondheim, Tapir.
- TØNNES, H. H., KRISTENSEN, S. & KARLSEN, J. 2008. Formulering av legemidler - et satsingsområde. *Norsk Farmaceutisk Tidsskrift*.
- VAN AKEN, G. A. 2006. Polysaccharides in Food Emulsions. In: STEPHEN, A. M., PHILLIPS, G. O. & WILLIAMS, P. A. (eds.) *Food Polysaccharides and Their Applications*. CRC Press.
- VAN AKEN, G. A., VINGERHOEDS, M. H. & DE WIJK, R. A. 2011. Textural perception of liquid emulsions: Role of oil content, oil viscosity and emulsion viscosity. *Food Hydrocolloids*, 25, 789-796.
- VEIS, A. 1964. *The macromolecular chemistry of gelatin*, New York: Academic Press.
- VU, C., ROBBLEE, J., WERNER, K. M. & FAIRMAN, R. 2001. Effects of charged amino acids at b and c heptad positions on specificity and stability of four-chain coiled coils. *Protein Science*, 10, 631-637.
- WARD, A. G. & COURTS, A. 1977. *The Science and technology of gelatin*, New York, Academic Press.
- WEICHENBERGER, C. X. & SIPPL, M. J. 2006. NQ-Flipper: validation and correction of asparagine/glutamine amide rotamers in protein crystal structures. *Bioinformatics*, 22, 1397-8.
- WIDMAIER, E. P., RAFF, H. & STRANG, K. T. 2010. *Vander's Human Physiology: The Mechanisms of Body Function*, McGraw-Hill College.
- WISHART, D. 2012. Human Metabolome Database (HMDB). 2005-16-11 ed.
- WOLD, I. M. 2011. *Investigation of gelatin based matrices for oral drug delivery*. Project work, NTNU.

List of appendices

Appendix A: Various calculations	1
A1. Preparation of artificial gastric acid for dissolution studies	1
A2. CCx matrices containing acetaminophen as marker for dissolution studies	1
A3. Standard solution of acetaminophen	2
A4. Blank samples of gelatin, sucralose and citric acid	2
A5. Stock solution of parabens	3
Appendix B: SEC-MALLS	4
Appendix C: Droplet size determination of Concordix	9
Appendix D: Shear Viscosity	11
D1. Shear viscosity for CCx	11
D2. Shear viscosity for CCx, NaCl, pH 7.5 or 8.5	14
D3. Shear viscosity for CCx, decreasing and increasing shear rate	16
Appendix E: Small strain oscillatory measurements	18
E1. Storage modulus	19
E2. Gelling temperature	19
E3. Melting temperature	20
Appendix F: Longitudinal deformation	21
F1. Instrument information	21
F2. Settings	21
F2.1. Young's modulus	21
F2.2. Break	21
F3. Example calculations	22
F3.1. Young's modulus	22
F3.2. Force at break	22
F3.3. Strain at break	22
F4. Data	23
F4.1. Young's modulus	23
F4.2. Force and strain at break	25
Appendix G: <i>In vitro</i> dissolution studies of Concordix matrices	27
G1. Data	27
G1.1. Concordix without oil	28
G1.2. Concordix with 10 wt % oil	32
G1.3. Concordix with 30 wt % oil	36
G1.4. Concordix with 50 wt % oil	41
G2. Linear regression	46
Appendix H: Stability study with double emulsions	49
H1. Data #1	49
H2. Data #2	50
H3. Data for Double emulsions dissolved at day 0	51
Appendix I: <i>In vitro</i> lipolysis of double emulsions	52
Appendix J: Statistical analysis	54
J1. Small strain oscillatory measurements	54
J2. Longitudinal deformation	55
Appendix K: Attached CD – information	57

Appendix A: Various calculations

A1. Preparation of artificial gastric acid for dissolution studies

Hydrochloric acid (HCl) was used as a solvent in the dissolution studies of Concordix matrices. Concentrated hydrochloric acid (37 wt %, 1 L = 1.19 kg, 36.45 g/mol) was used to prepare a 0.1 M solution of HCl. HCl (8.3 mL) was dissolved in MQ water (1 L) to obtain the final concentration of 0.1 M. The calculation is given below.

$$\frac{1.19\text{kg} / \text{L}}{0.03645\text{kg} / \text{mol}} \times 37\text{wt}\% = 12.08\text{mol} / \text{L}$$

$$\frac{0.1\text{mol}}{12.08\text{mol} / \text{L}} = 0.0082781\text{L} \approx 8.3\text{mL}$$

A2. CCx matrices containing acetaminophen as marker for dissolution studies

Concordix matrices containing acetaminophen (151.17 g/mol) as marker were prepared for the dissolution studies. The CCx matrix (1.5 g) was dissolved in artificial gastric acid (900 mL). The final concentration of acetaminophen in each gel was 0.1 mM:

$$0.1\text{mM} = 0.1 \times 10^{-3} \frac{\text{mol}}{\text{L}}$$

The acetaminophen concentration was multiplied with the volume of HCl to find the amount of moles:

$$0.1 \times 10^{-3} \frac{\text{mol}}{\text{L}} \times 0.9\text{L} = 9 \times 10^{-5} \text{mol}$$

The mass of acetaminophen in each CCx of 1.5 g was found by multiplying the amount of moles with the molecular weight of acetaminophen:

$$9 \times 10^{-5} \text{mol} \times 151.17 \frac{\text{g}}{\text{mol}} = 0.0136053\text{g}$$

A total of 30 g CCx matrix was prepared to ensure a sufficient amount for each study. From 30 g CCx a total of 20 matrix samples of 1.5 g can be obtained:

$$\frac{30\text{g}}{1.5\text{g}} = 20$$

The amount of acetaminophen in 30 g CCx is calculated below:

$$20 \times 0.0136053g = 0.272106g$$

The amount of CCx matrix needed is calculated below:

$$20 \times (1.5 - 0.0136053)g = 29.727894g$$

0.272106 g of acetaminophen was weighed out and added to 29.727894 g CCx matrix to obtain the desired concentration, and mixed with a spatula to obtain a homogeneous distribution of the marker in the gel matrix.

A3. Standard solution of acetaminophen

Acetaminophen was dissolved in HCl (1 L) to obtain a standard solution used for calculations in the dissolution studies. The standard solution was prepared by dissolving acetaminophen (151.17 g/mol) in HCl (0.1 M). The concentration of the final solution was 0.1 mM:

$$0.1mM = 0.1 \times 10^{-3} \frac{mol}{L}$$

The amount of acetaminophen was found by multiplying the final concentration of the solution with the molecular weight of acetaminophen:

$$0.1 \times 10^{-3} \frac{mol}{L} \times 151.17 \frac{g}{mol} \times 1L = 0.15117g$$

A4. Blank samples of gelatin, sucralose and citric acid

Blank samples with gelatin, sucralose and coffee flavor (C.F.) dissolved in artificial gastric acid, were prepared in order to subtract their contributions to the absorbance from the absorbance measurements of dissolved Concordix matrices during dissolution studies.

The concentration of gelatin, sucralose and C.F. in the digestion fluid (900 mL) was found by dividing the gel mass (1.5) on the total Concordix mass (39.97g) and multiplying with the amount of the current ingredients. The example shown below is for 0 wt % oil. Blank samples for Concordix with other oil contents were prepared the same way.

$$\text{Gelatin} : \frac{1.5g}{39.97g} \times 4.57g = 0.1715g$$

$$\text{Sucralose} : \frac{1.5g}{39.97} \times 0.17g = 0.00638g$$

$$\text{C.F.} : \frac{1.5g}{39.97} \times 0.29g = 0.0109g$$

The blank samples were made by dissolving the three components in 1 L HCl (0.1 M). The amount of each component was divided on the volume dissolution fluid to find the amount to be added:

$$\text{Gelatin} : \frac{0.1715g}{0.9} = 0.1906g$$

$$\text{Sucralose} : \frac{0.00638g}{0.9} = 0.00709g$$

$$\text{C.F.} : \frac{0.0109g}{0.9} = 0.0121g$$

A5. Stock solution of parabens

A stock solution with parabens was used as dissolution solvent in the stability studies of double emulsions to increase the shelf-life of the dissolved emulsions. Two different parabens, methyl 4-hydroxybenzoate sodium salt and propyl 4-hydroxybenzoate sodium salt, were dissolved in MQ water (250 mL).

0.4 wt % of methyl 4-hydroxybenzoate sodium salt:

$$\frac{250}{100} \times 0.4 = 1g$$

0.04 wt % of propyl 4-hydroxybenzoate sodium salt:

$$\frac{250}{100} \times 0.04 = 0.1g$$

Methyl 4-hydroxybenzoate sodium salt (1 g) and propyl 4-hydroxybenzoate sodium salt (0.1 g) were weighed out and dissolved in 250 mL MQ water.

Appendix B: SEC-MALLS

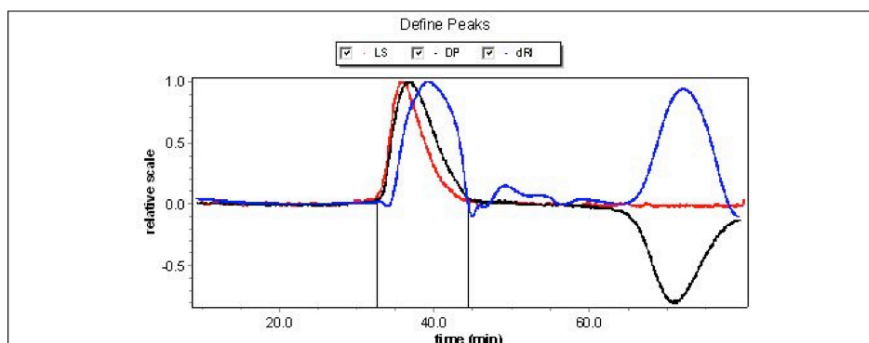
SEC-MALLS analysis were performed for Gelatin 160g Bloom, type A and B.

Raw data from SEC-MALLS analysis are found on the attached CD.

Summary reports from Astra for type A and B gelatin are shown below.

ASTRA 5.3.4 Summary Report for 1011004[1011ss]

Experiment name: C:\Ingvild\Resultater_lab\SEC-MALLS data IDA\New Folder\ 1011004[1011ss]
Sample: 1011 (A 160)
Processing Operator: Ingvild Haug
Collection Operator: Ann Sissel Ulset
Collection Astra Version: 5.3.4.20

**CONFIGURATION**

Viscometer: ViscoStar
Dilution factor: 0.4600
Light scattering instrument: DAWN HELEOS
Cell type: K5
Laser wavelength: 658.0 nm
Calibration constant: 2.8301e-5 1/(V cm)
RI Instrument: Optilab rEX
UV Instrument: n/a
Solvent: water
Refractive index: 1.331
Flow rate: 0.500 mL/min

PROCESSING

Processing time: Tuesday December 06, 2011 11:21 AM W. Europe Standard Time
Collection time: Thursday November 10, 2011 08:06 PM W. Europe Standard Time
Detectors used: 6 7 8 9 10 11 12 13 14 15
Concentration detector: RI
Mass results fitting: none (fit degree: n/a)
Radius results fitting: none (fit degree: n/a)

	Peak 1
Peak limits (min)	32.594 - 44.402
dn/dc (mL/g)	0.190
A ₂ (mol mL/g ²)	1.000e-3
UV ext. (mL/(g cm))	0.000
Model	Zimm
Fit degree	1
Eta Model	Huggins
Huggins Constant	0.0000
Kraemer Constant	0.0000
Injected mass (g)	2.0000e-4
Calc. mass (g)	1.3946e-4

RESULTS

1011004[1011ss]

Peak 1

Polydispersity
Mw/Mn 2.515 (21%)
Mz/Mn 13.690 (23%)

Molar mass moments (g/mol)
Mn 2.739e+4 (21%)
Mp 4.331e+4 (5%)
Mv n/a
Mw 6.890e+4 (5%)
Mz 3.750e+5 (10%)

rms radius moments (nm)
Rn n/a
Rw n/a
Rz 5.7 (515%)

Intrinsic viscosity moments (mL/g)
η_n 18.6 (0.8%)
η_w 32.3 (0.8%)
η_z 127.6 (10%)

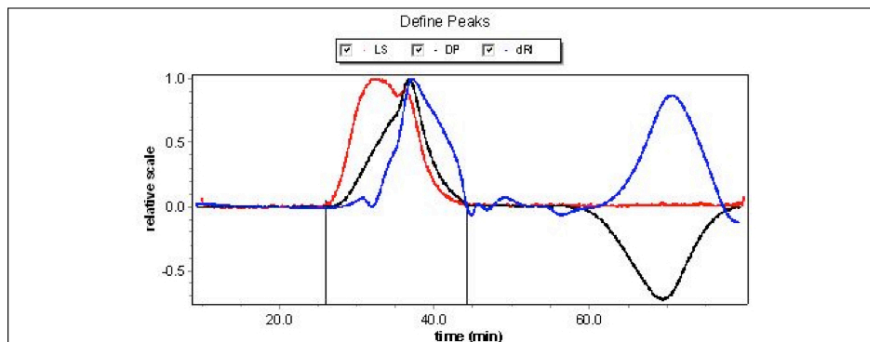
Hydrodynamic radius moments (nm)
Rh(n) 4.1 (5%)
Rh(w) 6.4 (2%)
Rh(z) 15.4 (3%)

Mark-Houwink-Sakurada parameters:
K: (2.943±0.008) e-2 mL/g
a: 0.638±0.000

1011008[1011ss]

ASTRA 5.3.4 Summary Report for 1011008[1011ss]

Experiment name: C:\Ingvild\Resultater_lab\SEC-MALLS data IDA\New Folder\ 1011008[1011ss]
Sample: 1011 (B 160)
Processing Operator: Ingvild Haug
Collection Operator: Ann Sissel Ulset
Collection Astra Version: 5.3.4.20



CONFIGURATION

Viscometer: ViscoStar
Dilution factor: 0.5000
Light scattering instrument: DAWN HELEOS
Cell type: K5
Laser wavelength: 658.0 nm
Calibration constant: 2.8301e-5 1/(V cm)
RI Instrument: Optilab rEX
UV Instrument: n/a
Solvent: water
Refractive index: 1.331
Flow rate: 0.500 mL/min

PROCESSING

Processing time: Tuesday December 06, 2011 11:23 AM W. Europe Standard Time
Collection time: Friday November 11, 2011 01:37 AM W. Europe Standard Time
Detectors used: 6 7 8 9 10 11 12 13 14 15
Concentration detector: RI
Mass results fitting: none (fit degree: n/a)
Radius results fitting: none (fit degree: n/a)

	Peak 1
Peak limits (min)	25.913 - 44.242
dn/dc (mL/g)	0.190
A₂ (mol mL/g²)	1.000e-3
UV ext. (mL/(g cm))	0.000
Model	Zimm
Fit degree	1
Eta Model	Huggins
Huggins Constant	0.0000
Kraemer Constant	0.0000
Injected mass (g)	1.0000e-4
Calc. mass (g)	1.3948e-4

RESULTS

1011008[1011ss]

Peak 1

Polydispersity
Mw/Mn 3.925 (21%)
Mz/Mn 67.518 (22%)

Molar mass moments (g/mol)
Mn 3.916e+4 (21%)
Mp 8.378e+4 (2%)
Mv n/a
Mw 1.537e+5 (3%)
Mz 2.644e+6 (6%)

rms radius moments (nm)
Rn 10.5 (644%)
Rw 5.1 (1214%)
Rz 19.2 (30%)

Intrinsic viscosity moments (mL/g)
 η_n 24.8 (0.6%)
 η_w 49.2 (1%)
 η_z 440.7 (17%)

Hydrodynamic radius moments (nm)
Rh(n) 5.0 (5%)
Rh(w) 8.9 (2%)
Rh(z) 41.4 (4%)

Mark-Houwink-Sakurada parameters:
K: (6.258±0.011)e-2 mL/g
a: 0.579±0.000

Appendix C: Droplet size determination of Concordix

The raw data from analysis of Concordix matrices by Mastersizer 3000 are provided in table C.1. The data are based on averages from five measurement replications, calculated by the software. The analysis report obtained from the Mastersizer software is presented in table C.2. Raw data is found on the attached CD.

Table C.1. Different droplet size classes (μm) obtained from analysis by Mastersizer 3000 of concordices with gelatin 160g Bloom (either type A or B) and different amounts of corn oil (10, 30 and 50 wt %). The amount in each size class is given as percentage of total droplets.

Size Classes (μm)	Results (%)					
	10 wt %		30 wt %		50 wt %	
	Type A	Type B	Type A	Type B	Type A	Type B
0.0278	0	0	0	0	0	0
0.0315	0	0	0	0	0	0
0.0358	0	0	0	0	0	0
0.0407	0	0	0	0	0	0
0.0463	0	0	0	0	0	0
0.0526	0	0	0	0	0	0
0.0597	0	0	0	0	0	0
0.0679	0	0	0	0	0	0
0.0771	0	0	0	0	0	0
0.0876	0	0	0	0	0	0
0.0995	0	0	0	0	0	0
0.113	0	0	0	0	0	0
0.128	0	0	0	0.15	0	0.17
0.146	0	0.21	0	0.4	0.21	0.44
0.166	0	0.51	0.18	0.78	0.56	0.85
0.188	0	0.96	0.43	1.28	1.11	1.4
0.214	0	1.52	0.8	1.87	1.86	2.05
0.243	0.28	2.16	1.29	2.52	2.77	2.77
0.276	0.79	2.83	1.87	3.17	3.79	3.5
0.314	1.64	3.47	2.55	3.78	4.84	4.19
0.357	2.81	4.05	3.3	4.3	5.83	4.74
0.405	4.27	4.56	4.11	4.72	6.66	5.12
0.46	5.93	5.05	5	5.07	7.26	5.3
0.523	7.67	5.61	6.02	5.42	7.6	5.32
0.594	9.33	6.35	7.17	5.89	7.71	5.26
0.675	10.71	7.34	8.43	6.55	7.64	5.25
0.767	11.54	8.52	9.66	7.42	7.44	5.39
0.872	11.61	9.61	10.56	8.35	7.15	5.74
0.991	10.76	10.15	10.56	9.01	6.71	6.22
1.13	9.03	9.69	9.95	8.99	6.05	6.64
1.28	6.68	8.07	8.12	8.03	5.12	6.78
1.45	4.21	5.64	5.63	6.24	3.97	6.49
1.65	2.11	3.11	3.13	4.05	2.75	5.71
1.88	0.56	0.58	0.98	2.01	1.61	4.53
2.13	0.05	0	0.05	0.01	0.73	3.15
2.42	0	0	0	0	0.2	1.85
2.75	0	0	0	0	0	0.86
3.12	0	0	0	0	0	0.26

3.55	0	0	0	0	0	0
4.03	0	0	0	0	0	0
4.58	0	0	0	0	0	0
5.21	0	0	0	0	0	0
5.92	0	0	0	0	0	0

Table C.2. Analysis report of data from analysis of concordices with gelatin 160g Bloom (type A or B), and varying amounts of oil (10, 30 and 50 wt%), by Mastersizer 3000. Data obtained from the instrument software.

Sample	10 wt % Type A	10 wt % Type B	30 wt % Type A	30 wt % Type B	50 wt % Type A	50 wt % Type B
Particle Absorption Index	0.010	0.010	0.010	0.010	0.010	0.010
Weighted Residual ¹ (%)	1.17	1.31	1.18	1.11	1.45	1.11
Particle Refractive Index	1.470	1.470	1.470	1.470	1.470	1.470
Dispersant Refractive Index	1.330	1.330	1.330	1.330	1.330	1.330
Laser Obscuration ² (%)	6.16	6.22	8.26	8.70	5.56	6.28
Concentration ³ (%)	0.0020	0.0021	0.0027	0.0029	0.0020	0.0021
Uniformity ⁴	0.336	0.412	0.377	0.459	0.546	0.613
Specific Surface area (m ² /kg) ⁵	8990	10390	9427	10820	11700	10770
D[3.2] ⁶ (µm)	0.742	0.642	0.707	0.616	0.570	0.619
D[4.3] ⁷ (µm)	0.876	0.863	0.899	0.873	0.805	0.988
Span ⁸	1.100	1.325	1.217	1.470	1.680	1.925
Result transformation type	Volume	Volume	Volume	Volume	Volume	Volume
Dv 10* µm	0.463	0.336	0.399	0.312	0.311	0.301
Dv 50* µm	0.825	0.832	0.862	0.824	0.673	0.836
Dv 90* µm	1.37	1.44	1.45	1.52	1.44	1.91

¹Indicates how well the calculated data was fitted to the measured data

²Measures the amount of lost laser beam when the sample is added

³Volume concentration

⁴Absolute derivation from the median

⁵Total area of particles divided by total weight

⁶Volume weighted mean

⁷Surface weighted mean

⁸Width of distribution

*Standard percentile readings from the analysis

Dv 10: size of particle below which 10% of the sample lies

Dv 50: size where 50% of the sample is smaller and 50% is larger

Dv 90: size of particle below which 90% of the sample lies

Appendix D: Shear Viscosity

D1. Shear viscosity for CCx

Information on the viscosity of the Concordix matrices with 160g Bloom gelatin type A and B, containing 0, 10, 30 or 50 wt % corn oil, were obtained from continuous shear measurements at 60°C, performed with a rheometer (StressTech, Lund Sweden). Table D1.1-D1.8 gives the viscosity (Pa s) at various shear rates (1/s) for the different CCx systems investigated.

Table D1.1. Shear viscosity for Concordix matrix with gelatin 160g Bloom, type A and 0 wt % corn oil (N=3, ± standard deviation).

Replications	1	2	3	Average	S.D.
Shear rate (1/s)	Viscosity (Pa s)	Viscosity (Pa s)	Viscosity (Pa s)	Viscosity (Pa s)	±
0.60	0.2908	0.2522	0.3493	0.2974	0.0489
0.80	0.2665	0.2414	0.3087	0.2722	0.0340
1.00	0.2402	0.2183	0.2725	0.2437	0.0273
2.00	0.1956	0.1641	0.2063	0.1887	0.0219
4.00	0.1597	0.1361	0.1591	0.1516	0.0135
7.00	0.1431	0.1238	0.1355	0.1341	0.0097
10.00	0.1342	0.1167	0.1269	0.1259	0.0088
20.00	0.1232	0.1081	0.1136	0.1150	0.0076
40.00	0.1151	0.1032	0.1047	0.1077	0.0065
60.00	0.1112	0.1014	0.1018	0.1048	0.0055
80.00	0.1089	0.1007	0.1000	0.1032	0.0049
100.00	0.1064	0.1001	0.0988	0.1018	0.0041

Table D1.2. Shear viscosity for Concordix matrix with gelatin 160g Bloom, type A and 10 wt % corn oil (N=3, ± standard deviation).

Replications	1	2	3	Average	S.D.
Shear rate (1/s)	Viscosity (Pa s)	Viscosity (Pa s)	Viscosity (Pa s)	Viscosity (Pa s)	±
0.60	0.1889	0.2077	0.2032	0.1999	0.0098
0.80	0.1786	0.1994	0.2104	0.1961	0.0161
1.00	0.1685	0.1922	0.2043	0.1883	0.0182
2.00	0.1653	0.1849	0.2006	0.1836	0.0177
4.00	0.1601	0.1772	0.1968	0.1780	0.0184
7.00	0.1568	0.1725	0.1925	0.1739	0.0179
10.00	0.1570	0.1719	0.1910	0.1733	0.0170
20.00	0.1532	0.1681	0.1845	0.1686	0.0157
40.00	0.1505	0.1653	0.1793	0.1650	0.0144
60.00	0.1491	0.1640	0.1768	0.1633	0.0139
80.00	0.1481	0.1628	0.1757	0.1622	0.0138
100.00	0.1479	0.1623	0.1748	0.1617	0.0135

Table D1.3. Shear viscosity for Concordix matrix with gelatin 160g Bloom, type A and 30 wt % corn oil (N=3, \pm standard deviation).

Replications	1	2	3	Average	S.D.
Shear rate (1/s)	Viscosity (Pa s)	Viscosity (Pa s)	Viscosity (Pa s)	Viscosity (Pa s)	\pm
0.60	3.6550	5.2200	5.9920	4.9557	1.1907
0.80	3.4410	4.9160	5.8780	4.7450	1.2275
1.00	3.3440	4.7830	5.4070	4.5113	1.0580
2.00	2.5020	3.5050	3.9720	3.3263	0.7511
4.00	1.9000	2.6000	2.9560	2.4853	0.5373
7.00	1.5550	2.0730	2.3680	1.9987	0.4116
10.00	1.3730	1.8140	2.0690	1.7520	0.3521
20.00	1.1130	1.4370	1.6440	1.3980	0.2676
40.00	0.9222	1.1700	1.3310	1.1411	0.2059
60.00	0.8307	1.0480	1.2050	1.0279	0.1880
80.00	0.7801	0.9777	1.1210	0.9596	0.1712
100.00	0.7423	0.9292	1.0640	0.9118	0.1616

Table D1.4. Shear viscosity for Concordix matrix with gelatin 160g Bloom, type A and 50 wt % corn oil (N=3, \pm standard deviation).

Replications	1	2	3	Average	S.D.
Shear rate (1/s)	Viscosity (Pa s)	Viscosity (Pa s)	Viscosity (Pa s)	Viscosity (Pa s)	\pm
0.60	91.3600	164.7000	76.0600	110.7067	47.3812
0.80	79.1500	140.9000	55.1500	91.7333	44.2382
1.00	69.1500	117.0000	41.8400	75.9967	38.0449
2.00	40.1900	69.4000	33.5800	47.7233	19.0613
4.00	25.1300	37.7300	20.3500	27.7367	8.7840
7.00	17.8300	26.6300	11.0000	18.4867	7.3570
10.00	14.0700	19.7800	8.9200	14.2567	5.4324
20.00	9.3620	13.1600	6.0480	9.5233	3.5587
40.00	5.9420	7.9840	4.2680	6.0647	1.8610

Table D1.5. Shear viscosity for Concordix matrix with gelatin 160g Bloom, type B and 0 wt % corn oil (N=3, \pm standard deviation).

Replications	1	2	3	Average	S.D.
Shear rate (1/s)	Viscosity (Pa s)	Viscosity (Pa s)	Viscosity (Pa s)	Viscosity (Pa s)	\pm
0.60	0.2310	0.2644	0.1362	0.2105	0.0665
0.80	0.2098	0.2459	0.1260	0.1939	0.0615
1.00	0.2055	0.2145	0.1328	0.1843	0.0448
2.00	0.1761	0.1818	0.1235	0.1605	0.0321
4.00	0.1576	0.1529	0.1163	0.1423	0.0226
7.00	0.1479	0.1345	0.1122	0.1315	0.0180
10.00	0.1417	0.1308	0.1102	0.1276	0.0160
20.00	0.1356	0.1225	0.1079	0.1220	0.0139
40.00	0.1313	0.1174	0.1061	0.1183	0.0126
60.00	0.1301	0.1159	0.1054	0.1171	0.0124
80.00	0.1295	0.1153	0.1051	0.1166	0.0123
100.00	0.1291	0.1148	0.1049	0.1163	0.0122

Table D1.6. Shear viscosity for Concordix matrix with gelatin 160g Bloom, type B and 10 wt % corn oil (N=3, \pm standard deviation).

Replications	1	2	3	Average	S.D.
Shear rate (1/s)	Viscosity (Pa s)	Viscosity (Pa s)	Viscosity (Pa s)	Viscosity (Pa s)	\pm
0.60	0.1752	0.1870	0.2250	0.1957	0.0260
0.80	0.1874	0.1963	0.2251	0.2029	0.0197
1.00	0.1878	0.1973	0.2191	0.2014	0.0160
2.00	0.1784	0.1871	0.2168	0.1941	0.0201
4.00	0.1798	0.1881	0.2140	0.1940	0.0178
7.00	0.1820	0.1896	0.2106	0.1941	0.0148
10.00	0.1804	0.1878	0.2104	0.1929	0.0156
20.00	0.1799	0.1863	0.2075	0.1912	0.0144
40.00	0.1788	0.1855	0.2056	0.1900	0.0139
60.00	0.1780	0.1850	0.2048	0.1893	0.0139
80.00	0.1774	0.1843	0.2040	0.1886	0.0138
100.00	0.1771	0.1841	0.2037	0.1883	0.0138

Table D1.7. Shear viscosity for Concordix matrix with gelatin 160g Bloom, type B and 30 wt % corn oil (N=3, \pm standard deviation).

Replications	1	2	3	Average	S.D.
Shear rate (1/s)	Viscosity (Pa s)	Viscosity (Pa s)	Viscosity (Pa s)	Viscosity (Pa s)	\pm
0.60	0.9736	1.0260	0.9548	0.9848	0.0369
0.80	0.9808	1.0330	0.9658	0.9932	0.0353
1.00	0.9733	1.0290	0.9539	0.9854	0.0390
2.00	0.9409	0.9915	0.9224	0.9516	0.0358
4.00	0.9206	0.9676	0.8992	0.9291	0.0350
7.00	0.9018	0.9458	0.8816	0.9097	0.0328
10.00	0.8886	0.9311	0.8665	0.8954	0.0328
20.00	0.8621	0.8975	0.8362	0.8653	0.0308
40.00	0.8272	0.8574	0.7974	0.8273	0.0300
60.00	0.8033	0.8311	0.7704	0.8016	0.0304
80.00	0.7838	0.8114	0.7534	0.7829	0.0290
100.00	0.7679	0.7960	0.7400	0.7680	0.0280

Table D1.8. Shear viscosity for Concordix matrix with gelatin 160g Bloom, type B and 50 wt % corn oil (N=3, \pm standard deviation).

Replications	1	2	3	Average	S.D.
Shear rate (1/s)	Viscosity (Pa s)	Viscosity (Pa s)	Viscosity (Pa s)	Viscosity (Pa s)	\pm
0.60	23.5000	13.4800	21.8000	19.5933	5.3621
0.80	21.2400	12.1200	20.2300	17.8633	4.9994
1.00	19.5800	11.1700	19.1300	16.6267	4.7310
2.00	15.5900	8.8700	16.2300	13.5633	4.0771
4.00	12.5600	7.2310	13.8000	11.1970	3.4902
7.00	10.5300	6.2170	11.9900	9.5790	3.0017
10.00	9.3080	5.6270	10.8700	8.6017	2.6919
20.00	7.2180	4.6320	8.9540	6.9347	2.1749
40.00	5.5410	3.8150	7.3160	5.5573	1.7506

D2. Shear viscosity for CCx, NaCl, pH 7.5 or 8.5

Information on the shear viscosity for Concordix matrices with 30 wt % corn oil, gelatin 160g Bloom, type A and B, and either with NaCl (250 mM) or pH 7.5 or 8.5 was obtained as described for the original CCx systems in D1. Viscosity (Pa s) at various shear rates (1/s) is presented in table D2.1-D2.5.

Table D2.1. Shear viscosity for Concordix matrix with gelatin 160g Bloom, type A, and 30 wt % corn oil, pH 8.5 (N=3, \pm standard deviation).

Replications	1	2	3	Average	S.D.
Shear rate (1/s)	Viscosity (Pa s)	Viscosity (Pa s)	Viscosity (Pa s)	Viscosity (Pa s)	\pm
0.60	2.0200	1.5940	2.4190	2.0110	0.4126
0.80	1.9780	1.5960	2.3980	1.9907	0.4012
1.00	1.9190	1.5660	2.3410	1.9420	0.3880
2.00	1.7190	1.4150	2.0970	1.7437	0.3417
4.00	1.5340	1.2730	1.8650	1.5573	0.2967
7.00	1.4010	1.1730	1.6970	1.4237	0.2627
10.00	1.3240	1.1100	1.5960	1.3433	0.2436
20.00	1.1950	1.0020	1.4310	1.2093	0.2149
40.00	1.0820	0.9106	1.2780	1.0902	0.1838
60.00	1.0140	0.8559	1.1840	1.0180	0.1641
80.00	0.9671	0.8170	1.1240	0.9694	0.1535
100.00	0.9363	0.7880	1.0790	0.9344	0.1455

Table D2.2. Shear viscosity for Concordix matrix with gelatin 160g Bloom, type B, and 30 wt % corn oil, pH 8.5 (N=3, \pm standard deviation).

Replications	1	2	3	Average	S.D.
Shear rate (1/s)	Viscosity (Pa s)	Viscosity (Pa s)	Viscosity (Pa s)	Viscosity (Pa s)	\pm
0.60	2.0330	1.7710	1.9090	1.9043	0.1311
0.80	2.0020	1.7420	1.8910	1.8783	0.1305
1.00	1.9650	1.7140	1.8670	1.8487	0.1265
2.00	1.8790	1.6560	1.7890	1.7747	0.1122
4.00	1.7970	1.5970	1.7260	1.7067	0.1014
7.00	1.7230	1.5410	1.6690	1.6443	0.0935
10.00	1.6790	1.5060	1.6250	1.6033	0.0885
20.00	1.5820	1.4350	1.5500	1.5223	0.0773
40.00	1.4790	1.3520	1.4600	1.4303	0.0685
60.00	1.4130	1.3000	1.4030	1.3720	0.0626
80.00	1.3690	1.2610	1.3610	1.3303	0.0602
100.00	1.3290	1.2340	1.3280	1.2970	0.0546

Table D2.3. Shear viscosity for Concordix matrix with gelatin 160g Bloom, type A, and 30 wt % corn oil, pH 7.5 (N=2).

Replications	1	2	Average
Shear rate (1/s)	Viscosity (Pa s)	Viscosity (Pa s)	Viscosity (Pa s)
0.60	2.2440	1.6980	1.9710
0.80	2.1600	1.6580	1.9090
1.00	2.0670	1.6180	1.8425
2.00	1.7120	1.3860	1.5490
4.00	1.4180	1.1910	1.3045
7.00	1.2380	1.0640	1.1510
10.00	1.1410	0.9912	1.0661
20.00	0.9861	0.8695	0.9278
40.00	0.8628	0.7753	0.8191
60.00	0.8053	0.7293	0.7673
80.00	0.7714	0.7044	0.7379
100.00	0.7484	0.6862	0.7173

Table D2.4. Shear viscosity for Concordix matrix with gelatin 160g Bloom, type B, and 30 wt % corn oil, pH 7.5 (N=2).

Replications	1	2	Average
Shear rate (1/s)	Viscosity (Pa s)	Viscosity (Pa s)	Viscosity (Pa s)
0.60	1.2510	0.9025	1.0768
0.80	1.2230	0.9100	1.0665
1.00	1.1810	0.8950	1.0380
2.00	1.1010	0.8444	0.9727
4.00	1.0240	0.8109	0.9175
7.00	0.9674	0.7827	0.8751
10.00	0.9364	0.7654	0.8509
20.00	0.8778	0.7286	0.8032
40.00	0.8212	0.6909	0.7561
60.00	0.7999	0.6671	0.7335
80.00	0.7782	0.6533	0.7158
100.00	0.7629	0.6400	0.7015

Table D2.5. Shear viscosity for Concordix matrix with gelatin 160g Bloom, type A and B, 30 wt % corn oil and NaCl (250 mM) (N=1). (Only one replica because the NaCl addition did not have any effect on the shear thinning)

Gel type	A	B
Shear rate (1/s)	Viscosity (Pa s)	Viscosity (Pa s)
0.60	5.0460	1.2410
0.80	4.8110	1.2170
1.00	4.4020	1.1930
2.00	3.2040	1.1510
4.00	2.3960	1.1020
7.00	1.9230	1.0630
10.00	1.6900	1.0380
20.00	1.3560	0.9858
40.00	1.1190	0.9278
60.00	1.0100	0.8920

80.00	0.9508	0.8619
100.00	0.9087	0.8373

D3. Shear viscosity for CCx, decreasing and increasing shear rate

The shear viscosity for Concordix matrices with 30 wt % corn oil and gelatin 160g Bloom, type A and B were obtained as described in D1. The shear rate started at 0.6 1/s and increased into 60 1/s before turning back to the start rate. The obtained viscosity is presented in table D3.1 to D3.3.

Table D3.1. Shear viscosity for Concordix matrix with gelatin 160g Bloom, type A and 30 wt % corn oil (N=2).

Replications	1	2	Average
Shear rate (1/s)	Viscosity (Pa s)	Viscosity (Pa s)	Viscosity (Pa s)
0.60	17.0300	16.3100	16.6700
0.80	15.0400	14.3400	14.6900
1.00	13.2800	12.6600	12.9700
2.00	8.6400	8.2940	8.4670
4.00	5.7690	5.4800	5.6245
7.00	4.2180	4.0070	4.1125
10.00	3.4640	3.2820	3.3730
20.00	2.4480	2.2860	2.3670
40.00	1.7790	1.6460	1.7125
60.00	1.4670	1.3770	1.4220
40.00	1.6400	1.5360	1.5880
20.00	2.0640	1.9270	1.9955
10.00	2.6970	2.5040	2.6005
7.00	3.2000	2.9670	3.0835
4.00	4.2000	3.8900	4.0450
2.00	6.1740	5.7070	5.9405
1.00	9.5900	8.8150	9.2025
0.80	11.6100	10.6500	11.1300
0.60	13.7700	12.4000	13.0850

Table D3.2. Shear viscosity for Concordix matrix with gelatin 160g Bloom, type B and 30 wt % corn oil (N=2).

Replications	1	2	Average
Shear rate (1/s)	Viscosity (Pa s)	Viscosity (Pa s)	Viscosity (Pa s)
0.60	1.2070	1.1950	1.2010
0.80	1.1650	1.1720	1.1685
1.00	1.1560	1.1550	1.1555
2.00	1.0770	1.0760	1.0765
4.00	1.0160	1.0170	1.0165
7.00	0.9718	0.9778	0.9748
10.00	0.9441	0.9496	0.9469
20.00	0.8936	0.9044	0.8990
40.00	0.8467	0.8571	0.8519
60.00	0.8158	0.8275	0.8217
40.00	0.8444	0.8570	0.8507
20.00	0.8910	0.8999	0.8955
10.00	0.9374	0.9451	0.9413
7.00	0.9618	0.9700	0.9659
4.00	1.0030	1.0100	1.0065
2.00	1.0670	1.0710	1.0690
1.00	1.1490	1.1460	1.1475
0.80	1.1650	1.1630	1.1640
0.60	1.1980	1.1900	1.1940

Table D3.3. Shear viscosity for Concordix matrix with gelatin 160g Bloom, type B and 30 wt % corn oil. Sample A1 and A2 are the same, but a break time of 15 minutes without shear was performed between the two measurements.

Sample	A1	A2
Shear rate (1/s)	Viscosity (Pa s)	Viscosity (Pa s)
0.60	4.083	5.094
0.80	3.928	5.045
1.00	3.783	4.751
2.00	3.009	3.477
4.00	2.36	2.543
7.00	1.949	2.022
10.00	1.729	1.756
20.00	1.384	1.382
40.00	1.12	1.107
60.00	0.997	0.9917
40.00	1.076	1.072
20.00	1.266	1.258
10.00	1.53	1.521
7.00	1.754	1.721
4.00	2.15	2.091
2.00	2.816	2.731
1.00	3.838	3.716
0.80	4.482	4.321
0.60	4.986	4.882

Appendix E: Small strain oscillatory measurements

Small strain oscillatory measurements were performed with a rheometer (StressTech, Lund Sweden) and the parameters examined were storage modulus (G'), gelling temperature (T_g) and melting temperature (T_m). The temperature of the water bath was 20°C and 30°C for measurements at 60°C and 70°C , respectively. The rheometer was coupled to the software *Rheoexplorer*, which was used to analyze the data obtained. A typical plot obtained from oscillatory measurements is given in figure E1. The first 20 minutes is a cooling process, thereafter a holding period for 15 minutes, followed by a heating process for 20 minutes. The storage modulus is found at the transition between holding and heating, at the highest value of the primary y-axis. The gelling temperature is found during the cooling period, at the intersection between temperature (secondary y-axis) and phase degree of 45° , and the melting temperature is the temperature at phase degree of 45° in the heating period.

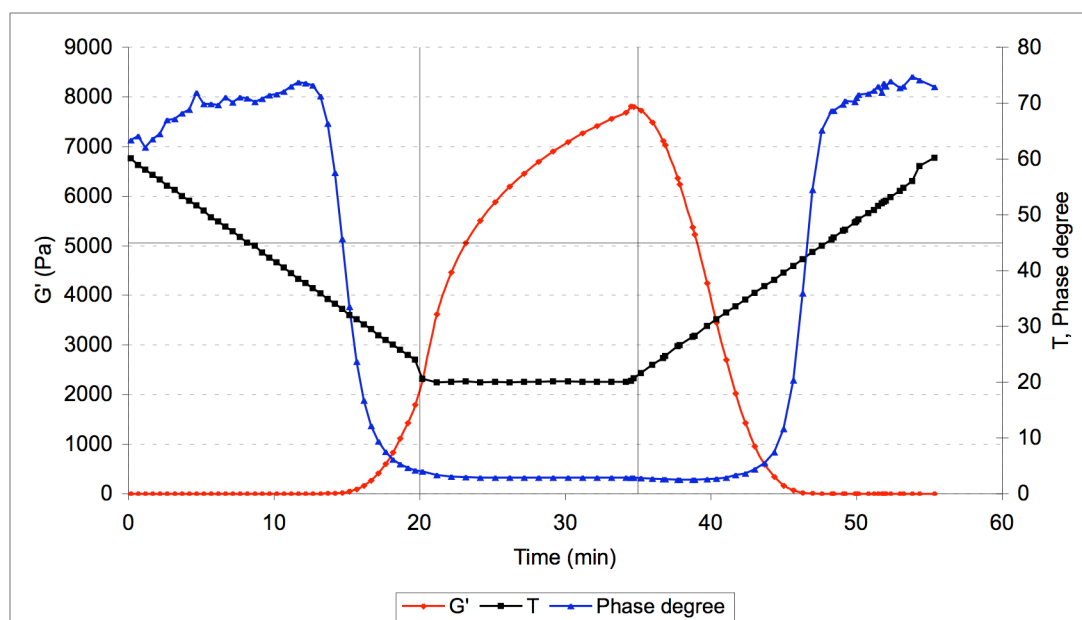


Figure E1. Example plot from small strain oscillatory measurement of Concordix matrix with 160g Bloom, type A gelatin and 0 wt % oil. Storage modulus (G') is given as a function of time on the primary y-axis, and temperature (T) and phase degree as a function of time on the secondary y-axis. The vertical, grey lines are marking the transition from, cooling, holding and heating periods (from left to right), and the horizontal grey line shows the phase degree of 45° .

E1. Storage modulus

The storage modulus (G') is the peak value at 20°C, as shown in figure E1 above, and the value of G' was extracted from the result table obtained from *Rheoexplorer*. Table E1.1 gives the values of G' for Concordix matrices with gelatin 160g Bloom, type A and B, and different weight percentages (wt %) of corn oil.

Table E1.1 Storage modulus (G') for Concordix matrices containing 0, 10, 30 and 50 wt % corn oil, gelatin 160g Bloom, type A and B (N=6), average G' and standard deviation (S.D.).

Gel type and oil (%)	G'1 (Pa)	G'2 (Pa)	G'3 (Pa)	G'4 (Pa)	G'5 (Pa)	G'6 (Pa)	Average G' (Pa)	S.D. (Pa)
Type A, 0	7814	7288	6839	6739	6987	6698	7061	426
Type B, 0	7129	8480	6772	7097	6636	5627	6957	925
Type A, 10	8769	9284	10080	6932	7340	8156	8427	1189
Type B, 10	7819	8099	7839	7530	7122	7999	7735	357
Type A, 30	11090	12180	13150	12270	10730	13260	12113	1037
Type B, 30	11020	10990	10750	11360	11320	11140	11097	227
Type A, 50	21690	19860	20200	23050	17010	17760	19928	2287
Type B, 50	16660	15280	15000	12950	15400	14820	15018	1202

E2. Gelling temperature

The gelling temperature (T_g) is the temperature corresponding to the phase degree of 45°, obtained from the cooling period, found by interpolation of phase angles and corresponding temperatures at the two measured points above and below phase angle of 45°. The interpolation was performed when a phase angle of exactly 45° was not obtained as a measurement point. Table E2.1 gives the values of T_g for Concordix matrices with gelatin 160g Bloom, type A and B, and different weight percentages of corn oil.

Table E2.1. Gelling temperature (T_g) for Concordix matrices containing 0, 10, 30 and 50 wt % corn oil, gelatin 160g Bloom, type A and B (N=6), average G' and standard deviation (S.D.).

Gel type and oil (%)	T_g 1 (°C)	T_g 2 (°C)	T_g 3 (°C)	T_g 4 (°C)	T_g 5 (°C)	T_g 6 (°C)	Average T_g (°C)	S.D. (°C)
Type A, 0	33.1	33.3	32.9	32.9	33.0	32.8	33.0	0.2
Type B, 0	35.0	35.7	34.5	34.8	34.7	34.4	34.9	0.5
Type A, 10	32.4	32.4	32.3	32.2	32.6	32.4	32.4	0.1
Type B, 10	34.9	34.8	34.5	34.1	34.3	34.4	34.5	0.3
Type A, 30	38.1	38.9	39.2	36.6	37.0	36.2	37.7	1.2
Type B, 30	36.4	36.0	36.2	35.1	34.6	34.6	35.5	0.8

E3. Melting temperature

The melting temperature (T_m) is the temperature corresponding to the phase degree of 45°, obtained from the heating period, found as described in section E.2.1 above. Table E.3.1 gives the values of T_m for Concordix matrices with gelatin 160g Bloom, type A and B, and different weight percentages of corn oil.

Table E3.1. Melting temperature (T_m) for Concordix matrices containing 0, 10, 30 and 50 wt % corn oil, gelatin 160g Bloom, type A and B (N=6), average G' and standard deviation (S.D.).

Gel type and oil (%)	T_{m1} (°C)	T_{m2} (°C)	T_{m3} (°C)	T_{m4} (°C)	T_{m5} (°C)	T_{m6} (°C)	Average T_m (°C)	S.D. (°C)
Type A, 0	42.6	42.7	42.3	42.3	42.4	42.4	42.4	0.2
Type B, 0	43.9	44.3	43.5	43.7	43.6	43.0	43.6	0.4
Type A, 10	41.8	41.7	41.8	41.4	41.9	41.8	41.7	0.2
Type B, 10	43.9	43.6	43.3	43.3	43.5	43.7	43.5	0.2
Type A, 30	51.9	53.4	53.2	51.0	51.7	50.2	51.9	1.2
Type B, 30	45.1	44.7	45.1	44.6	48.3	44.0	45.3	1.5

Appendix F: Longitudinal deformation

F1. Instrument information

A texture analyzer (TA.XT.-Plus Texture Analyser, Stable Micro Systems, serial number: 11085, Surrey, UK) were utilized to determine Young's modulus, force and strain at break for Concordix gels. The instrument was coupled to the software "Exponent", which was used for data acquisition and analysis. A 5 kg load cell was used for all measurements.

F2. Settings

F2.1. Young's modulus

Young's modulus was found by detecting the gradient (N/m) by compression of Concordix gels with a 50 mm diameter cylindrical probe (p/50). The parameter settings used are given in table F2.1.

Table F2.1. Settings used for Young's modulus measurement.

Parameter	Value
Test mode	Compression
Load cell	5 kg
Test speed	0.1 mm/sec
Target mode	Distance (mm)
Distance	2 mm
Trigger type	Auto (force)
Trigger force	1.5 g

F2.2. Break

Force and strain at break was obtained with a 2 mm penetration probe (p/2). The parameter settings used are given in table F.2.2

Table F.2.2. Settings used for measurements of force and strain at break.

Parameter	Value
Test mode	Compression
Load cell	5 kg
Test speed	0.1 mm/sec
Target mode	Distance (mm)
Distance	18 mm
Trigger type	Auto (force)
Trigger force	1.5 g

F3. Example calculations

F3.1. Young's modulus

Equations 2.1 and 2.2 from the main report were used to calculate Young's modulus. Force (N) as function of distance (mm) was registered from the compression of Concordix gels, and the software provided a force-distance curve. A macro was programmed to find the gradient, $F/\Delta L$ (N/m) from the curve, by determining the slope in the region of 0.10-0.15 mm. Linear regression ($y=Ax+B$) was performed to ensure that the region was linear, and R^2 values above 0.98 were considered to be linear, and was included in the result. The gel heights (L_0) and diameters (d) were measured with a digital caliper, however the height was also measured by the probe, and the value registered by the probe was used in the calculations of Young's moduli. An example calculation is presented below, for sample 1 in table F4.1:

Height = 0.01937 m

Diameter = 0.017 m

$$Area = A_0 = \pi \left(\frac{d}{2} \right)^2 = \pi \left(\frac{0.017}{2} \right)^2 = 0.000227 m^2$$

$$Gradient = 245.9 \frac{N}{m}$$

$$E = 245.9 \frac{N}{m} \left(\frac{0.01937}{0.000227 m^2} \right) \approx 20983 \frac{N}{m^2} = 20,98 kPa$$

F3.2. Force at break

The software determined force at break as the first peak obtained from the force-distance curve, which corresponds to the first break in the gel. The force at break appeared automatically in the result file.

F3.3. Strain at break

Strain at break is the deformation at break, and was found by dividing the distance at break (mm) by the original height of the gel, and multiplied by 100 to obtain a percentage deformation. An example calculation is presented below, for sample 3 in table F4.7:

Height = 19.373 mm

Diameter = 7.634 mm

$$Strain(\%) = \frac{7.634 mm}{19.373 mm} = 0.394 \times 100 = 39.4\%$$

F4. Data

F4.1. Young's modulus

The original height (L_0), diameter (d), area (A), gradient and calculated values for Young's modulus (E) are presented in table F.4.1-F.4.6.

Table F4.1. Calculation of Young's modulus (E) from texture analyzing of Concordix gels containing 0 wt % corn oil, gelatin 160g Bloom, type A (N=4).

Sample	L_0 (m)	d (m)	A (m^2)	Gradient (N/m)	E (kPa)
1	0.01937	0.0170	0.000227	245.9	20.98
2	0.01959	0.0170	0.000227	205.8	17.76
3	0.01947	0.0168	0.0002217	212.4	18.65
6	0.01965	0.0170	0.000227	191.6	16.56
Average					18.49
\pm S.D.					1.87

Table F4.2. Calculation of Young's modulus (E) from texture analyzing of Concordix gels containing 0 wt % corn oil, gelatin 160g Bloom, type B (N=7).

Sample	L_0 (m)	D (m)	A (m^2)	Gradient (N/m)	E (kPa)
2	0.01929	0.017	0.000227	225.3	19.15
3	0.01977	0.017	0.000227	235.7	20.53
4	0.01987	0.017	0.000227	236.0	20.66
6	0.01986	0.017	0.000227	238.0	20.82
7	0.01997	0.017	0.000227	237.2	20.87
8	0.01985	0.017	0.000227	185.8	16.25
9	0.01973	0.017	0.000227	228.0	19.82
Average					19.73
\pm S.D.					1.66

Table F4.3. Calculation of Young's modulus (E) from texture analyzing of Concordix gels containing 10 wt % corn oil, gelatin 160g Bloom, type A (N=8).

Sample	L_0 (m)	D (m)	A (m^2)	Gradient (N/m)	E (kPa)
2	0.019565	0.0169	0.0002243	179.2	15.63
3	0.019466	0.017	0.000227	132.7	11.38
5	0.019082	0.017	0.000227	154.9	13.02
6	0.019219	0.0168	0.0002217	232.3	20.14
7	0.019523	0.0168	0.0002217	201.3	17.73
8	0.019455	0.01685	0.000223	196.9	17.18
9	0.019209	0.0167	0.000219	146.0	12.81
10	0.019543	0.0167	0.000219	212.4	18.95
Average					15.86
\pm S.D.					3.18

Table F.4.4. Calculation of Young's modulus (E) from texture analyzing of Concordix gels containing 10 wt % corn oil, gelatin 160g Bloom, type B ($N=7$).

Sample	L_0 (m)	D (m)	A (m^2)	Gradient (N/m)	E (kPa)
2	0.019348	0.0168	0.0002217	258.8	22.59
3	0.019259	0.0167	0.000219	263.2	23.15
6	0.019317	0.01675	0.0002204	296.4	25.98
7	0.019596	0.0165	0.0002138	163.7	15.00
8	0.019248	0.0165	0.0002138	174.8	15.73
9	0.019369	0.0167	0.000219	185.8	16.43
10	0.019461	0.0167	0.000219	179.2	15.92
Average					19.26
\pm S.D.					4.49

Table F4.5. Calculation of Young's modulus (E) from texture analyzing of Concordix gels containing 30 wt % corn oil, gelatin 160g Bloom, type A ($N=8$).

Sample	L_0 (m)	D (m)	A (m^2)	Gradient (N/m)	E (kPa)
1	0.01986	0.0168	0.0002217	305.3	27.35
3	0.019837	0.0166	0.0002164	252.2	23.12
4	0.019752	0.0165	0.0002138	221.2	20.44
5	0.019672	0.0166	0.0002164	380.5	34.59
6	0.019712	0.01645	0.0002125	367.2	34.06
7	0.019753	0.01645	0.0002125	380.5	35.37
8	0.019518	0.0167	0.000219	396.0	35.29
10	0.019485	0.0168	0.0002217	373.9	32.86
Average					30.39
\pm S.D.					5.94

Table F4.6. Calculation of Young's modulus (E) from texture analyzing of Concordix gels containing 30 wt % corn oil, gelatin 160g Bloom, type B ($N=8$).

Sample	L_0 (m)	D (m)	A (m^2)	Gradient (N/m)	E (kPa)
1	0.019426	0.0163	0.0002087	134.9	12.56
3	0.019471	0.0167	0.000219	267.7	23.80
5	0.019602	0.01665	0.0002177	269.9	24.30
6	0.019642	0.0167	0.000219	320.8	28.77
7	0.019714	0.0167	0.000219	329.6	29.67
8	0.019521	0.01665	0.0002177	194.7	17.46
9	0.01944	0.01665	0.0002177	150.4	13.43
10	0.019617	0.0165	0.0002138	294.2	26.99
Average					22.12
\pm S.D.					6.77

F4.2. Force and strain at break

The original height (L_0), diameter (d), area (A), and force and strain at break are presented in table F.4.7-F.4.12.

Table F4.7. Calculation of force and strain at break from texture analyzing of Concordix gels containing 0 wt % corn oil, gelatin 160g Bloom, type A (N=4).

Sample	Highth (mm)	Distance (mm)	Strain (%)	Force (N)
1	19.314	6.934	35.9	0.837
2	19.389	7.448	38.4	0.915
3	19.373	7.634	39.4	0.970
6	19.373	6.972	36.0	0.835
Aveage			37.4	0.890
±S.D.			1.8	0.065

Table F4.8. Calculation of force and strain at break from texture analyzing of Concordix gels containing 0 wt % corn oil, gelatin 160g Bloom, type B (N=7).

Sample	Highth (mm)	Distance (mm)	Strain (%)	Force (N)
2	19.616	7.722	39.4	1.023
3	19.720	7.153	36.3	1.070
4	19.628	7.009	35.7	0.858
6	19.759	7.278	36.8	0.877
7	19.874	7.366	37.1	0.925
8	19.687	7.345	37.3	0.906
9	19.612	7.925	40.4	0.956
Aveage			37.6	0.945
±S.D.			1.7	0.077

Table F4.9. Calculation of force and strain at break from texture analyzing of Concordix gels containing 10 wt % corn oil, gelatin 160g Bloom, type A (N=8).

Sample	Highth (mm)	Distance (mm)	Strain (%)	Force (N)
2	19.110	5.741	30.0	0.616
3	19.565	5.454	27.9	0.533
5	19.466	5.343	27.4	0.546
6	19.082	5.754	30.2	0.539
7	19.219	5.706	29.7	0.591
8	19.455	5.858	30.1	0.585
9	19.209	6.054	31.5	0.576
10	19.543	5.982	30.6	0.554
Aveage			29.7	0.567
±S.D.			1.4	0.029

Table F4.10. Calculation of force and strain at break from texture analyzing of Concordix gels containing 10 wt % corn oil, gelatin 160g Bloom, type B (N=7).

Sample	Highth (mm)	Distance (mm)	Strain (%)	Force (N)
2	19.202	7.934	41.3	1.152
3	19.348	7.823	40.4	1.055
6	19.259	7.932	41.2	1.100
7	20.265	8.678	42.8	1.326
8	19.416	8.776	45.2	1.330
9	19.317	8.748	45.3	1.329
10	19.596	9.076	46.3	1.384
Average			42.7	1.206
±S.D.			2.7	0.155

Table F4.11. Calculation of force and strain at break from texture analyzing of Concordix gels containing 30 wt % corn oil, gelatin 160g Bloom, type A (N=8).

Sample	Highth (mm)	Distance (mm)	Strain (%)	Force (N)
1	19.860	4.278	21.5	0.644
3	19.837	4.689	23.6	0.641
4	19.752	4.994	25.3	0.689
5	19.672	4.890	24.9	0.690
6	19.712	4.771	24.2	0.660
7	19.753	5.083	25.7	0.735
8	19.474	4.646	23.9	0.625
10	19.485	4.580	23.5	0.722
Average			24.1	0.676
±S.D.			1.3	0.040

Table F4.12. Calculation of force and strain at break from texture analyzing of Concordix gels containing 30 wt % corn oil, gelatin 160g Bloom, type B (N=8).

Sample	Highth (mm)	Distance (mm)	Strain (%)	Force (N)
1	19.426	6.996	36.0	1.078
3	19.732	5.051	25.6	0.659
5	19.753	7.344	37.2	1.160
6	19.602	6.227	31.8	0.876
7	19.642	7.573	38.6	0.995
8	19.714	6.826	34.6	1.212
9	19.44	7.479	38.5	1.190
10	19.617	6.580	33.5	0.964
Average			34.5	1.017
±S.D.			4.3	0.186

Appendix G: *In vitro* dissolution studies of Concordix matrices

G1. Data

The dissolution studies were performed as two independent experiments, each with two replications for type A gelatin and two replications for type B gelatin (N=2), for Concordix matrices with 0, 10, 30 and 50 wt % corn oil. Two replications of A and two replications of B were studied at the same time in the dissolution unit. Together the two independent experiments gave four replications for each gelatin type. The absorbance was measured at 243.3 nm to find the amount of acetaminophen released from the matrices, and standard curves were used to determine the corresponding percentage release. The standard curves were made from a stock solution of acetaminophen (see appendix A, section A3). The stock solution was used to make five dilutions (1:50, 1:40, 1:30, 1:20 and 1:10). A blank sample with gelatin, sucralose and citric acid was subtracted from the measured absorbance of each sample, to avoid contribution to the absorbance.

Section G.1.1-4 presents the raw data and percentage concentration of acetaminophen, corresponding to the dissolved Concordix matrix, for gels with 0, 10, 30 and 50 wt % oil, respectively. Calculation examples and standard curves are also presented for each gel.

G1.1. Concordix without oil

Table G1.1: Dissolution study of Concordix matrices with gelatin 160g Bloom, type A and B, and 0 wt % oil (N=2). Independent study #1.

	Absorbance (nm)	Subtracting the blank sample A or B	Percentage dissolved acetaminophen
Blank	0.001		
Blank	0		
Standard curve (1:50)	0.1555		
Standard curve (1:40)	0.2076		
Standard curve (1:30)	0.2773		
Standard curve (1:20)	0.4126		
Standard curve (1:10)	0.8243		
Blank	0		
Type A1 (1 min)	0.1314	0.0536	6.6626
Type A1 (6 min)	0.4844	0.4066	49.1928
Type A1 (11 min)	0.9139	0.8361	100.9398
Type A1 (16 min)	1.0759	0.9981	120.4578
Type A1 (21 min)	1.0902	1.0124	122.1807
Type A1 (26 min)	1.0905	1.0127	122.2169
Type A1 (36 min)	1.0912	1.0134	122.3012
Type A1 (46 min)	1.0913	1.0135	122.3132
Type A1 (56 min)	1.0924	1.0146	122.4458
Type A1 (66 min)	1.0936	1.0158	122.5904
Blank	0.0717		
Type A2 (1 min)	0.0941	0.0163	2.1687
Type A2 (6 min)	0.4686	0.3908	47.2892
Type A2 (11 min)	0.9036	0.8258	99.6988
Type A2 (16 min)	1.0663	0.9885	119.3012
Type A2 (21 min)	1.0846	1.0068	121.5060
Type A2 (26 min)	1.0846	1.0068	121.5060
Type A2 (36 min)	1.0869	1.0091	121.7831
Type A2 (46 min)	1.0879	1.0101	121.9036
Type A2 (56 min)	1.0897	1.0119	122.1205
Type A2 (66 min)	1.0915	1.0137	122.3373
Blank	0.0825		
Type B1 (1 min)	0.0874	0.0103	1.4458
Type B1 (6 min)	0.5003	0.4232	51.1928
Type B1 (11 min)	0.8944	0.8173	98.6747
Type B1 (16 min)	1.0555	0.9784	118.0843
Type B1 (21 min)	1.0743	0.9972	120.3494
Type B1 (26 min)	1.0755	0.9984	120.4940
Type B1 (36 min)	1.079	1.0019	120.9157
Type B1 (46 min)	1.0834	1.0063	121.4458
Type B1 (56 min)	1.0865	1.0094	121.8193
Type B1 (66 min)	1.0892	1.0121	122.1446
Blank	0.0828		
Type B2 (1 min)	0.0778	0.0007	0.2892
Type B2 (6 min)	0.4669	0.3898	47.1687
Type B2 (11 min)	0.8742	0.7971	96.2410
Type B2 (16 min)	1.0782	1.0011	120.8193
Type B2 (21 min)	1.1005	1.0234	123.5060
Type B2 (26 min)	1.103	1.0259	123.8072
Type B2 (36 min)	1.1055	1.0284	124.1084

Type B2 (46 min)	1.1078	1.0307	124.3855
Type B2 (56 min)	1.1107	1.0336	124.7349
Type B2 (66 min)	1.1152	1.0381	125.2771
Blank	0		
Blank A	0.0778		
Blank B	0.0771		

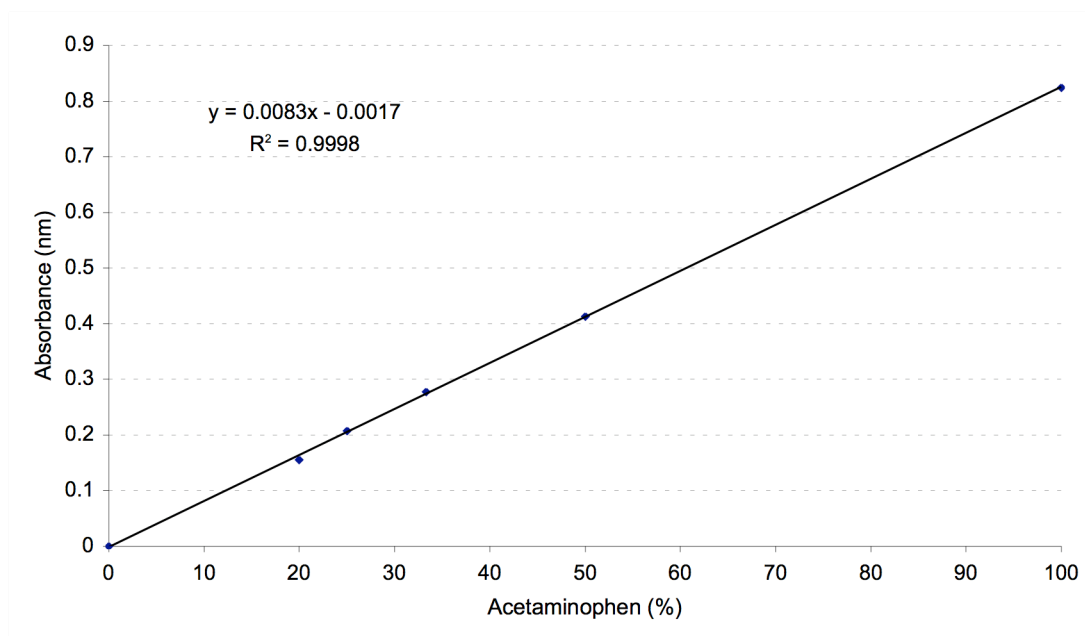


Figure G1.1. Absorbance (nm) as function of known concentrations of acetaminophen, giving a standard curve.

Table G1.2. Dissolution study of Concordix matrices with gelatin 160g Bloom, type A and B, and 0 wt % oil (N=2). Independent study #2.

	Absorbance (nm)	Subtracting the blank sample A or B	Percentage dissolved acetaminophen
Blank	0		
Blank	0		
Standard curve (1:50)	0.1626		
Standard curve (1:40)	0.2043		
Standard curve (1:30)	0.271		
Standard curve (1:20)	0.4087		
Standard curve (1:10)	0.8197		
Blank	0		
Type A1 (1 min)	0.1184	0.0406	5.0854
Type A1 (6 min)	0.5543	0.4765	58.2439
Type A1 (11 min)	0.9546	0.8768	107.0610
Type A1 (16 min)	1.0259	0.9481	115.7561
Type A1 (21 min)	1.0425	0.9647	117.7805
Type A1 (26 min)	1.0453	0.9675	118.1220
Type A1 (36 min)	1.043	0.9652	117.8415
Type A1 (46 min)	1.0449	0.9671	118.0732
Type A1 (56 min)	1.0469	0.9691	118.3171
Type A1 (66 min)	1.0396	0.9618	117.4268
Blank	0.0827		
Type A2 (1 min)	0.1007	0.0229	2.9268
Type A2 (6 min)	0.5745	0.4967	60.7073
Type A2 (11 min)	0.9438	0.866	105.7439
Type A2 (16 min)	0.9985	0.9207	112.4146
Type A2 (21 min)	1.0069	0.9291	113.4390
Type A2 (26 min)	1.0045	0.9267	113.1463
Type A2 (36 min)	1.0257	0.9479	115.7317
Type A2 (46 min)	1.028	0.9502	116.0122
Type A2 (56 min)	1.0388	0.961	117.3293
Type A2 (66 min)	1.0368	0.959	117.0854
Blank	0		
Type B1 (1 min)	0.1219	0.0448	5.5976
Type B1 (6 min)	0.4955	0.4184	51.1585
Type B1 (11 min)	0.8827	0.8056	98.3780
Type B1 (16 min)	0.973	0.8959	109.3902
Type B1 (21 min)	0.9863	0.9092	111.0122
Type B1 (26 min)	0.9815	0.9044	110.4268
Type B1 (36 min)	0.9778	0.9007	109.9756
Type B1 (46 min)	0.9802	0.9031	110.2683
Type B1 (56 min)	0.9812	0.9041	110.3902
Type B1 (66 min)	0.9824	0.9053	110.5366
Blank	0		
Type B2 (1 min)	0.1158	0.0387	4.8537
Type B2 (6 min)	0.525	0.4479	54.7561
Type B2 (11 min)	0.9113	0.8342	101.8659
Type B2 (16 min)	1.0015	0.9244	112.8659
Type B2 (21 min)	1.0059	0.9288	113.4024
Type B2 (26 min)	1.0125	0.9354	114.2073
Type B2 (36 min)	1.0065	0.9294	113.4756
Type B2 (46 min)	1.008	0.9309	113.6585
Type B2 (56 min)	1.0042	0.9271	113.1951

Type B2 (66 min)	1.0068	0.9297	113.5122
Blank	0.1097		
Blank A	0.0778		
Blank B	0.0771		

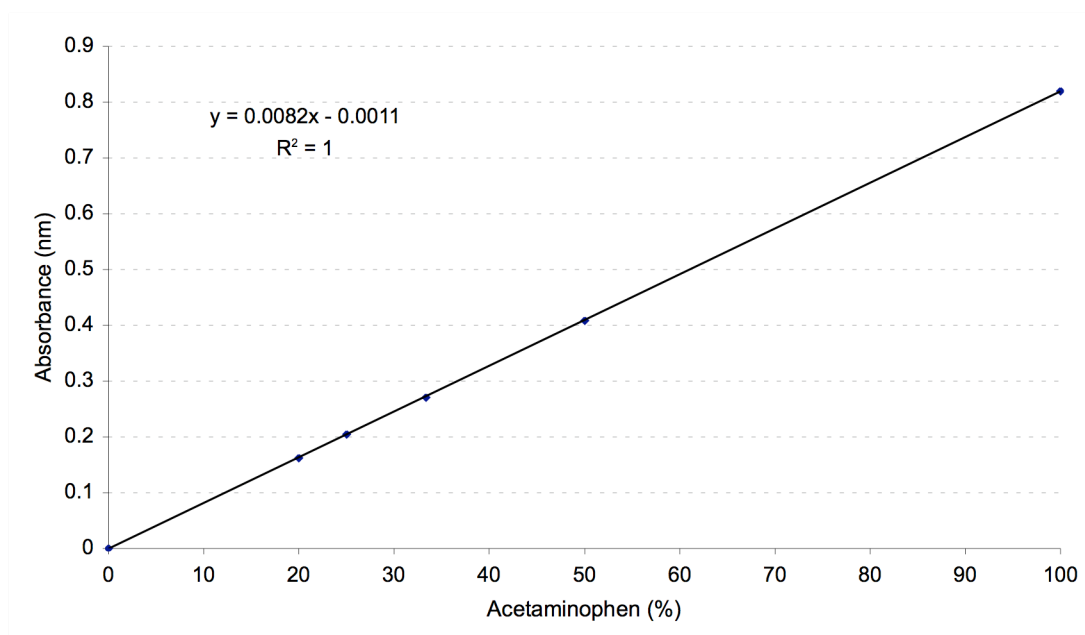


Figure G1.2: Absorbance (nm) as function of known concentrations of acetaminophen, giving a standard curve.

The equation in figure G1.1 was used to find the percentage acetaminophen dissolved from the matrixes at each measurement time in table G1.1, and the equation in figure G1.2 was used to find the percentage acetaminophen listed in table G1.2. An example is shown below.

Sample A1 (1 min) from table G2.2.

Absorbance: 0.1184

Subtracting the Blank A: $0.1184 - 0.0778 = 0.0406$

Finding the amount acetaminophen dissolved from the matrix:

$$0.0406 = 0.0082x - 0.0011$$

$$(0.0406 + 0.0011) / 0.0082 = 5.0854$$

For the measurement taken at 1 minute, the average acetaminophen dissolved was found by summarizing *Percentage dissolved acetaminophen* for A1 (1 min) and A2 (1 min) in table G1.1 and A1 (2 min) and A2 (2 min) in table G1.2, and dividing the number by four, as shown below:

Acetaminophen dissolved after 1 minute:

$$(6.6626 + 2.1687 + 5.0854 + 2.9268) / 4 = 4.2109$$

G1.2. Concordix with 10 wt % oil

Table G2.1. Dissolution study of Concordix matrices with 10 wt % corn oil and gelatin 160g Bloom, type A and B (N=2). Independent study #1.

	Absorbance (nm)	Subtracting the blank sample A or B	Percentage dissolved acetaminophen
Blank	0.002		
Blank	0.0014		
Standard curve (1:50)	0.1761		
Standard curve (1:40)	0.2217		
Standard curve (1:30)	0.2954		
Standard curve (1:20)	0.4407		
Standard curve (1:10)	0.8751		
Blank	0.0018		
Type A1 (2 min)	0.4378	0.3694	42.2299
Type A1 (6 min)	0.728	0.6596	75.5862
Type A1 (10 min)	0.9573	0.8889	101.9425
Type A1 (14 min)	1.0028	0.9344	107.1724
Type A1 (18 min)	1.013	0.9446	108.3448
Type A1 (23 min)	0.9985	0.9301	106.6782
Type A1 (28 min)	1.0019	0.9335	107.0690
Type A1 (38 min)	1.0051	0.9367	107.4368
Type A1 (48 min)	1.0021	0.9337	107.0920
Type A1 (58 min)	1.0071	0.9387	107.6667
Blank	0.0013		
Type A2 (2 min)	0.4116	0.3432	39.2184
Type A2 (6 min)	0.6858	0.6174	70.7356
Type A2 (10 min)	0.9555	0.8871	101.7356
Type A2 (14 min)	0.9977	0.9293	106.5862
Type A2 (18 min)	0.9954	0.927	106.3218
Type A2 (23 min)	1.0046	0.9362	107.3793
Type A2 (28 min)	1.0087	0.9403	107.8506
Type A2 (38 min)	1.0167	0.9483	108.7701
Type A2 (48 min)	1.0028	0.9344	107.1724
Type A2 (58 min)	1.0052	0.9368	107.4483
Blank	0.0018		
Type B1 (2 min)	0.3039	0.2326	26.5057
Type B1 (6 min)	0.6387	0.5674	64.9885
Type B1 (10 min)	0.92	0.8487	97.3218
Type B1 (14 min)	0.9879	0.9166	105.1264
Type B1 (18 min)	1.0011	0.9298	106.6437
Type B1 (23 min)	0.9964	0.9251	106.1034
Type B1 (28 min)	0.9962	0.9249	106.0805
Type B1 (38 min)	0.9973	0.926	106.2069
Type B1 (48 min)	0.9983	0.927	106.3218
Type B1 (58 min)	0.9946	0.9233	105.8966
Blank	0.0017		
Type B2 (2 min)	0.2982	0.2269	25.8506
Type B2 (6 min)	0.6581	0.5868	67.2184
Type B2 (10 min)	0.9384	0.8671	99.4368
Type B2 (14 min)	1.0005	0.9292	106.5747
Type B2 (18 min)	0.9982	0.9269	106.3103
Type B2 (23 min)	0.9992	0.9279	106.4253
Type B2 (28 min)	0.9993	0.928	106.4368

Type B2 (38 min)	0.9949	0.9236	105.9310
Type B2 (48 min)	0.9926	0.9213	105.6667
Type B2 (58 min)	0.9912	0.9199	105.5057
Blank	0.0004		
Blank A	0.0684		
Blank B	0.0713		

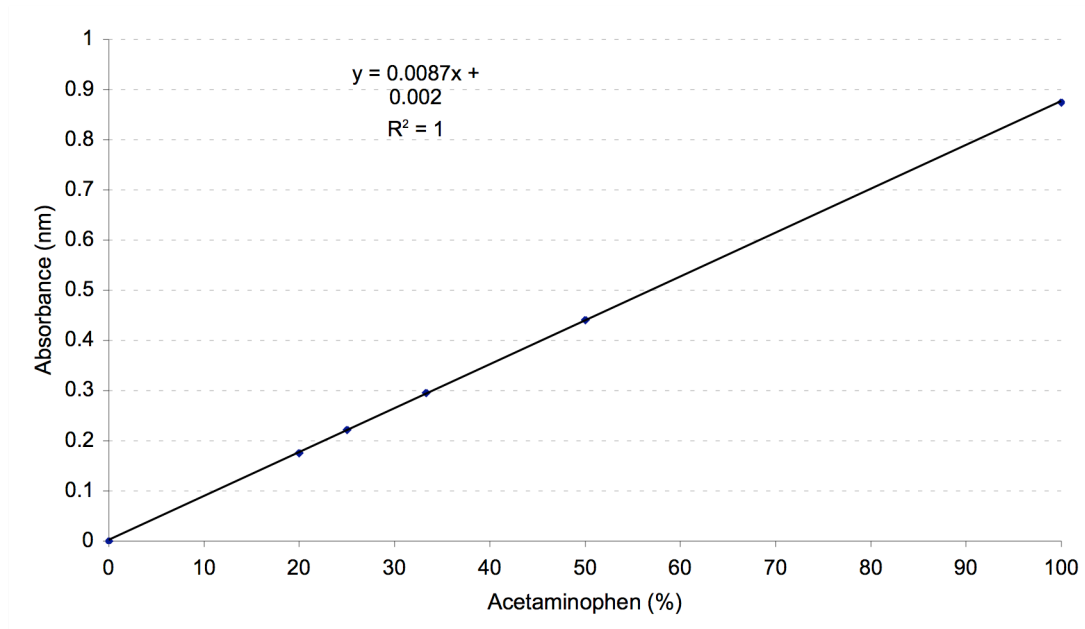


Figure G2.1. Absorbance (nm) as function of known concentrations of acetaminophen, giving a standard curve.

Table G2.2. Dissolution study of Concordix matrices with 10 wt % corn oil and gelatin 160g Bloom, type A and B (N=2). Independent study #2.

Sample	Absorbance (nm)	Subtracting the blank sample A or B	Percentage dissolved acetaminophen
Blank	0.0014		
Blank	0.0011		
Standard curve (1:50)	0.1759		
Standard curve (1:40)	0.2194		
Standard curve (1:30)	0.2947		
Standard curve (1:20)	0.4369		
Standard curve (1:10)	0.8666		
Blank	0.0018		
Type A1 (2 min)	0.1749	0.1065	11.9080
Type A1 (6 min)	0.4276	0.3592	40.9540
Type A1 (10 min)	0.6712	0.6028	68.9540
Type A1 (14 min)	0.8297	0.7613	87.1724
Type A1 (18 min)	0.9486	0.8802	100.8391
Type A1 (23 min)	0.9676	0.8992	103.0230
Type A1 (28 min)	0.9736	0.9052	103.7126
Type A1 (38 min)	0.982	0.9136	104.6782
Type A1 (48 min)	0.9861	0.9177	105.1494
Blank	0.0024		
Type A2 (2 min)	0.21	0.1416	15.9425
Type A2 (6 min)	0.4496	0.3812	43.4828
Type A2 (10 min)	0.6895	0.6211	71.0575
Type A2 (14 min)	0.8714	0.803	91.9655
Type A2 (18 min)	0.9354	0.867	99.3218
Type A2 (23 min)	0.9407	0.8723	99.9310
Type A2 (28 min)	0.96	0.8916	102.1494
Type A2 (38 min)	0.953	0.8846	101.3448
Type A2 (48 min)	0.9548	0.8864	101.5517
Blank	0.002		
Type B1 (2 min)	0.2189	0.1476	16.6322
Type B1 (6 min)	0.4526	0.3813	43.4943
Type B1 (10 min)	0.6744	0.6031	68.9885
Type B1 (14 min)	0.8971	0.8258	94.5862
Type B1 (18 min)	0.9648	0.8935	102.3678
Type B1 (23 min)	0.9747	0.9034	103.5057
Type B1 (28 min)	0.9767	0.9054	103.7356
Type B1 (38 min)	0.9691	0.8978	102.8621
Type B1 (48 min)	0.9755	0.9042	103.5977
Blank	0.0031		
Type B2 (2 min)	0.1628	0.0915	10.1839
Type B2 (6 min)	0.4286	0.3573	40.7356
Type B2 (10 min)	0.7212	0.6499	74.3678
Type B2 (14 min)	0.9283	0.857	98.1724
Type B2 (18 min)	0.9615	0.8902	101.9885
Type B2 (23 min)	0.966	0.8947	102.5057
Type B2 (28 min)	0.9595	0.8882	101.7586
Type B2 (38 min)	0.9706	0.8993	103.0345
Type B2 (48 min)	0.9716	0.9003	103.1494
Blank	0.0027		
Blank A	0.0684		
Blank B	0.0713		

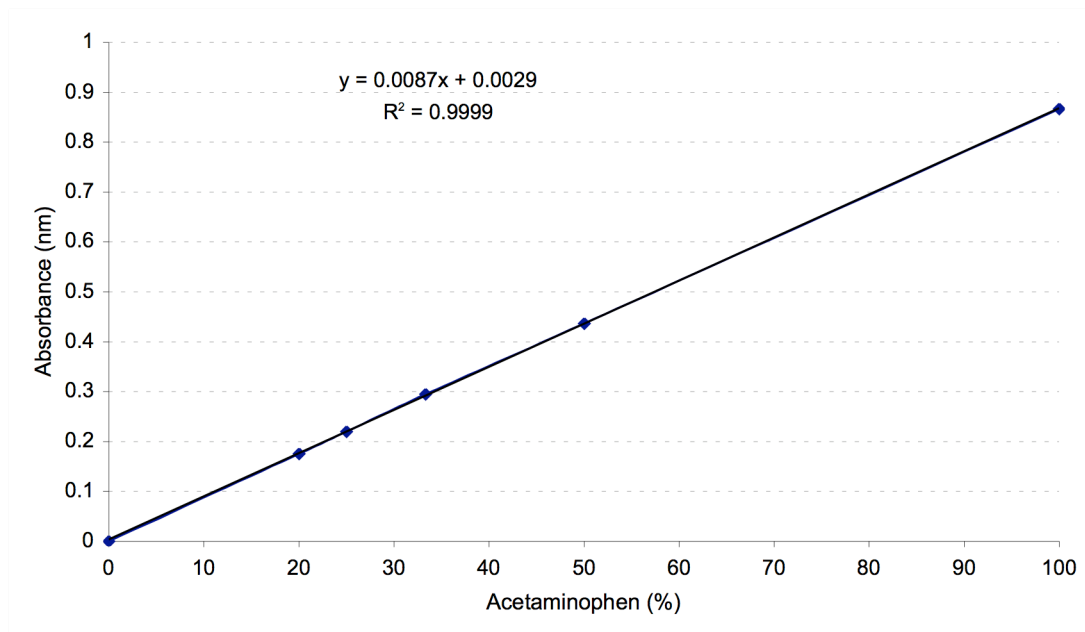


Figure G2.2. Absorbance (nm) as function of known concentrations of acetaminophen, giving a standard curve.

The equation in figure G2.1 was used to find the percentage acetaminophen dissolved from the matrixes at each measurement time in table G2.1, and the equation in figure G2.2 was used to find the percentage acetaminophen listed in table G2.2. An example is shown below.

Sample A1 (2 min) from table G2.2.

Absorbance: 0.1749

Subtracting the Blank A: $0.1749 - 0.0684 = 0.1065$

Finding the amount acetaminophen dissolved from the matrix:

$$0.1065 = 0.0087x + 0.0029$$

$$(0.1065 - 0.0029) / 0.0087 = 11.9080$$

For the measurement taken at 2 minutes, the average acetaminophen dissolved was found by summarizing *Percentage dissolved acetaminophen* for A1 (2 min) and A2 (2 min) in table G2.1 and A1 (2 min) and A2 (2 min) in table G2.2, and dividing the number by four, as shown below:

Acetaminophen dissolved after 2 minutes:

$$(42.2299 + 39.2184 + 11.9080 + 15.9425) / 4 = 27.3247$$

G1.3. Concordix with 30 wt % oil

Table G3.1. Dissolution study of Concordix matrices with 30 wt % corn oil and gelatin 160g Bloom, type A and B (N=2). Independent study #1.

	Absorbance (nm)	Subtracting the blank sample A or B	Percentage dissolved acetaminophen
Blank	0.0005		
Blank	0.0001		
Standard curve (1:50)	0.1729		
Standard curve (1:40)	0.2167		
Standard curve (1:30)	0.291		
Standard curve (1:20)	0.4341		
Standard curve (1:10)	0.8743		
Blank	0		
Type A1 (2 min)	0.1123	0.0535	6.3161
Type A1 (6 min)	0.1252	0.0665	7.7989
Type A1 (10 min)	0.1936	0.1349	15.6609
Type A1 (14 min)	0.2251	0.1664	19.2816
Type A1 (18 min)	0.2751	0.2164	25.0287
Type A1 (23 min)	0.3294	0.2707	31.2701
Type A1 (28 min)	0.4116	0.3529	40.7184
Type A1 (38 min)	0.5333	0.4746	54.7069
Type A1 (48 min)	0.6549	0.5962	68.6839
Type A1 (58 min)	0.7664	0.7077	81.5000
Type A1 (68 min)	0.9387	0.8800	101.3046
Blank	0.0007		
Type A2 (2 min)	0.1187	0.0600	7.0517
Type A2 (6 min)	0.1335	0.0748	8.7529
Type A2 (10 min)	0.178	0.1193	13.8678
Type A2 (14 min)	0.2266	0.1679	19.4540
Type A2 (18 min)	0.2789	0.2202	25.4655
Type A2 (23 min)	0.352	0.2933	33.8678
Type A2 (28 min)	0.4225	0.3638	41.9713
Type A2 (38 min)	0.5866	0.5279	60.8333
Type A2 (48 min)	0.7338	0.6751	77.7529
Type A2 (58 min)	0.8686	0.8099	93.2471
Type A2 (68 min)	1.019	0.9603	110.5345
Blank	0.0012		
Type B1 (2 min)	0.131	0.0766	8.9598
Type B1 (6 min)	0.3295	0.2751	31.7759
Type B1 (10 min)	0.5556	0.5012	57.7644
Type B1 (14 min)	0.7717	0.7173	82.6034
Type B1 (18 min)	0.904	0.8496	97.8103
Type B1 (23 min)	1.0073	0.9529	109.6839
Type B1 (28 min)	1.0201	0.9657	111.1552
Type B1 (38 min)	1.0356	0.9812	112.9368
Type B1 (48 min)	1.0269	0.9725	111.9368
Type B1 (58 min)	1.0319	0.9775	112.5115
Type B1 (68 min)	1.0312	0.9768	112.4310
Blank	0.0022		
Type B2 (2 min)	0.1201	0.0657	7.7069
Type B2 (6 min)	0.2854	0.2310	26.7069
Type B2 (10 min)	0.4821	0.4277	49.3161
Type B2 (14 min)	0.6839	0.6295	72.5115

Type B2 (18 min)	0.873	0.8186	94.2471
Type B2 (23 min)	0.9987	0.9443	108.6954
Type B2 (28 min)	1.0265	0.9721	111.8908
Type B2 (38 min)	1.0307	0.9763	112.3736
Type B2 (48 min)	1.0328	0.9784	112.6149
Type B2 (58 min)	1.0509	0.9965	114.6954
Type B2 (68 min)	1.0525	0.9981	114.8793
Blank	0.0005		
Blank A	0.0588		
Blank B	0.0545		

Table G3.2. Dissolution study of Concordix matrices with 30 wt % corn oil and gelatin 160g Bloom, type A and B (N=2). Independent study #2.

	Absorbance (nm)	Subtracting the blank sample A or B	Percentage dissolved acetaminophen
Blank	0.0048		
Blank	0.0025		
Standard curve (1:50)	0.1729		
Standard curve (1:40)	0.2167		
Standard curve (1:30)	0.291		
Standard curve (1:20)	0.4341		
Standard curve (1:10)	0.8743		
Blank	0.0035		
Type A1 (2 min)	0.1025	0.0438	5.1897
Type A1 (6 min)	0.134	0.0753	8.8103
Type A1 (10 min)	0.1686	0.1099	12.7874
Type A1 (14 min)	0.194	0.1353	15.7069
Type A1 (18 min)	0.2369	0.1782	20.6379
Type A1 (23 min)	0.2875	0.2288	26.4540
Type A1 (28 min)	0.3454	0.2867	33.1092
Type A1 (38 min)	0.4393	0.3806	43.9023
Type A1 (48 min)	0.5475	0.4888	56.3391
Type A1 (58 min)	0.6835	0.6248	71.9713
Type A1 (68 min)	0.824	0.7653	88.1207
Type A1 (78 min)	0.9509	0.8922	102.7069
Blank	0.0043		
Type A2 (2 min)	0.2113	0.1526	17.6954
Type A2 (6 min)	0.1804	0.1217	14.1437
Type A2 (10 min)	0.1905	0.1318	15.3046
Type A2 (14 min)	0.2313	0.1726	19.9943
Type A2 (18 min)	0.2787	0.2200	25.4425
Type A2 (23 min)	0.3373	0.2786	32.1782
Type A2 (28 min)	0.3935	0.3348	38.6379
Type A2 (38 min)	0.4914	0.4327	49.8908
Type A2 (48 min)	0.6053	0.5466	62.9828
Type A2 (58 min)	0.734	0.6753	77.7759
Type A2 (68 min)	0.8995	0.8408	96.7989
Type A2 (78 min)	0.9813	0.9226	106.2011
Blank	0.005		
Type B1 (2 min)	0.2389	0.1845	21.3621
Type B1 (6 min)	0.3255	0.2711	31.3161
Type B1 (10 min)	0.4975	0.4431	51.0862
Type B1 (14 min)	0.6681	0.6137	70.6954
Type B1 (18 min)	0.8203	0.7659	88.1897
Type B1 (23 min)	0.9554	0.9010	103.7184
Type B1 (28 min)	0.9939	0.9395	108.1437
Type B1 (38 min)	1.017	0.9626	110.7989
Type B1 (48 min)	1.0107	0.9563	110.0747
Type B1 (58 min)	1.019	0.9646	111.0287
Type B1 (68 min)	1.0129	0.9585	110.3276
Type B1 (78 min)	1.0193	0.9649	111.0632
Blank	0.0049		
Type B2 (2 min)	0.1459	0.0915	10.6724
Type B2 (6 min)	0.3396	0.2852	32.9368
Type B2 (10 min)	0.518	0.4636	53.4425

Type B2 (14 min)	0.6984	0.6440	74.1782
Type B2 (18 min)	0.8525	0.7981	91.8908
Type B2 (23 min)	0.9497	0.8953	103.0632
Type B2 (28 min)	0.9915	0.9371	107.8678
Type B2 (38 min)	0.9818	0.9274	106.7529
Type B2 (48 min)	1.0023	0.9479	109.1092
Type B2 (58 min)	0.9935	0.9391	108.0977
Type B2 (68 min)	0.9914	0.9370	107.8563
Type B2 (78 min)	1.0104	0.9560	110.0402
Blank	0.0041		
Blank A	0.0588		
Blank B	0.0545		

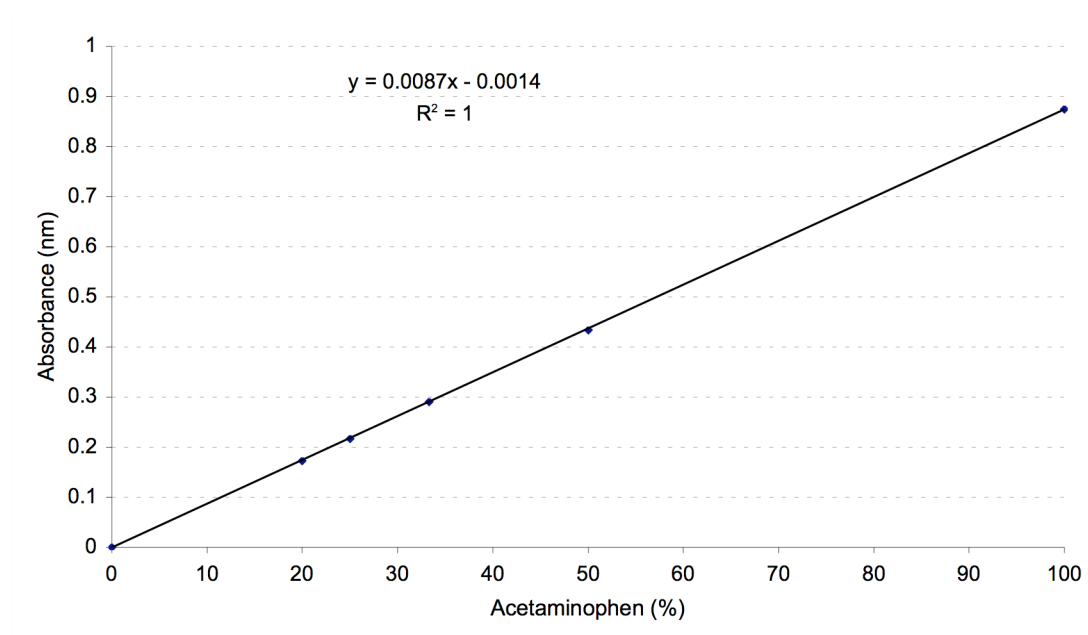


Figure G3.1. Absorbance (nm) as function of known concentrations of acetaminophen, giving a standard curve.

The equation in figure G3.1 was used to find the percentage acetaminophen dissolved from the matrixes at each measurement time. The same standard curve was used for the dissolution study performed 10.11 and 7.12. An example is shown below.

Sample A1 (2 min) from table G3.1.

Absorbance: 0.1123

Subtracting the Blank A: $0.1123 - 0.0588 = 0.0535$

Finding the amount acetaminophen dissolved from the matrix:

$$0.0535 = 0.0087x - 0.0014$$

$$(0.0535 + 0.0014) / 0.0087 = 6.31$$

For the measurement taken at 2 minutes, the average acetaminophen dissolved was found by summarizing *Percentage dissolved acetaminophen* for A1 (2 min) and A2 (2 min) in table G3.1 and A1 (2 min) and A2 (2 min) in table G3.2, and dividing the

number by four, as shown below:

Acetaminophen dissolved after 2 minutes:

$$(6.3161+7.0517+5.1897+17.6954)/4= 9.0632$$

G1.4. Concordix with 50 wt % oil

Table G4.1. Dissolution study of Concordix matrices with 50 wt % corn oil and gelatin 160g Bloom, type A and B (N=2). Independent study #1.

	Absorbance (nm)	Subtracting the blank sample A or B	Percentage dissolved acetaminophen
Blank	0.0054		
Blank	0.0039		
Standard curve (1:50)	0.1846		
Standard curve (1:40)	0.2321		
Standard curve (1:30)	0.3059		
Standard curve (1:20)	0.4584		
Standard curve (1:10)	0.9045		
Blank	0.0014		
Type A1 (2 min)	0.1578	0.1151	12.3444
Type A1 (7 min)	0.2884	0.2457	26.8556
Type A1 (12 min)	0.3818	0.3391	37.2333
Type A1 (17 min)	0.4571	0.4144	45.6000
Type A1 (22 min)	0.5132	0.4705	51.8333
Type A1 (27 min)	0.5678	0.5251	57.9000
Type A1 (37 min)	0.6495	0.6068	66.9778
Type A1 (47 min)	0.7298	0.6871	75.9000
Type A1 (57 min)	0.7815	0.7388	81.6444
Type A1 (67 min)	0.8377	0.795	87.8889
Type A1 (127 min)	0.9446	0.9019	99.7667
Type A1 (187 min)	1.0145	0.9718	107.5333
Type A1 (247 min)	1.1032	1.0605	117.3889
Blank	0.0014		
Type A2 (2 min)	0.1736	0.1309	14.1000
Type A2 (7 min)	0.2969	0.2542	27.8000
Type A2 (12 min)	0.3848	0.3421	37.5667
Type A2 (17 min)	0.4506	0.4079	44.8778
Type A2 (22 min)	0.5101	0.4674	51.4889
Type A2 (27 min)	0.5604	0.5177	57.0778
Type A2 (37 min)	0.6505	0.6078	67.0889
Type A2 (47 min)	0.7084	0.6657	73.5222
Type A2 (57 min)	0.7605	0.7178	79.3111
Type A2 (67 min)	0.7962	0.7535	83.2778
Type A2 (127 min)	0.9611	0.9184	101.6000
Type A2 (187 min)	1.0081	0.9654	106.8222
Type A2 (247 min)	1.0596	1.0169	112.5444
Blank	0.0021		
Type B1 (2 min)	0.129	0.089	9.4444
Type B1 (7 min)	0.3103	0.2703	29.5889
Type B1 (12 min)	0.5532	0.5132	56.5778
Type B1 (17 min)	0.8143	0.7743	85.5889
Type B1 (22 min)	0.9859	0.9459	104.6556
Type B1 (27 min)	1.2136	1.1736	129.9556
Type B1 (37 min)	1.4487	1.4087	156.0778
Type B1 (47 min)	1.3894	1.3494	149.4889
Type B1 (57 min)	1.5131	1.4731	163.2333
Type B1 (67 min)	1.4747	1.4347	158.9667
Type B1 (127 min)	1.0612	1.0212	113.0222
Type B1 (187 min)	1.1159	1.0759	119.1000

Type B1 (247 min)	1.1096	1.0696	118.4000
Blank	0.0016		
Type B2 (2 min)	0.1212	0.0812	8.5778
Type B2 (7 min)	0.2947	0.2547	27.8556
Type B2 (12 min)	0.5162	0.4762	52.4667
Type B2 (17 min)	0.6755	0.6355	70.1667
Type B2 (22 min)	0.902	0.862	95.3333
Type B2 (27 min)	1.0808	1.0408	115.2000
Type B2 (37 min)	1.372	1.332	147.5556
Type B2 (47 min)	1.4111	1.3711	151.9000
Type B2 (57 min)	1.3657	1.3257	146.8556
Type B2 (67 min)	1.3827	1.3427	148.7444
Type B2 (127 min)	1.0256	0.9856	109.0667
Type B2 (187 min)	1.0918	1.0518	116.4222
Type B2 (247 min)	1.1296	1.0896	120.6222
Blank	0		
Blank A	0.0427		
Blank B	0.0400		

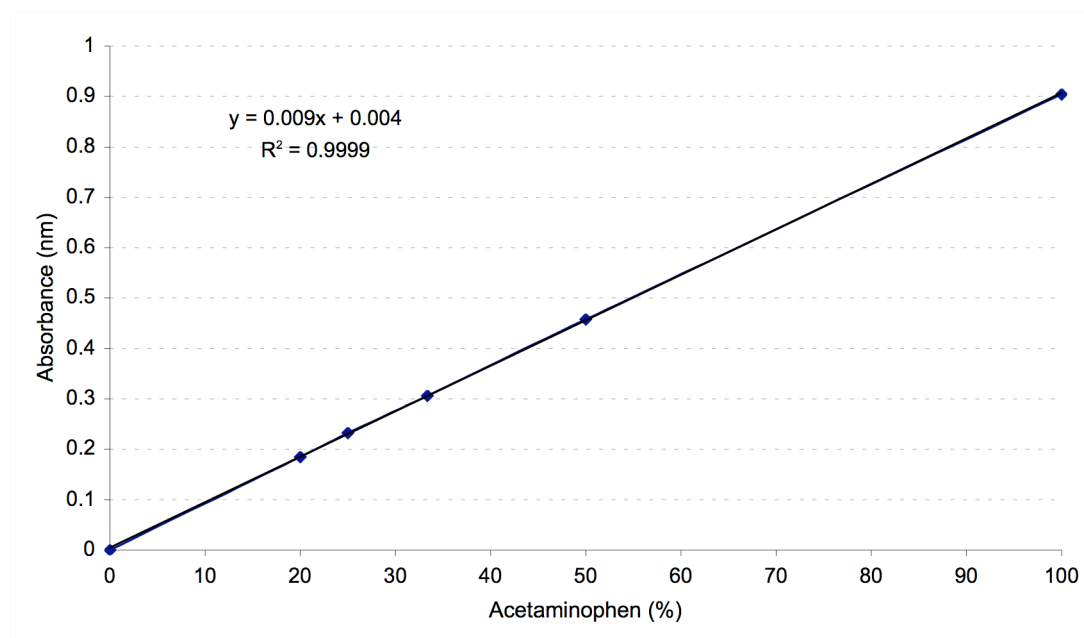


Figure G4.1. Absorbance (nm) as function of known concentrations of acetaminophen, giving a standard curve.

Table G4.2. Dissolution study of Concordix matrices with 50 wt % corn oil and gelatin 160g Bloom, type A and B (N=2). Independent study #2.

	Absorbance (nm)	Subtracting the blank sample A or B	Percentage dissolved acetaminophen
Blank	0.0040		
Blank	0.0044		
Standard curve (1:50)	0.1547		
Standard curve (1:40)	0.2083		
Standard curve (1:30)	0.2750		
Standard curve (1:20)	0.4078		
Standard curve (1:10)	0.7946		
Blank	0.1139		
Type A1 (2 min)	0.1151	0.0724	8.5250
Type A1 (7 min)	0.1650	0.1223	14.7625
Type A1 (12 min)	0.2115	0.1688	20.5750
Type A1 (17 min)	0.2570	0.2143	26.2625
Type A1 (22 min)	0.3031	0.2604	32.0250
Type A1 (27 min)	0.3393	0.2966	36.5500
Type A1 (37 min)	0.4019	0.3592	44.3750
Type A1 (47 min)	0.4638	0.4211	52.1125
Type A1 (57 min)	0.5199	0.4772	59.1250
Type A1 (67 min)	0.5677	0.525	65.1000
Type A1 (127 min)	0.7653	0.7226	89.8000
Type A1 (187 min)	0.9162	0.8735	108.6625
Type A1 (247 min)	1.0102	0.9675	120.4125
Blank	0.1285		
Type A2 (2 min)	0.1315	0.0888	10.5750
Type A2 (7 min)	0.2121	0.1694	20.6500
Type A2 (12 min)	0.2516	0.2089	25.5875
Type A2 (17 min)	0.2861	0.2434	29.9000
Type A2 (22 min)	0.3251	0.2824	34.7750
Type A2 (27 min)	0.3675	0.3248	40.0750
Type A2 (37 min)	0.4232	0.3805	47.0375
Type A2 (47 min)	0.4939	0.4512	55.8750
Type A2 (57 min)	0.5493	0.5066	62.8000
Type A2 (67 min)	0.5973	0.5546	68.8000
Type A2 (127 min)	0.7283	0.6856	85.1750
Type A2 (187 min)	0.8600	0.8173	101.6375
Type A2 (247 min)	1.0014	0.9587	119.3125
Blank	0.1573		
Type B1 (2 min)	0.1178	0.0778	9.2000
Type B1 (7 min)	0.2082	0.1682	20.5000
Type B1 (12 min)	0.3290	0.289	35.6000
Type B1 (17 min)	0.4850	0.445	55.1000
Type B1 (22 min)	0.6615	0.6215	77.1625
Type B1 (27 min)	0.8460	0.806	100.2250
Type B1 (37 min)	1.0655	1.0255	127.6625
Type B1 (47 min)	1.2235	1.1835	147.4125
Type B1 (57 min)	1.2756	1.2356	153.9250
Type B1 (67 min)	1.2761	1.2361	153.9875
Type B1 (127 min)	1.0412	1.0012	124.6250
Type B1 (187 min)	1.0432	1.0032	124.8750
Type B1 (247 min)	1.0730	1.033	128.6000
Blank	0.1373		

Type B2 (2 min)	0.1299	0.0899	10.7125
Type B2 (7 min)	0.2117	0.1717	20.9375
Type B2 (12 min)	0.3515	0.3115	38.4125
Type B2 (17 min)	0.4999	0.4599	56.9625
Type B2 (22 min)	0.6492	0.6092	75.6250
Type B2 (27 min)	0.7855	0.7455	92.6625
Type B2 (37 min)	0.9800	0.94	116.9750
Type B2 (47 min)	1.1029	1.0629	132.3375
Type B2 (57 min)	1.1798	1.1398	141.9500
Type B2 (67 min)	1.1873	1.1473	142.8875
Type B2 (127 min)	1.0421	1.0021	124.7375
Type B2 (187 min)	1.0476	1.0076	125.4250
Type B2 (247 min)	1.0654	1.0254	127.6500
Blank	0.1308		
Blank A	0.0427		
Blank B	0.0400		

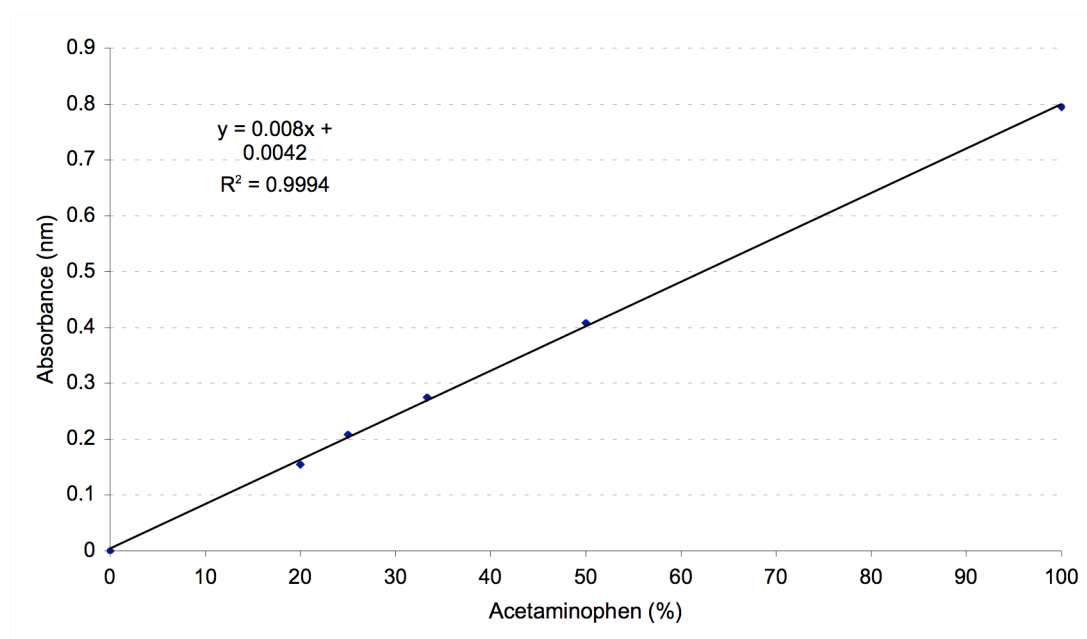


Figure G4.2. Absorbance (nm) as function of known concentrations of acetaminophen, giving a standard curve.

The equation in figure G4.1 was used to find the percentage acetaminophen dissolved from the matrixes at each measurement time in table G4.1, and the equation in figure G4.2 was used to find the percentage acetaminophen listed in table G4.2. An example is shown below.

Sample A1 (2 min) from table G4.2.

Absorbance: 0.1151

Subtracting the Blank A: $0.1151 - 0.0427 = 0.0724$

Finding the amount acetaminophen dissolved from the matrix:

$$0.0724 = 0.008x + 0.0042$$

$$(0.0724 - 0.0042) / 0.008 = 8.525$$

For the measurement taken at 2 minutes, the average acetaminophen dissolved was found by summarizing *Percentage dissolved acetaminophen* for A1 (2 min) and A2 (2 min) in table G4.1 and A1 (2 min) and A2 (2 min) in table G4.2, and dividing the number by four, as shown below:

Acetaminophen dissolved after 2 minutes:
 $(12.3444+14.1000+8.5250+10.5750)/4= 11.3861$

G2. Linear regression

The dissolution curves of the Concordix matrices (figure 3.5.1-3.5.4 in the main report) were subjected to linear regression in the initial linear region of the dissolution curves. This was performed in order to obtain the initial dissolution rate (dm/dt) for the Concordix matrices.

The initial dissolution rate for Concordix matrices with 0 wt % oil was found by linear regression between $t=1$ and $t=11$, figure G2.1.

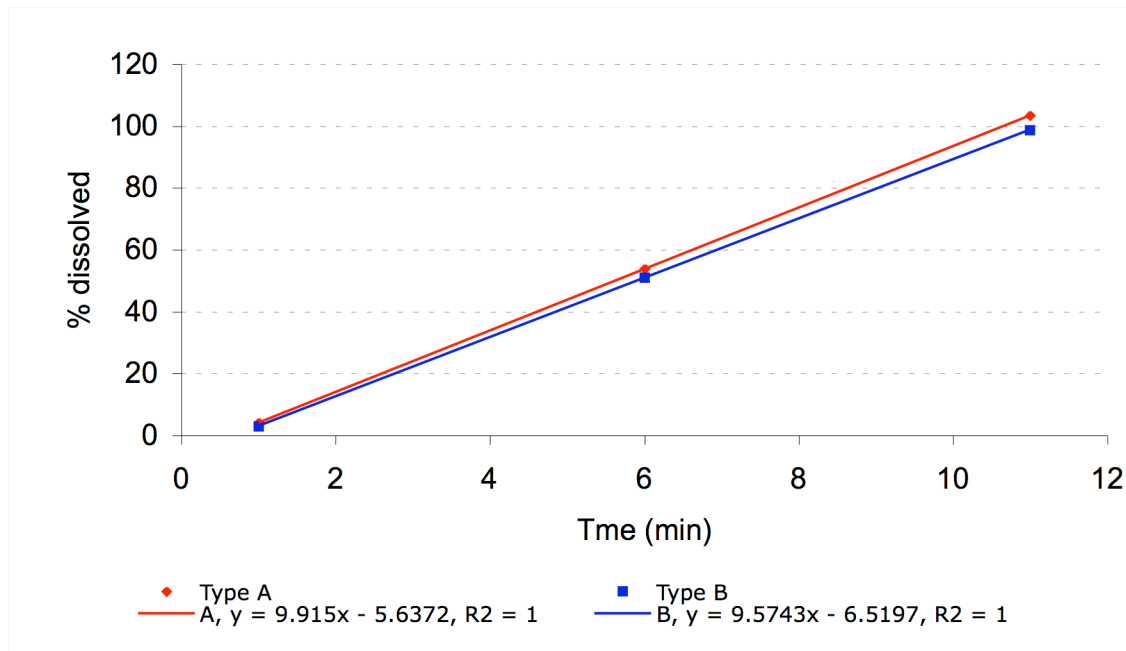


Figure G2.1. Linear regressions between $t=1$ and $t=11$ for Concordix matrices with 0 wt % oil, gelatin 160g Bloom, type A and B. The slope in the equations corresponds to the initial dissolution rate.

The initial dissolution rate for Concordix matrices with 10 wt % oil was found by linear regression between $t=2$ and $t=10$, figure G2.2.

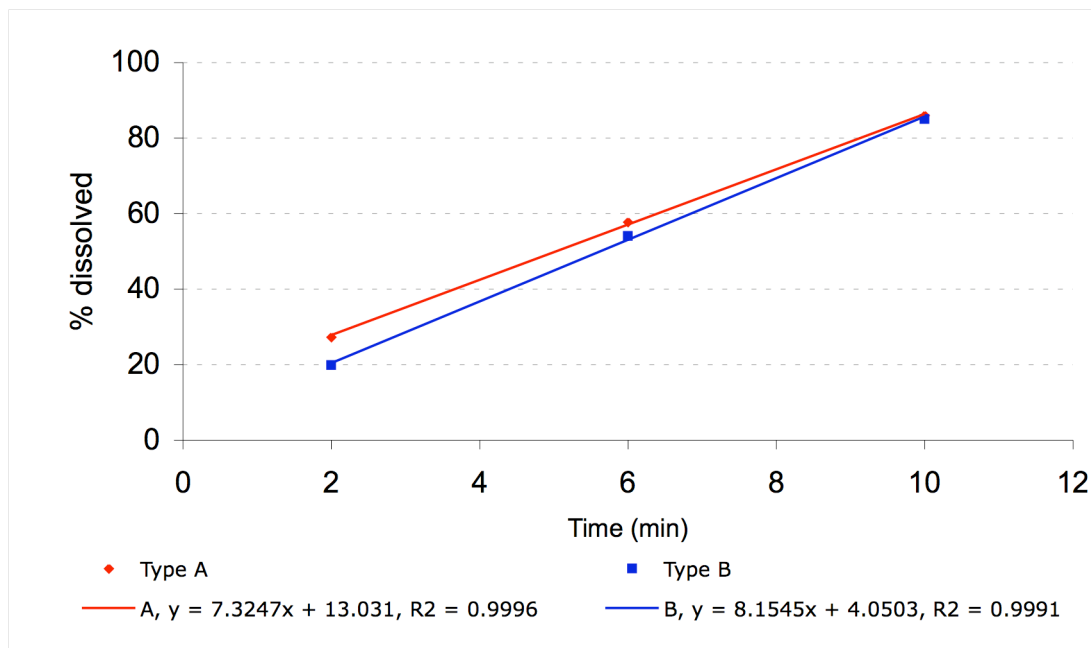


Figure G2.2. Linear regressions between $t=2$ and $t=10$ for Concordix matrices with 10 wt % oil, gelatin 160g Bloom, type A and B. The slope in the equations corresponds to the initial dissolution rate.

The initial dissolution rate for Concordix matrices with 30 wt % oil was found by linear regression between $t=6$ and $t=14$, figure G2.3.

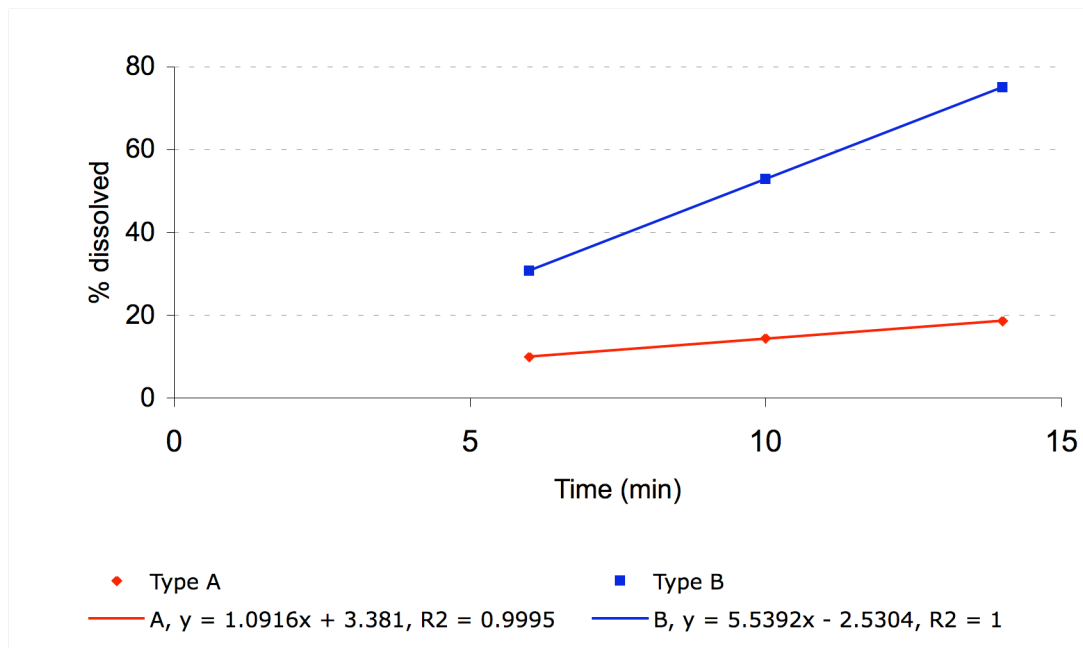


Figure G2.3. Linear regressions between $t=6$ and $t=14$ for Concordix matrices with 30 wt % oil, gelatin 160g Bloom, type A and B. The slope in the equations corresponds to the initial dissolution rate.

The initial dissolution rate for Concordix matrices with 50 wt % oil was found by linear regression between $t=2$ and $t=12$, figure G2.4.

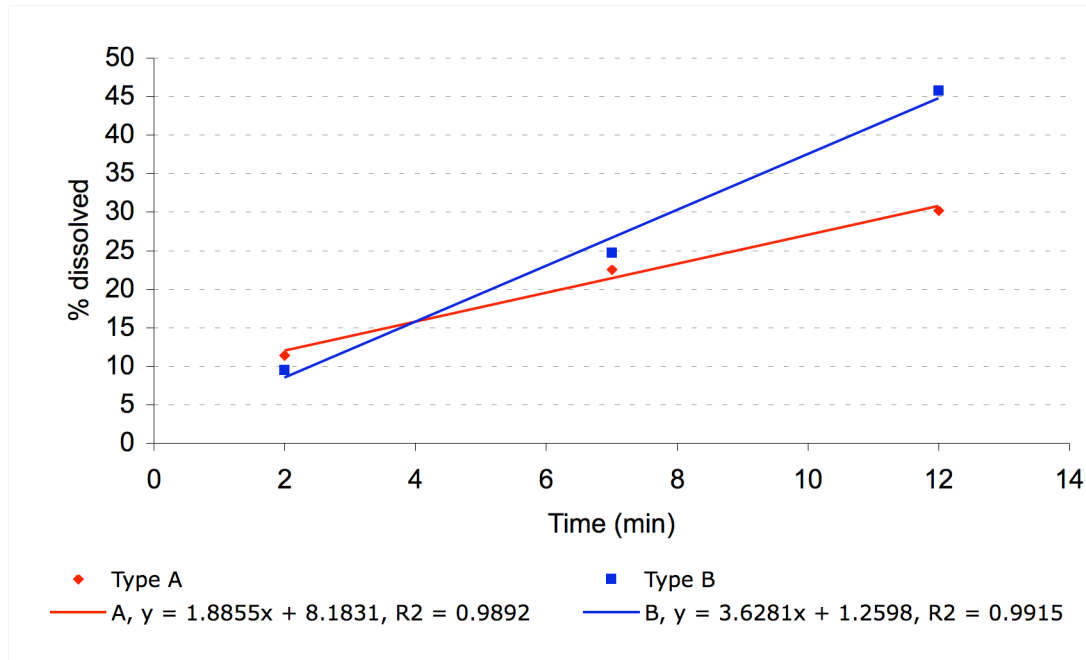


Figure G2.4. Linear regressions between $t=2$ and $t=12$ for Concordix matrices with 50 wt % oil, gelatin 160g Bloom, type A and B. The slope in the equations corresponds to the initial dissolution rate.

Appendix H: Stability study with double emulsions

H1. Data #1

Raw data from stability studies of w/o/w double emulsions made by *method I* (see section 2.2.8 in the main report) are given in table H1.1-2, together with % tartrazine released. The amount of tartrazine release was found for each sampling time by dividing the control on the negative control and multiplying with 100.

Table H1.1. Raw data from stability studies of w/o/w double emulsions stabilized with gelatin 226g Bloom, type B. Absorbance (nm), for control (C) and negative control (Neg), at every sampling day, together with the amount tartrazine released (%). Emulsions were made by method I.

Time (days)	C (nm)	Neg (nm)	Tartrazine Release (%)
0	0.0127	1.0365	1.2253
8	0.0075	1.0449	0.7178
15	0.0465	1.0404	4.4694
29	0.0199	1.0456	1.9032
43	0.0354	1.1484	3.0825
57	0.0403	1.1754	3.4286
78	0.0044	1.2280	0.3583

Table H1.2. Raw data from stability studies of w/o/w double emulsions stabilized with tween80. Absorbance (nm), for control (C) and negative control (Neg), at every sampling day, together with the amount tartrazine released (%). Emulsions were made by method I.

Time (days)	C (nm)	Neg (nm)	Tartrazine Release (%)
0	0.0028	0.9615	0.2912
8	0.0422	1.0548	4.0008
15	0.0047	1.0253	0.4584
29	0.0090	1.0294	0.8743
43	0.0146	1.0333	1.4129
57	0.0185	1.0454	1.7697
78	0.0133	1.0332	1.2873

H2. Data #2

Raw data from stability studies of w/o/w double emulsions is given in table H2.1-2, together with % tartrazine released. This data is from the result obtained for double emulsions made by *method II*, see section 2.2.8 in the main report. The amount of tartrazine release was found as described in H1.

Table H2.1. Raw data from stability studies of w/o/w double emulsions stabilized with gelatin 226g Bloom, type B. Absorbance (nm), for control (C) and negative control (Neg), at every sampling day, together with the amount tartrazine released (%). Emulsions were made by method II.

Time (days)	C (nm)	Neg (nm)	Tartrazine Release (%)
0	0.0057	0.9472	0.6018
8	0.0044	1.0099	0.4357
15	0.0035	1.0083	0.3471
29	0.0043	0.9927	0.4332
43	0.0014	1.4205	0.0986
57	0.0061	1.5267	0.3996
78	0.0044	1.1448	0.3843

Table H2.2. Raw data from stability studies of w/o/w double emulsions stabilized with tween80. Absorbance (nm), for control (C) and negative control (Neg), at every sampling day, together with the amount tartrazine released (%). Emulsions were made by method II.

Time (days)	C (nm)	Neg (nm)	Tartrazine Release (%)
0	0.0027	0.9585	0.2817
8	0.0056	0.9988	0.5607
15	0.0075	1.0101	0.7425
29	0.0098	1.0174	0.9632
43	0.0056	1.0188	0.5497
57	0.0157	1.0239	1.5334
78	0.0131	1.0315	1.267

H3. Data for Double emulsions dissolved at day 0

Raw data from stability studies of w/o/w double emulsions is given in table H3.1-2, together with % tartrazine released. These data are from the results obtained for double emulsions made by *method II* and dissolved at day 0, see section 2.2.8 in the main report. The amount of tartrazine release was found as described in H1.

Table H3.1. Raw data from stability studies of w/o/w double emulsions stabilized with gelatin 226g Bloom, type B. Absorbance (nm), for control (C) and negative control (Neg), at every sampling day, together with the amount tartrazine released (%). Emulsions were made by method II and dissolved at day 0.

Time (days)	C (nm)	Neg (nm)	Tartrazine Release (%)
0	0.0057	0.9472	0.6018
8	0.0064	0.9595	0.667
15	0.0098	0.9644	1.0162
29	0.0073	0.9602	0.7603
43	0.0044	0.9802	0.4489
57	0.0117	0.9763	1.1984
78	0.0126	0.987	1.2766

Table H3.2. Raw data from stability studies of w/o/w double emulsions stabilized with tween80. Absorbance (nm), for control (C) and negative control (Neg), at every sampling day, together with the amount tartrazine released (%). Emulsions were made by method II and dissolved at day 0.

Time (days)	C (nm)	Neg (nm)	Tartrazine Release (%)
0	0.0027	0.9585	0.2817
8	0.0283	0.9828	2.8795
15	0.0468	0.9759	4.7956
29	0.0591	0.9749	6.0622
43	0.1123	0.9763	11.5026
57	0.6137	0.9956	61.6412
78	0.2678	1.0191	26.2781

Appendix I: *In vitro* lipolysis of double emulsions

Raw data from *in vitro* lipolysis studies of w/o/w double emulsions are given in table I.1-4, together with % tartrazine released. Dividing the control on the negative control and multiplying with 100, was done for each sampling time, to find the release of tartrazine, see example below for time=10, table I.1:

$$\frac{0.1076}{0.2366} \approx 0.4548 \times 100 = 45\%$$

Table I.1 and I.2 present the two replicates performed. The control studies without bile extracts and /or pancreatic enzymes are presented in table I.3 and I.4, respectively.

Table I.1. Raw data from in vitro lipolysis of w/o/w double emulsions with Tartrazine entrapped in the inner water phase. Absorbance (nm) for the control (C) and negative control (Neg) at every sampling time (min) for of replication 1, together with the amount tartrazine released (%).

Time (min)	C (nm)	C (- blank) Blank=0.017	Neg (nm)	Neg (- blank) Blank=0.017	Tartrazine Release (%)
10 ¹	0.1246	0.1076	0.2536	0.2366	45
15	0.1704	0.1534	0.2826	0.2656	58
20	0.2412	0.2242	0.3117	0.2947	76
25	0.2586	0.2416	0.3201	0.3031	80
30	0.3303	0.3133	0.3659	0.3489	90
40	0.3141	0.2971	0.3537	0.3367	88
50	0.3136	0.2966	0.3423	0.3253	91

¹Immediately after addition of lipases

Table I.2. Raw data from in vitro lipolysis of w/o/w double emulsions with Tartrazine entrapped in the inner water phase. Absorbance (nm) for every sampling time (min) for the control (C) and negative control (Neg) of replication 2, together with the amount tartrazine released (%).

Time (min)	C (nm)	C (- blank) Blank=0.0491	Neg (nm)	Neg (- blank) Blank=0.0491	Tartrazine Release (%)
10 ¹	0.4561	0.407	0.9465	0.8974	45.3532
10 ²	0.0995	0.0504	0.1732	0.1241	40.6124
13	0.1371	0.088	0.1664	0.1173	75.0213
16	0.1613	0.1122	0.1857	0.1366	82.1376
19	0.2029	0.1538	0.1901	0.141	109.0780
25	0.1983	0.1492	0.2184	0.1693	88.1276
30	0.2127	0.1636	0.2429	0.1938	84.4169
40	0.2437	0.1946	0.2535	0.2044	95.2055

¹Immediately after addition of lipases

²Just prior to lipase addition

Table I.3. Raw data from in vitro dissolution of w/o/w double emulsions with Tartrazine entrapped in the inner water phase, in absence of both pancreatic enzymes and bile extracts. Absorbance (nm) for the control (C) and negative control (Neg), together with the amount tartrazine released (N=6).

Replicate	C (nm)	C (- blank) Blank=0.0049	Neg (nm)	Neg (- blank) Blank=0.0049	Tartrazine Release (%)
1	0.0101	0.0052	1.0201	1.0152	0.5122
2	0.0105	0.0056	1.0303	1.0254	0.5461
3	0.0114	0.0065	1.0315	1.0266	0.6332
4	0.011	0.0061	1.0321	1.0272	0.5938
5	0.0126	0.0077	1.0334	1.0285	0.7487
6	0.0165	0.0116	1.0371	1.0322	1.1238
Average					0.693

Table I.4. Raw data from in vitro dissolution of w/o/w double emulsions with Tartrazine entrapped in the inner water phase, in absence of pancreatic enzymes. Absorbance (nm) for every sampling time (min) for the control (C) and negative control (Neg) of replication 2, together with the amount tartrazine released (%).

Time (min)	C (nm)	C (- blank) Blank=0.0221	Neg (nm)	Neg (- blank) Blank=0.0221	Tartrazine Release (%)
10	0.1068	0.0847	1.0161	0.994	8.5211
13	0.1207	0.0986	1.0466	1.0245	9.6242
16	0.1552	0.1331	1.0560	1.0339	12.8736
19	0.1701	0.148	1.0649	1.0428	14.1926
30	0.3035	0.2814	1.0803	1.0582	26.5923
40	0.4551	0.433	1.1196	1.0975	39.4533
70	1.2865	1.2644	1.2941	1.272	99.4025

The negative control were used as references for 100 % tartrazine in outer water phase, and the amount released from inner to outer water phase was found by dividing the absorbance for the control on the negative control at every sampling time.

Calculation example for replication 1 at 50 min is presented below (table I.1):

$$\frac{0.2966}{0.3253} \approx 0.911581 \times 100 = \underline{91.1581\%}$$

Appendix J: Statistical analysis

Statistical analyses on the results from the studies of Concordix matrices (storage modulus, gelling temperature, melting temperature, young's modulus and strain and force at break) were performed using Minitab 16.

The different gel properties listed above, were compared for type A and B gels with same amount of oil, and for either type A or B with different oil content, by performing 2-sample t-tests. The test compares data from two independent, random samples, based on the following hypotheses (H):

$$H_0: \mu(A) = \mu(B)$$

$$H_1: \mu(A) \neq \mu(B)$$

$\mu(A)$ and $\mu(B)$ are the mean value from the two independent samples.

It was assumed that the results obtained were random, independent and normally distributed. The analyses were performed with a confidence level of 0.95 and a corresponding p-value of 0.05. The results were considered as significant if the p-value was above 0.05.

J1. Small strain oscillatory measurements

p-values obtained from two-sample t-test comparison of the storage modulus, gelling and melting temperature for Concordix matrices (either type A or B) with varying amounts of oil is presented in table J.1-3.

Storage modulus

Table J.1. p-values obtained from a 2-sample t-test comparing the storage modulus between different Concordix matrices. Bold numbers are significant and regular numbers are not significant.

Gels compared	p-value
A0 and B0	0.810
A10 and B10	0.230
A30 and B30	0.066
A50 and B50	0.002
A0 and A10	0.038
A10 and A30	0.000
A30 and A50	0.000
B0 and B10	0.103
B10 and B30	0.000
B30 and B50	0.001

Gelling temperature

Table J.2. *p*-values obtained from a 2-sample *t*-test comparing the gelling temperature between different Concordix matrices. Bold numbers are significant and regular numbers are not significant.

Gels compared	p-value
A0 and B0	0.000
A10 and B10	0.000
A30 and B30	0.007
A0 and A10	0.000
A10 and A30	0.000
B0 and B10	0.165
B10 and B30	0.029

Melting temperature

Table J.3. *p*-values obtained from a 2-sample *t*-test comparing the melting temperature between different Concordix matrices. Bold numbers are significant and regular numbers are not significant.

Gels compared	p-value
A0 and B0	0.001
A10 and B10	0.000
A30 and B30	0.000
A0 and A10	0.000
A10 and A30	0.000
B0 and B10	0.625
B10 and B30	0.042

J2. Longitudinal deformation

p-values obtained from two-sample *t*-test comparison of Young's modulus, force and strain at break for Concordix gels (either type A or B) with varying amounts of oil is presented in table J.4-6.

Young's modulus

Table J.4. *p*-values obtained from a 2-sample *t*-test comparing Young's modulus between different Concordix gels. Bold numbers are significant and regular numbers are not significant.

Gels compared	p-value
A0 and B0	0.320
A10 and B10	0.126
A30 and B30	0.022
A0 and A10	0.105
A10 and A30	0.000
B0 and B10	0.802
B10 and B30	0.348

Force at break

Table J.5. *p*-values obtained from a 2-sample *t*-test comparing force at break between different Concordix gels. Bold numbers are significant and regular numbers are not significant.

Gels compared	p-value
A0 and B0	0.248
A10 and B10	0.000
A30 and B30	0.001
A0 and A10	0.003
A10 and A30	0.000
B0 and B10	0.002
B10 and B30	0.046

Strain at break

Table J.6. *p*-values obtained from a 2-sample *t*-test comparing strain at break between different Concordix gels. Bold numbers are significant and regular numbers are not significant.

Gels compared	p-value
A0 and B0	0.904
A10 and B10	0.000
A30 and B30	0.000
A0 and A10	0.002
A10 and A30	0.000
B0 and B10	0.001
B10 and B30	0.001

Appendix K: Attached CD – information

Additional raw data are found on the attached CD. Table K.1 provides information on the files, with corresponding folder names.

Table K.1. The content on the attach CD: Files with corresponding folder names.

File	Folder name
SEC-MALLS, raw data, word file	SEC-MALLS
Mastersizer 3000 raw data files	Mastersizer
Texture analyser raw data files	TextureAnalyser
MiniTab projects and worksheets	Minitab